

Desorption kinetics from albumin and the influence on hepatic metabolism

Dissertation

zur Erlangung des Doktorgrades der Naturwissenschaften
(Dr. rer. nat.)

der

Naturwissenschaftlichen Fakultät II
Chemie, Physik und Mathematik

der Martin-Luther-Universität
Halle-Wittenberg

vorgelegt von

Frau Sophia Krause

geboren am 09.03.1990 in Zwickau

Gutachter: 1. Prof. Dr. Kai-Uwe Goss
2. Prof. Dr. Martin Scheringer

Verteidigt am: 6. Dezember 2018

Wir werden nicht klüger ohne zu verstehen, dass wir eine Menge Fehler begangen haben.

August von Hayek

Abstract

Albumin is a highly abundant protein in blood that functions as a transport protein for many endogenous ligands like fatty acids, steroid hormones and metabolites. Due to its broad binding capacity, albumin also binds a lot of exogenous ligands like pharmaceuticals or contaminants. All bound ligands have to desorb from albumin again to be distributed into surrounding tissues or eliminating organs, because only the freely dissolved forms of the compounds are able to permeate across cell membranes. For hydrophobic compounds, hepatic metabolism is the major route of elimination. Desorption kinetics from albumin can thus affect a compound's elimination kinetics inside an organism, because slow desorption from albumin can limit the uptake of the compound into the metabolizing organ. By this, desorption kinetics from albumin is a potentially important parameter for pharmacokinetic and toxicokinetic modelling.

The purpose of this work was to investigate how fast desorption from albumin typically occurs and to quantify to which extent desorption kinetics impacts hepatic elimination of compounds. For experimental investigation of desorption kinetics, albumin-bound test chemicals were extracted in a time-resolved manner. For each test chemical a desorption rate constant was determined based on the measured extraction profile via transport modelling. The set of test chemicals comprised 15 neutral organic chemicals, including contaminants like polycyclic aromatic hydrocarbons and the pesticide chlorpyrifos. The corresponding experimentally determined desorption rate constants ranged from 0.1 s^{-1} up to 1.8 s^{-1} . Furthermore, a correlation between the determined desorption rate constant of a chemical and the chemical's molar mass was observed. Consideration of desorption as a transport process across the phase boundary between albumin and the surrounding aqueous phase provided a mechanistic explanation for this observed relationship. By this, the empirically calibrated relationship between desorption rate constant and molar mass can be considered as a predictive tool for desorption rate constants of other organic chemicals.

With the determined desorption rate constants, the question how desorption kinetics affects hepatic elimination of compounds was explored. For this purpose, suitable models of hepatic metabolism that allow consideration of desorption kinetics were developed based on the two most common modelling approaches for liver models: the well-stirred and the parallel tube liver model. The first one considers the whole liver as one well-stirred compartment, i.e. all components of the liver are assumed to be in instantaneous equilibrium with respect to chemical partitioning. The well-stirred liver model accounts for blood flow limitation but desorption of the compound from albumin and permeation of the compound into the hepatocytes cannot be considered when instantaneous equilibrium within the liver is assumed. The parallel tube liver model considers the

liver as an aggregation of identical cylindrical tubes with a concentration gradient along the tubes. Most commonly, the parallel tube model also considers only blood flow limitation and neglects permeation and desorption kinetics by assuming instantaneous equilibrium between blood and hepatocytes at any point of the tube.

To enable consideration of desorption kinetics, both models were extended in a way that albumin is represented as a separate compartment that exchanges compound with the aqueous portion of blood. Additionally, further compartmentalization was applied so that also permeation is represented as a kinetic process and consideration of permeability limitation is theoretically possible. However, to focus in the presented work exclusively on limitation caused by desorption kinetics, permeability was always set to high values that cause no additional limitations. Combination of different desorption rate constants with physiologically realistic values for hepatic blood flow and metabolism kinetics showed that slow desorption can reduce hepatic elimination of a compound by more than one order of magnitude. Such a strong reduction in hepatic elimination, though, only occurred when the lowest known desorption rate constant from the literature of 0.02 s^{-1} was assumed for a compound that was highly bound to albumin and quickly metabolized.

Considering the relationship between desorption rate constant and molar mass of a compound, it follows that such a low desorption rate constant is only realistic for high molar mass compounds. For less extreme scenarios of compounds with intermediate molar masses of 200 to 300 g/mol, desorption was faster and hepatic extraction efficiency decreased by no more than a factor three. This effect reduced even more, if compounds were slowly metabolized or only a minor fraction of the compound was bound to albumin. Consequently, compound-specific estimations are required to quantify the impact of desorption kinetics on hepatic metabolism accurately. The here presented relationship for prediction of desorption rate constants together with the derived models for hepatic metabolism provides the instruments needed for such estimations and thus enables comprehensive assessment of the importance of desorption kinetics.

Zusammenfassung

Albumin ist ein im Blut vorkommendes Protein, das Transporterfunktion für zahlreiche endogene Liganden, wie beispielsweise Fettsäuren, Steroidhormone und Metabolite übernimmt. Aufgrund seiner weitgefächerten Bindungskapazität bindet Albumin auch zahlreiche Substanzen exogenen Ursprungs, wie etwa Pharmaka oder Schadstoffe. Für die Verteilung in umliegende Gewebe oder abbauende Organe ist die Desorption der gebundenen Substanzen von Albumin notwendig, da nur die freigelösten Formen der Substanzen Zellmembranen passieren können. Ein besonders wichtiges Organ für den Abbau zahlreicher Substanzen ist die Leber, für hydrophobe Substanzen ist der hepatische Metabolismus der zentrale Pfad der Elimination. Die Desorptionskinetik kann die Eliminationskinetik von Substanzen innerhalb eines Organismus beeinflussen, da eine langsame Desorption die Aufnahme in das abbauende Organ limitieren kann. Infolgedessen ist die Desorptionskinetik von Albumin ein potenziell wichtiger Parameter für die pharmako- und toxikokinetische Modellierung.

Ziel dieser Arbeit war es zu untersuchen, wie schnell die Desorption von Albumin typischerweise abläuft und in welchem Maß die Desorptionskinetik den hepatischen Abbau von Chemikalien beeinflusst. Für die experimentelle Bestimmung der Desorptionskinetik wurden Albumin-gebundene Testchemikalien zeitaufgelöst extrahiert. Auf Basis der so aufgezeichneten Extraktionsprofile wurden die Desorptionsratenkonstanten der Testchemikalien mit Hilfe eines Transportmodells ermittelt. Die Auswahl an Testchemikalien umfasste 15 neutrale organische Verbindungen, einschließlich Schadstoffen wie polyzyklische aromatische Kohlenwasserstoffe und das Pestizid Chlorpyrifos. Die ermittelten Desorptionsratenkonstanten lagen im Bereich von $0,1 \text{ s}^{-1}$ bis $1,8 \text{ s}^{-1}$. Außerdem wurde eine Korrelation zwischen der Desorptionsratenkonstante einer Testchemikalie und ihrer molaren Masse beobachtet. Diese Beziehung konnte mechanistisch erklärt werden, indem die Desorption als Transportprozess über eine Phasengrenze hinweg betrachtet wurde. Mit dieser mechanistischen Grundlage kann die empirisch kalibrierte Korrelation zwischen Desorptionsratenkonstante und Molekulargewicht als eine Möglichkeit zur Vorhersage von Desorptionsratenkonstanten anderer Chemikalien angesehen werden.

Auf Basis der vorhandenen Daten wurde dann die Frage nach dem Einfluss der Desorptionskinetik auf den hepatischen Abbau von Chemikalien untersucht. Zu diesem Zweck wurden zwei Modellierungsansätze entwickelt. Die beiden Modellierungsansätze basierten dabei auf den zwei am häufigsten verwendeten Lebermodellen: dem „well-stirred“ und dem „parallel tube liver model“. Das sogenannte „well-stirred liver model“ behandelt die Leber als ein einziges gutdurchmischtes Kompartiment. In diesem Modell wird instantanes Gleichgewicht zwischen allen

Komponenten der Leber angenommen. Eine potenzielle Limitierung des Abbaus durch den Blutfluss wird im existierenden Modell bereits berücksichtigt, weitere eventuelle Limitierungen aufgrund langsamer Desorption oder langsamer Permeation der Chemikalien in die Hepatozyten hinein werden durch die Annahme von instantanem Gleichgewicht jedoch vernachlässigt. Das sogenannte „parallel tube liver model“ hingegen bildet die Leber als eine Ansammlung identischer Blut-durchflossener Röhren ab und berücksichtigt die Entstehung von Konzentrationsgradienten in den durchflossenen Röhren. In der Regel repräsentiert auch dieses Modell nur die potenzielle Blutflusslimitierung, Desorption und Permeation werden durch die Annahme von instantanem Gleichgewicht zwischen Blut und Hepatozyten an jedem beliebigen Punkt der Röhre ebenfalls vernachlässigt.

Um die Desorptionskinetik von Albumin in die Modelle einbauen zu können, wurden beide Modelle so erweitert, dass Albumin als ein separates Kompartiment abgebildet wird und im Austausch mit dem wässrigen Anteil des Blutes steht. Zugleich wurden die Modelle dahingehend erweitert, dass auch Permeation abgebildet ist und folglich auch die Berücksichtigung einer etwaigen Permeationslimitierung möglich wäre. Um vorerst jedoch den Fokus ausschließlich auf den Effekt der Desorption zu legen, wurde die Permeabilität in allen Berechnungen stets so hoch gesetzt, dass keine Permeationslimitierung auftrat. Die Kombination verschiedener Desorptionsratenkonstanten mit physiologisch realistischen Werten für hepatischen Blutfluss und Abbaukinetik zeigte, dass eine langsame Desorption den hepatischen Abbau um mehr als eine Größenordnung reduzieren kann. Ein so starker Effekt tritt allerdings nur auf, wenn die kleinste aus der Literatur bekannte Desorptionsratenkonstante von 0.02 s^{-1} im Modell mit einer Chemikalie kombiniert wird, die im Blut zu einem hohen Grad am Albumin gebunden vorliegt und die gleichzeitig schnell abgebaut wird.

Berücksichtigt man die Korrelation zwischen Desorptionsratenkonstante und molarer Masse einer Chemikalie, zeigt sich, dass eine so geringe Desorptionsratenkonstante nur für Chemikalien mit hohen molaren Massen realistisch ist. Für weniger extreme Szenarien mit Chemikalien, deren molaren Massen im Bereich von 200 – 300 g/mol liegen, ist die Desorption schneller und die hepatische Extraktionseffizienz verringert sich um nicht mehr als Faktor drei. Dieser Effekt nimmt noch weiter ab, wenn die Abbaukinetik langsam ist oder nur ein geringer Anteil der Substanz am Albumin gebunden vorliegt. Um den Einfluss der Desorptionskinetik auf den hepatischen Abbau einer Substanz exakt zu quantifizieren, sind demnach substanzspezifische Abschätzungen notwendig. Die hier präsentierten Modelle des hepatischen Abbaus stellen zusammen mit der Korrelation zur Vorhersage von Desorptionsratenkonstanten geeignete Werkzeuge für diese Abschätzungen dar und ermöglichen somit eine umfassende Beurteilung der Relevanz der Desorptionskinetik in verschiedensten Szenarien.

Preface

The present work was performed from June 2015 to June 2018 at the Helmholtz Centre for Environmental Research Leipzig in the Department Analytical Environmental Chemistry. The thesis is written as monograph.

A version of chapter 3 has been published in the Journal Archives of Toxicology: Krause, S., N. Ulrich, and K.-U. Goss, Desorption kinetics of organic chemicals from albumin. Archives of Toxicology, 2018. 92(3): p. 1065-1074.

The first author conducted the experiments, analyzed the data and wrote the manuscript. N. Ulrich contributed to the design of the experiments and provided technical assistance. K.-U. Goss coordinated the study and contributed to the development of the transport model. N. Ulrich and K.-U. Goss critically revised the manuscript.

Parts of chapter 4 also have been published in the Journal Archives of Toxicology: Krause, S. and K.-U. Goss, The impact of desorption kinetics from albumin on hepatic extraction efficiency and hepatic clearance: a model study. Archives of Toxicology, 2018. 92(7): p. 2175-2182.

The first author derived the model, performed the simulations and wrote the manuscript. K.-U. Goss contributed to the model development and critically revised the manuscript.

Note that text passages and figures in this monograph are partly taken from the published papers without further indication. The published papers are included at the end (appendix D).

Content

Abstract	I
Zusammenfassung	III
Preface	V
1. Introduction	1
2. Objective	3
3. Experimental investigation of desorption kinetics	4
3.1. Materials & Methods	4
3.1.1. Experimental principle	4
3.1.2. Method development & materials	4
3.1.3. Time-resolved extraction experiments	5
3.1.4. Limitations of the method	6
3.1.5. Data analysis via transport modelling	8
3.2. Results	12
3.2.1. Determination of extraction rate constants	12
3.2.2. Comparison between HSA and BSA	13
3.2.3. Determination of desorption rate constants	13
3.3. Discussion	16
3.3.1. Desorption from BSA and HSA	16
3.3.2. Comparison to published k_{des}	17
3.3.3. Calibration of a prediction method based on a mechanistic concept	18
3.3.4. A first glance on physiological relevance of desorption kinetics from albumin	23
4. Modelling the impact of desorption kinetics from albumin on hepatic metabolism	24
4.1. Calculations using a well-stirred liver model approach	24
4.1.1. Implementation of desorption kinetics into a well-stirred liver model	24
4.1.2. Physiological input data	27
4.2. Calculations using a parallel tube liver model approach	30
4.2.1. Implementation of desorption kinetics into a parallel tube liver model	30
4.2.2. Physiological input data	32
4.3. Comparison of the results of both liver models	33
4.3.1. Partition properties of the compound affect E	33
4.3.2. Slow desorption can reduce E significantly	36
4.3.3. Fast metabolism is a prerequisite for relevance of desorption kinetics	38

4.4. Discussion	39
5. Conclusion	42
6. Abbreviations	44
7. References	45
Appendix	49
A. Rearranging the mass balance equations of the well-stirred modelling approach	49
B. Calculation of hepatocyte-water partition coefficients	53
C. References	57
D. Published Papers	58
D.1. Desorption kinetics of organic chemicals from albumin.....	58
D.2. The impact of desorption kinetics from albumin on hepatic extraction efficiency and hepatic clearance: a model study.....	68
List of figures	77
List of tables	78
Danksagung	79
Angaben zur Person und zum Bildungsgang	80
Publikationen und Konferenzbeiträge	81
Eidesstattliche Erklärung.....	82

1. Introduction

Accurate predictions how fast and to which extent a chemical is eliminated from an organism are demanded for by various fields: In environmental sciences such information is needed for bioaccumulation assessment, in pharmacology it is required for estimations of *in vivo* pharmacokinetics and in toxicology such information is used for modelling of internal exposure in risk assessment. For hydrophobic chemicals, the major route of elimination is hepatic metabolism. The kinetics of the hepatic metabolism not only depends on the kinetics of the metabolizing enzymes but also on kinetics of compound delivery to the metabolically active sites. Compound delivery inside organisms mostly happens via blood stream. In blood, however, most chemicals are not present freely dissolved but bound to certain blood components instead. Among these components, the protein albumin, the most important transport protein in blood, is commonly regarded as an especially important compartment for binding.

It follows that chemicals have to desorb from the protein before they can be taken up into surrounding tissues, because only the freely dissolved forms of chemicals can permeate into cells [1]. By this, desorption from albumin is a potentially rate limiting step for hepatic metabolism, because blood passes through the liver within seconds [2]. Although this issue was already raised in the 1980s [3], the question how big the impact of desorption kinetics on hepatic metabolism is has not been answered conclusively yet. In fact, despite its potential relevance, desorption kinetics are currently neglected in models of hepatic metabolism by assuming instantaneous sorption equilibrium.

One reason for this might be that only limited data of experimentally determined desorption rate constants exists. The existing data is restricted to a few compounds and shows broad variation with desorption rate constants ranging over two orders of magnitude [4-11]. To improve the data basis, generation of a consistent dataset of experimentally determined desorption rate constants is necessary. A suitable method for such measurements is the time-resolved in-tube solid phase microextraction, that was presented in the literature a few years ago for investigation of desorption kinetics from dissolved organic matter [12]. In this experimental method, the test chemicals were extracted from suspensions containing dissolved organic matter in a time-resolved manner via pumping through a capillary coated with an extraction material. Adapting this method for investigation of desorption kinetics is appealing, because this experimental set-up would mimic the physiological situation of blood capillaries surrounded by hepatocytes. In the experimental set-up, the extraction material functions as a sink for the test chemical, whereas in the

physiological situation the hepatocytes are an infinite sink for the chemicals due to the metabolic activity. As a result of this functional analogy, qualitative information on whether desorption affects the *in vivo* uptake kinetics of the test chemical can be directly deduced from the experiments.

With an improved data basis of experimentally determined desorption rate constants, it is possible to revisit the question whether desorption kinetics is an important parameter for prediction of hepatic metabolism. For modelling of hepatic metabolism, two commonly used liver models exist. The so-called well-stirred liver model [13] considers the entire liver as one single well-stirred compartment, whereas the so-called parallel tube liver model [14] considers the liver as an aggregation of identical cylindrical tubes through which blood continuously flows. The well-stirred model is mathematically simpler than the parallel tube model. However, it neglects the concentration gradient that develops for well metabolized compounds during passage through the liver capillaries, the so called sinusoids, and is known to underestimate hepatic metabolism for some cases [15, 16].

Usually, both models neglect desorption kinetics by assuming instantaneous equilibrium within the liver. One has to note that, by this, not only desorption kinetics but also permeation kinetics, i.e. the transport of the freely dissolved chemical from sinusoid blood into the hepatocytes, is neglected. In order to enable consideration of desorption kinetics, both models require modifications and extensions. Two parameters that describe the metabolic capacity of the liver are then most convenient for quantification of the impact of desorption kinetics on hepatic metabolism: hepatic clearance and extraction efficiency. The parameter hepatic clearance was first mentioned in pharmacology literature in the 1940s [17] and is defined as 'the average volume of blood cleared of drug per unit time' [13]. In a mathematical sense, hepatic clearance corresponds to the metabolic rate constant multiplied by a volume. The parameter extraction efficiency describes to which extent a chemical is removed from blood by the liver. Extraction efficiency is calculated as the difference between chemical concentration in inflowing and in outflowing blood divided by chemical concentration in inflowing blood [18].

2. Objective

The aim of this work was to quantify the impact of desorption kinetics from albumin on hepatic metabolism. For this goal, a dataset of desorption rate constants was determined experimentally and, in a second part, models of hepatic metabolism considering desorption kinetics from albumin were developed.

For experimental investigation of desorption kinetics from albumin, time-resolved extraction of test chemicals from albumin suspensions was performed. To ensure a structurally diverse data set of neutral organic test chemical, chemicals from different compound classes were chosen as test chemicals, e.g. substituted ethers, substituted benzenes and polycyclic aromatic hydrocarbons. Based on the observed extraction profiles, the desorption rate constants had to be determined via transport modelling.

For the second part, the quantification of the impact of desorption kinetics on hepatic metabolism, two modelling approaches based on the two most commonly used liver models were developed: the well-stirred liver model and the parallel tube liver model. To enable consideration of desorption kinetics, these models had to be modified in a way that albumin is represented as a separate compartment. The so generated models were then used to quantify the impact of desorption kinetics on hepatic metabolism by combining different desorption rate constants with physiological values of hepatic blood flow and metabolism kinetics. The simultaneous application of the well-stirred and the parallel tube modelling approach additionally allowed critical comparison and quantification of the differences between both models.

3. Experimental investigation of desorption kinetics

3.1. Materials & Methods

3.1.1. Experimental principle

The principle used for measurement of desorption kinetics from albumin was a time-resolved extraction of the test chemicals from albumin suspensions. For time-resolved extraction, an albumin suspension spiked with test chemical is pumped through a capillary that has a coating of sorbing polymer (poly(dimethylsiloxane), PDMS) on its inner surface. The flow rates that were used for pumping determined the residence time of the sample inside the capillary. As soon as the test chemical desorbed from albumin inside the capillary, it was removed from the sample solution due to sorption into the polymer and the test chemical's concentration in the sample solution thus decreased. Only that fraction of the test chemical, which did not desorb fast enough from the albumin, passed through the capillary. This remaining concentration of the test chemical in the capillary effluent was compared to the concentration in the input suspension. By variation of the flow rates used for pumping, concentration-residence time profiles for the extractions were measured. These concentration-residence time profiles allowed determination of the desorption rate constants.

3.1.2. Method development & materials

The used method was a modification of the method introduced by Eisert and Pawliszyn [19] and extended by Kopinke et al. [12]. Essentially, two differences to the system used by Kopinke et al. existed: 1) the PDMS coating of the capillary was thicker (8 μm instead of 1 μm) and 2) a PDMS-coated glass fibre (30 μm coating thickness) instead of a metal wire was inserted in the capillary. Both changes resulted in a gain of sorption capacity due to a bigger PDMS volume. Inserting a PDMS-coated glass fibre into the capillary (Fig. 1) reduced the maximum diffusion path length from the albumin suspension to the PDMS phase perpendicular to flow direction from 177 μm (empty capillary) to ≈ 25.5 μm (filled capillary, assuming non-centred glass fibre position). A reduced diffusion path length leads to a faster extraction of the test chemical from the sample solution into the PDMS, which is essential for successful application of the method.

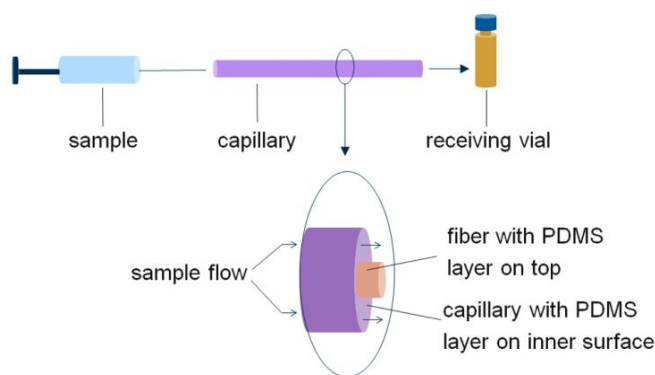


Fig. 1 Schematic representation of the experimental set-up for time-resolved extraction experiments

The capillaries used for the time-resolved extraction experiments were pieces of a standard gas chromatography (GC) column that were cut to 20 cm length. The used 007-1 GC column (inner diameter 0.25 mm, layer 100% PDMS, layer thickness 8 μm) was purchased from Quadrex Corporation. The inserted PDMS coated glass fibres (diameter of the glass core 0.123 mm, PDMS layer thickness 30 μm) were purchased from Polymicro Technologies Inc. GC capillaries and fibers were cleaned before usage by purging with methanol.

For the experiments, stock solutions of the test chemicals were prepared either in methanol or in isopropanol. Lyophilized human and bovine serum albumin was obtained from Sigma Life Science (> 98%, essentially fatty acid free) and dissolved in a phosphate buffer (150 mM NaCl, 10 mM phosphate, pH 7.40). Albumin suspensions were spiked with stock solutions of each test chemical to prepare the sample solutions. The methanol or isopropanol content did not exceed 0.5 v/v %. The sample solutions were gently shaken (RS-TR05, Phoenix Instrument) overnight at room temperature for equilibration.

3.1.3. Time-resolved extraction experiments

At first, pure aqueous solutions (clean water without albumin, $V = 200 \mu\text{L}$) of the test chemicals were pumped (VIT-FIT syringe pump, Lambda Laboratory Instruments) through the capillary with flow rates ranging from 24 mL/h to 2.4 mL/h corresponding to residence times inside the capillary ranging from 0.5 s up to 5 s. These reference experiments allowed investigation of the extraction kinetics and derivation of the extraction rate constants k_{extr} of the freely dissolved chemical from the water phase into the PDMS. The capillary effluent was directly collected in septum-closed vials after passage through the capillary in order to avoid losses by volatilization. For concentration determination via gas chromatography-mass spectrometry (GC-MS) (7890A/5975C and 7890B/7010, Agilent Technologies), the

vials were pre-filled with cyclohexane as extraction solvent. Cyclohexane contained hexachlorobenzene as internal standard. For extraction, samples were gently shaken for 3 minutes. Efficiency of extraction was calculated for each chemical using partition coefficients estimated based on the compound's physicochemical properties [20] and did not undershoot 99%. The input suspension was extracted in the same manner. For analysis, the cyclohexane extracts were injected in cold splitless mode, separated with an HP-5 column (HP-5MS UI, 30 m, inner diameter 0.25 mm, film thickness 0.25 μm , Agilent Technologies) and analyzed in SIM or MRM mode.

In a next step, experiments were conducted with albumin suspensions. The sample solution (albumin suspension spiked with test chemical, $V = 200 \mu\text{L}$) was pumped through the capillary with defined flow rates ranging from 24 mL/h to 0.2 mL/h. These flow rates corresponded to residence times of the sample inside the capillary ranging from 0.5 s to 60 s. Again, the capillary effluent was collected and concentrations were determined as described for the reference experiments with pure aqueous solutions. In the experiments conducted with albumin suspensions, the overall transport kinetics that we measured had contributions from two kinetic steps: a) desorption from albumin itself into the freely dissolved state and b) extraction from the freely dissolved state into PDMS. Obviously, a sensitive determination of the sole desorption kinetics from albumin is only possible if the extraction kinetics from the water phase are corrected for in the experiments with albumin. This was why the reference experiments with water were needed.

For the experiments with albumin suspension, human serum albumin (HSA) as well as bovine serum albumin (BSA) were used in order to reveal possible differences in desorption kinetics. The used albumin concentrations ranged from 0.1 g/L to 10 g/L, individually chosen for each chemical according to its partition properties. Albumin was always present in excess in the sample solutions (moles albumin \gg moles test chemical) to avoid saturation of binding sites and to assume 1:1-binding of the chemical. Under these conditions, desorption from albumin could be assumed as independent from the used albumin concentration, i. e. experiments with different albumin concentrations should result in the same desorption rate constants k_{des} for a given chemical. Based on this assumption, each chemical was extracted from two albumin suspensions, differing in their concentrations. This procedure allowed confirmation of the determined k_{des} . All experiments were conducted at room temperature.

3.1.4. Limitations of the method

For successful application of the method, the following conditions had to be met:

- 1) the albumin-bound fraction of the chemical in the input albumin suspension would preferably be above 70-80%
- 2) sufficient capacity of PDMS for nearly complete extraction of the chemical from the albumin suspension under equilibrium conditions
- 3) extraction from water into PDMS faster than desorption from albumin into water
- 4) negligible loss of albumin due to sorption to the PDMS coating inside the capillary

To ensure a high albumin-bound fraction in the input suspension, the used albumin concentrations were adapted for each chemical according to its partition properties. Partitioning between albumin and water was calculated using BSA-water-partition coefficients either from literature [21] or (in case no literature data was available) from the LSER (linear solvation energy relationship)-database [20], which provides partition coefficients estimated based on a compound's physicochemical properties. Only in a few experiments the sorbed amount was smaller than 70%, which resulted in a loss of accuracy in the derived desorption rate constants due to a smaller measuring range.

In order to meet the second condition of sufficient PDMS capacity, the experimental set-up was optimized by testing GC capillaries with different layer thicknesses. The optimal set-up consisted of a capillary with a 8 μm PDMS coating into which a glass fibre with a 30 μm PDMS coating was inserted. Fast extraction of the test chemicals from water into PDMS was confirmed via comparing results from reference experiments with aqueous solutions of the chemicals to results from albumin suspension extraction.

In order to check to which extent a loss of albumin due to sorption to the PDMS coating inside the capillary occurs, the albumin concentration of the capillary effluent was determined and compared with the albumin concentration of the input suspension. Concentration determination was performed via absorption measurements at 280 nm as well as at 595 nm (Bradford assay, [22]). Two different albumin concentrations were tested with two different flow rates (resulting in different residence times - 1 s and 10 s - inside the capillary). The shown results (Table 1) represent the averaged recoveries of seven measurements with its corresponding standard deviations (SD).

Table 1: Albumin recoveries after pumping albumin suspensions through the capillary.

BSA concentration	mass BSA in effluent/mass BSA in input (mean \pm SD)	
	t = 1 s	t = 10 s
1 g/L	0.991 (\pm 0.028)	1.020 (\pm 0.044)
10 g/L	0.999 (\pm 0.034)	1.015 (\pm 0.055)

The calculated mean recoveries did not undershoot 99.1%, the loss of albumin thus could be considered as negligible.

3.1.5. Data analysis via transport modelling

The desorption rate constants could not be read directly from the measured concentration-time profiles, but needed to be determined via transport modelling. Fig. 2 illustrates the situation inside the capillary for the experiments with water and with albumin suspension.

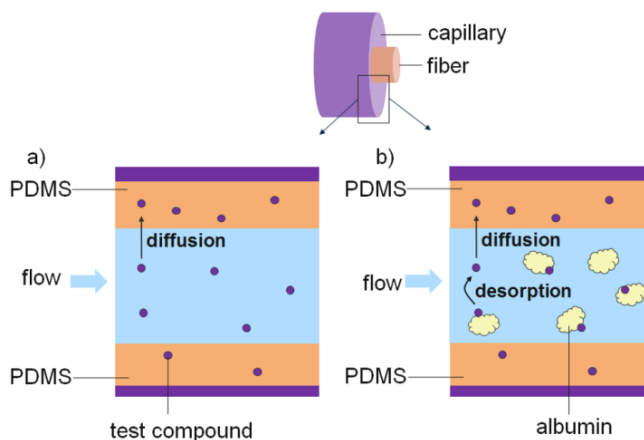


Fig. 2 Detailed scheme of the used experimental set-up. Part a) shows the situation in the capillary when the test chemical is extracted from water, part b) shows the situation in the capillary when the test chemical is extracted from an albumin suspension

The measured concentration-time profiles in the experiments with albumin suspension depended on two kinetic steps: desorption kinetics from albumin and extraction kinetics into the PDMS. The extraction of the test chemical into the PDMS created the chemical gradient, that was the driving factor for desorption from albumin. This extraction of the chemical into the PDMS was driven by diffusion. In detail, diffusion within the slit water volume, diffusion across the phase boundary between slit water and PDMS and diffusion within the PDMS occurred.

To represent these transport processes, a diffusion model was developed. In the diffusion model, the experimental set-up was represented by a sample solution compartment and two neighbouring PDMS compartments (Fig. 3).

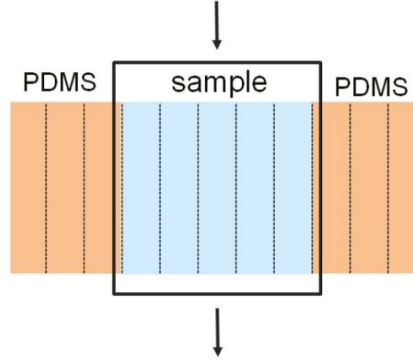


Fig. 3 Scheme of the spatial discretization in the diffusion model

The continuous pumping of the sample through the capillary was represented by a block by block exchange of the sample solution compartment; the frequency of exchange resulted from flow rate and slit volume. To model the compound flux from the sample solution compartment into the PDMS, the different compartments were spatially discretized into layers parallel to flow direction. For data analysis of the experiments with water, the sample solution compartment was depicted by 14 layers, the PDMS coating of the capillary was depicted by 4 layers and the PDMS coating of the glass fibre was depicted by 10 layers. Each of them was assumed to be well-mixed. Perpendicular to flow direction no additional spatial discretization was applied. The compound flux across the layers was calculated based on Fick's law:

$$J = -D \frac{\partial C}{\partial x} \quad (1)$$

The flux J of the test chemical (mol/cm²/s) was given by the diffusion coefficient D (cm²/s) of the unbound chemical in water and in PDMS respectively, the concentration gradient (mol/cm³) and diffusion path length x (cm). Diffusion coefficients in water were available in the literature or LSER-calculated [23] for each test chemical and ranged from 3.5×10^{-6} to 8.4×10^{-6} cm²/s. For PDMS, the diffusion coefficient was estimated to be 6.6×10^{-7} cm²/s from the literature [24, 25]. For compound flux across the phase boundary between slit water and PDMS, the partitioning of the compound between the two different phases needed to be considered. Rearrangement of Fick's law with the PDMS-water partition coefficient $K_{PDMS/W}$ (L/L) gives an equation describing the flux across the phase boundary:

$$J_{water \rightarrow PDMS} = \frac{1}{\frac{x_{PDMS}}{D_{PDMS}} * \frac{1}{K_{PDMS/W}} + \frac{x_{water}}{D_{water}}} * (C_w - \frac{C_{PDMS}}{K_{PDMS/W}}) \quad (2)$$

Numerical solution in MS Excel of these equations showed that diffusion in PDMS was not limiting for compound transport from the water phase into PDMS. In order to reproduce the measured extraction profiles from water via modelling, though, it was necessary to consider dispersion along the direction of convective flow. For this purpose, we introduced stagnant water layers next to the PDMS layers as a simplified representation of dispersion.

In a second step, the extraction of an albumin suspension was modelled. We extended the existing model by adding albumin as an additional phase represented by an additional layer next to each water layer. Compound flux J (mol/s) from albumin into water is described by a first order desorption kinetics:

$$J = -k_{des} * C^b * V_{alb} + k_{sorb} * C^u * V_{water} \quad (3)$$

where k_{des} referred to the desorption rate constant (s^{-1}) and k_{sorb} (s^{-1}) to the adsorption rate constant, C^u and C^b were the unbound and bound concentrations of the chemical and V_{alb} and V_{water} were the albumin or water volume respectively. To solve the equations numerically, they were implemented into a visual basic script to conduct automated computations in MS excel. The discretization in time was 0.0001 s.

As expected, this model could not yet represent the experimental data satisfactorily unless facilitated transport of the chemical by albumin was taken into account. This facilitated transport resulted from diffusion of the albumin bound fraction of the chemical together with the albumin perpendicular to the flow direction, which happened in addition to diffusion of the freely dissolved chemical. The facilitated transport was implemented by considering the diffusion of the albumin bound portion of the chemical as a second flux J^b from water to PDMS in addition to the flux of the freely dissolved portion:

$$J^b = -D^b \frac{C_{alb} * \partial C^b}{\partial x} \quad (4)$$

Here, D^b represented the diffusion coefficient of the bound chemical, which is given by the diffusion coefficient of albumin in water ($D^b = 3.6 \times 10^{-7} \text{ cm}^2/\text{s}$ from the literature) and C_{alb} was the albumin concentration [26].

This diffusion model was used to optimize the dimensions of the experimental set-up (e.g. thickness of PDMS layer, diffusion path length in the water perpendicular to the flow direction) to ensure fast extraction from the water phase into the PDMS and sufficient sorption capacity of the PDMS for the test chemicals. Good agreement between the results from this model and the experiments with aqueous solutions of the chemicals indicated that the mechanistic understanding of the extraction from pure water was sufficiently good. However, this model was not well suited to evaluate the eventual experiments that were

dominated by the desorption kinetics from albumin. For these experiments, it was important to describe the convective and dispersive transport through the capillary more correctly than this is done by a blockwise replacement of the sample solution layers.

As a result a second numerical model was developed based on dispersion and convection. In these transport calculations, albumin, water and PDMS were represented as different compartments and were discretized into 100 sections perpendicular to flow direction (Fig. 4).

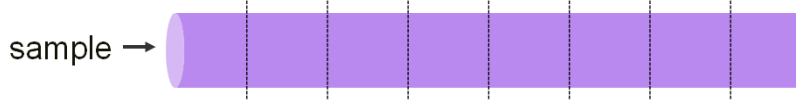


Fig. 4 Scheme of the spatial discretization in the dispersion-convection model

Each section was assumed as well-mixed. The discretization in time again was 0.0001 s. In order to keep the computational effort affordable, we did not discretize the water parallel to the flow direction into various layers. By doing so, the flux of the test chemical from the water phase into PDMS (extraction) was not explicitly treated as a diffusional process but instead this process was described by first order kinetics. The flux of the test chemical from albumin into the water phase (desorption) was also assumed to be a first order kinetics.

The continuous transport of albumin, albumin-bound chemical and unbound chemical was calculated based on convection and dispersion:

$$J = -D \frac{\partial C}{\partial x} + v C \quad (5)$$

Here, D referred to the dispersion coefficient and v to the convective velocity. The dispersion coefficient was determined based on a measured breakthrough curve and the convective velocity was given by the flow rate.

Additionally, the model included the facilitated transport of the test chemicals from the suspension to the PDMS. The facilitated transport was represented by using accelerated extraction rate constants when modelling the albumin extraction experiments. These accelerated extraction rate constants were calculated individually for each chemical and albumin concentration based on the extraction rate constants found in the reference experiments with clean water. For this calculation, we used an approach analogue to the one from Kramer et al. [27], representing the total flux (J^{total}) of the chemical as sum of the flux of bound and unbound chemical:

$$J^{total} = - (J^u + J^b) \quad (6)$$

Using eq. (1) and eq. (3), substituting C^b for $K_{AW} * C^u$ and rearranging J^{total} , the ratio of fluxes in albumin containing and in clean water solutions (FTR) can be rewritten as:

$$FTR = 1 + \frac{D^b}{D^u} * K_{AW} * C_{alb} \quad (7)$$

Here, D^u referred to the diffusion coefficient of the chemical in water and D^b to the diffusion coefficient of albumin in water, K_{AW} referred to the albumin-water partition coefficient, C_{alb} was the albumin concentration. According to this, the accelerated extraction rate constants $k_{accelerated\ extr}$ for extractions from albumin suspensions were calculated (eq. (8)) based on the extraction rate constant determined for the extraction of clean water.

$$k_{accelerated\ extr} = k_{extr} * FTR \quad (8)$$

The model was implemented into a visual basic script, which conducted the computations in MS excel. By fitting this transport model to the measured concentration-time profiles, the desorption rate constants for each test chemical were determined.

3.2. Results

3.2.1. Determination of extraction rate constants

The obtained extraction profiles showed that extraction kinetics from water were similar for all chemicals. This observation is in agreement with expectations because diffusion of the used chemicals in water is very similar (estimated diffusion coefficients range from 3.5×10^{-6} to 8.4×10^{-6} cm²/s [23]) and diffusion of the chemicals in PDMS itself had been shown not to be rate limiting in our set-up. Fig. 5 shows the extraction profiles of three different chemicals as an example. Shown are mean values of duplicates, standard deviations are indicated as error bars. While the PDMS-water partition coefficients of these chemicals differed by about 1 log-unit, sorption equilibrium was reached for all chemicals within 3 seconds residence time in the capillary and all chemicals were extracted to about 99%.

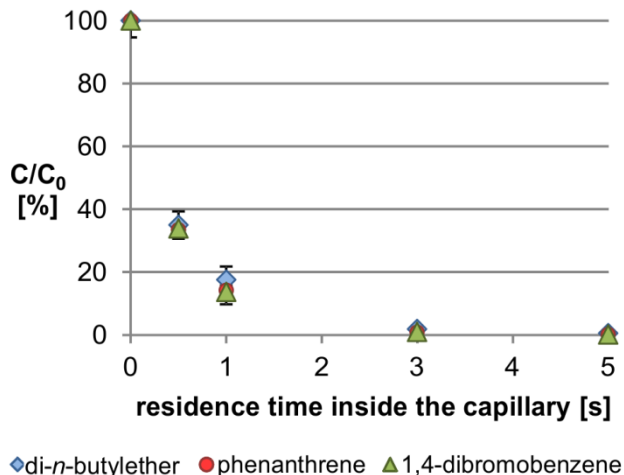


Fig. 5 Extraction of di-*n*-butylether ($C_0 = 1$ mg/L), phenanthrene ($C_0 = 0.05$ mg/L) and 1,4-dibromobenzene ($C_0 = 0.2$ mg/L) from water, all test chemicals were extracted to about 99% within 3 s. Shown are mean values of duplicates, standard deviations are indicated as error bars. In cases where error bars are invisible, they are covered by the symbols

Fitting the curves with the transport model revealed a rate constant $k_{extr} = 2.7$ s⁻¹ for extraction of the most chemicals. The only exceptions were chlorpyrifos, 1-nitrooctane and 1-chlorooctane, for which slightly different extraction rate constants were determined ($k_{extr} = 2.3$ s⁻¹ for chlorpyrifos and $k_{extr} = 2.9$ s⁻¹ for 1-nitrooctane and 1-chlorooctane). The determined extraction rate constants were used to calculate the accelerated extraction rate constants, which were needed for transport modelling of the extractions from albumin suspensions.

3.2.2. Comparison between HSA and BSA

The experiments with HSA instead of BSA yielded extraction profiles, which were overlaying to the extraction profiles measured in the BSA experiments. These experiments thus showed no evidence for dependence of desorption kinetics on the albumin type. Further comparison between HSA and BSA was omitted and the succeeding experiments were all conducted with BSA.

3.2.3. Determination of desorption rate constants

All experiments showed a substantially slower extraction from the albumin suspension compared to the extraction from water. Fig. 6 shows the extraction of 1,2,3,4-tetrachlorobenzene from BSA compared to its extraction from water. Again, mean values of duplicates are shown and standard deviations are indicated as error bars.

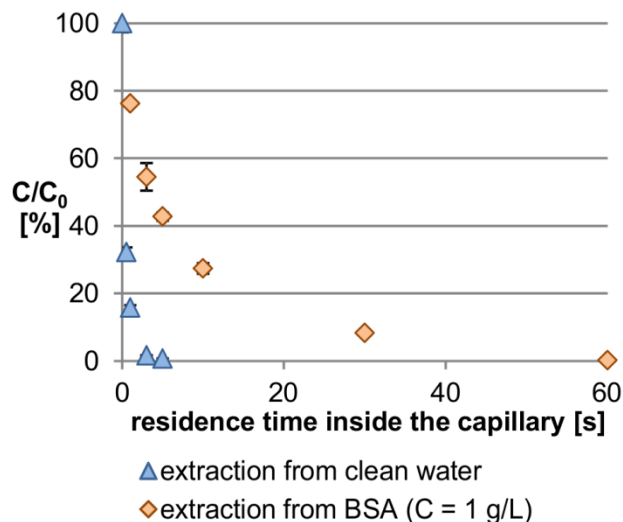


Fig. 6 Extraction of 1,2,3,4-tetrachlorobenzene ($C_0 = 0.1$ mg/L) from water and from a BSA suspension ($C = 1$ g/L). Shown are mean values of duplicates, standard deviations are indicated as error bars. In cases where error bars are invisible, they are covered by the symbols

After 60 s residence time in the capillary, the remaining concentration of 1,2,3,4-tetrachlorobenzene in the sample was almost zero. Obviously, 60 s were sufficient for desorption and establishment of partition equilibrium between water, albumin and PDMS. With shorter residence times the remaining concentration increased due to incomplete desorption. For the shortest residence time, the concentration in the capillary effluent was mainly governed by the partition equilibrium between water and albumin in the input suspension indicating no significant desorption going on during passage through the column.

Summarizing these observations, the edges of the extraction profiles can be considered as dominated by the partition properties of the chemicals whereas the steepness of the intermediate part of the extraction profile mostly reflects the influence of the desorption rate constant.

The generated data were modelled with the developed transport model to obtain desorption rate constants for each chemical. For confirmation, each chemical was extracted from two albumin suspensions with different concentrations. Assuming that the desorption kinetics were independent from the albumin concentration, the desorption rate constant had to be the same for both experiments (Fig. 7). This allowed confirmation of the predetermined k_{extr} and the fitted k_{des} : while a single extraction curve could still be fitted equally well with different combinations of k_{extr} and k_{des} (because a wrong k_{extr} could be corrected by fitting an also wrong k_{des}), the simultaneous fitting of two extraction curves with different albumin concentrations could only succeed if both rate constants were correct.

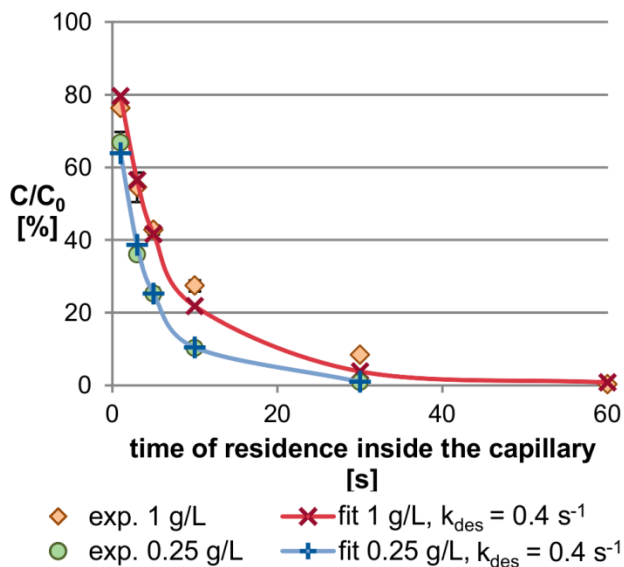


Fig. 7 Extraction of 1,2,3,4-tetrachlorobenzene ($C_0 = 0.1 \text{ mg/L}$) from bovine serum albumin suspensions. Different BSA concentrations are indicated as diamonds (1 g/L) and dots (0.25 g/L). Shown are mean values of duplicates, standard deviations are indicated as error bars. In cases where error bars are invisible, they are covered by the symbols. Corresponding fits with a desorption rate constant $k_{des} = 0.4 \text{ s}^{-1}$ are indicated as crosses with interpolated lines between the calculated data points

Table 2 shows the determined desorption rate constants for 15 test chemicals. Additionally, the corresponding partition coefficients (from literature [21] or estimated based on the physicochemical properties of the compound [20]) used for calculating equilibria and transport modelling are shown. All partition coefficients were corrected for the salting-out effect [28], because the salt content of the used buffer influences the partitioning of the chemicals. In some cases the published albumin-water partition coefficients were additionally adjusted (by 0.3 log units maximum) to fit our data. This adjustment lies within the typical range of accuracy of the methods by which the albumin-water partition coefficients were determined. One exception was naphthalene, whose albumin-water partition coefficient needed to be adjusted by about 0.5 log units.

Table 2: List of test chemicals with determined desorption rate constants (k_{des}) and corresponding albumin-water and PDMS-water partition coefficients ($K_{BSA/water}$ and $K_{PDMS/water}$, from literature or estimated based on the physicochemical properties of the compound).

test chemical	k_{des} [s^{-1}]	$\log K_{BSA/water}$ [L/L]	$\log K_{PDMS/water}$ [L/L]
1-nitrooctane	0.5	3.55	3.03
1-chlorooctane	0.6	3.50	4.40
1,8-dibromooctane	0.3	3.70	4.30
di- <i>n</i> -butylether	1.4	2.20	3.24
di- <i>n</i> -pentylether	0.9	2.92	3.85
<i>n</i> -propylbenzene	1.8	3.00	3.49
<i>n</i> -hexylbenzene	0.9	4.34	5.04
allylbenzene	1.6	3.10	2.98
1,4-dibromobenzene	0.3	3.60	3.49
1,2,4-trichlorobenzene	0.8	3.90	3.70
1,2,3,4-tetrachlorobenzene	0.4	4.11	4.11
naphthalene	1.4	3.90	2.78
phenanthrene	0.6	4.05	3.95
pyrene	0.6	4.90	4.20
chlorpyrifos	0.2	3.30	3.85

3.3. Discussion

3.3.1. Desorption from BSA and HSA

Rate constants for desorption of 15 neutral organic chemicals from albumin were determined. Initially, experiments were performed with both HSA and BSA to check for possible differences. These experiments showed no differences in desorption kinetics. Consequently, we assume that results from desorption experiments are transferable between the two species. Apart from our test with HSA and BSA, this assumption is also plausible in consideration of the similarities between the two proteins: both the amino acid sequence and the structure of the folded protein are very similar for HSA and BSA. The amino acid sequence homology between the two albumins is 76% [29], HSA consisting of 585 residues and BSA consisting of 583 residues [30]. Both amino acid chains are folded into three homologous domains, each domain consists of two subdomains [29, 31].

According to the literature, these structural similarities between the two albumin types may result in similar binding of chemicals to HSA and BSA: A recent study [32] suggested that albumin binding effects for many chemicals arise from the 3D structure of the molecule. In this study, binding for about 80 neutral and 40 ionic chemicals to albumin could be

explained by considering three-dimensional features but without discrimination between different binding sites. Based on the structural similarities between the both proteins and our own results from initial tests, we thus assume that the found desorption rate constants from BSA also describe desorption from HSA.

3.3.2. Comparison to published k_{des}

The here determined desorption rate constants varied from 0.2 s^{-1} for the lowest to 1.8 s^{-1} for the highest desorption rate constant. Thus, our results are in a similar range as the kinetic data published by Yoo, Chen and Rich [4, 7, 9, 10]. Chen and Rich investigated the desorption kinetics of warfarin from HSA. Rich used surface plasmon resonance spectroscopy with BIACORE for real time detection of the desorption process and determined a desorption rate constant of 1.2 s^{-1} at $37 \text{ }^\circ\text{C}$, Chen found desorption rate constants of 0.56 s^{-1} and 0.66 s^{-1} at $37 \text{ }^\circ\text{C}$ by using noncompetitive peak decay analysis in HSA-containing columns. Also applying a noncompetitive peak decay method, Yoo determined desorption rate constants from human serum albumin for twelve drugs ranging from 0.29 s^{-1} to 0.78 s^{-1} at $37 \text{ }^\circ\text{C}$. The fastest desorption rate constant with 3.96 s^{-1} was measured by Zheng [11] for desorption of chlorpromazine from HSA at $37 \text{ }^\circ\text{C}$ using ultrafast affinity extraction in a HSA microcolumn.

In contrast, Svenson, Faerch and Gray investigated the desorption kinetics of bilirubin from albumin and found desorption rate constants smaller than our smallest value by around one order of magnitude [5, 6, 8]. Svenson used partitioning between soluble and immobilized albumin in combination with spectrophotometry and determined 0.009 s^{-1} as desorption rate constant from HSA at $25 \text{ }^\circ\text{C}$. Faerch determined a desorption rate constant of 0.03 s^{-1} from BSA at $37 \text{ }^\circ\text{C}$ by an enzymatic degradation method.

Again using a spectrophotometrical method, Gray determined a desorption rate constant of 0.01 s^{-1} from HSA at $4 \text{ }^\circ\text{C}$. Bilirubin was extracted from the HSA sample by adding BSA, the kinetics were monitored in a stopped flow spectrometer by means of the different absorption spectra of the two complexes.

These dramatic differences between the desorption rate constants of bilirubin, independently measured by three groups with different methods, and the desorption rate constants of all the other chemicals that we and other groups measured raise questions about the plausibility of the different results. Reinvestigation of the chemicals used in the literature with the here presented time-resolved extraction method was not feasible, because PDMS is not a suitable extraction material for these chemicals. We thus checked if a

mechanistic consideration of the desorption process can provide an explanation for these differences.

3.3.3. Calibration of a prediction method based on a mechanistic concept

From a mechanistic point of view, the desorption process can be considered as a transport across a phase boundary. This transport requires diffusion within the albumin from the actual sorption sites to the water phase and diffusion across a stagnant water layer into the well-mixed water phase adjacent to the albumin. The detailed mathematical description of transport processes across phase boundaries can be found in the literature [33].

At the albumin-water interface, substance exchange is assumed to be immediate and concentrations are at equilibrium. Consequently, the concentration of the test chemical in water at the interface C_W^* and the concentration of the test chemical in albumin in the interface C_A^* always abide the albumin-water partition coefficient K_{AW} . The concentration of the test chemical in the bulk phases (C_A and C_W) may differ from the concentrations directly at the interface. This leads to substance fluxes J ($\text{mol cm}^{-2}\text{s}^{-1}$) across the stagnant layers, which can be described by Fick's first law:

$$J_{bulk\ albumin \rightarrow interface} = \frac{D_{alb}}{x_{alb}} * (C_A - C_A^*) \quad (9)$$

and

$$J_{interface \rightarrow bulk\ water} = \frac{D_{water}}{x_{water}} * (C_W^* - C_W) \quad (10)$$

Here, D_{alb} and D_{water} are the diffusion coefficients of the test chemical in albumin or in water and x_{alb} and x_{water} are the diffusion path lengths in the two phases. Neither the stagnant layers nor the interface are a sink for the test chemical. It thus follows from mass conservation that the two fluxes across the two stagnant layers have to be the same at any given time. Consequently, the flux across the complete phase boundary $J_{bulk\ albumin \rightarrow bulk\ water}$ is identical to the flux across each of the stagnant layers. Continuing with eq. (9) and substituting C_A^* gives:

$$J_{bulk\ albumin \rightarrow bulk\ water} = \frac{D_{alb}}{x_{alb}} * (C_A - K_{AW}C_W^*) \quad (11)$$

Equating (10) and (11) allows rearrangement for C_W^* :

$$C_W^* = \frac{\frac{D_{alb}}{x_{alb}} * C_A + \frac{D_{water}}{x_{water}} * C_W}{\frac{D_{alb}}{x_{alb}} * K_{AW} + \frac{D_{water}}{x_{water}}} \quad (12)$$

Substituting this in eq. (11) reveals the mechanistic meaning of k_{des} as the separate term, which is multiplied by the concentration gradient:

$$J_{bulk\ albumin \rightarrow bulk\ water} = \frac{1}{\frac{x_{water}}{D_{water}} * K_{AW} + \frac{x_{alb}}{D_{alb}}} * (C_A - C_W K_{AW}) \quad (13)$$

Equation (13) shows that k_{des} mechanistically corresponds to a permeability. Permeability is defined as the reciprocal of resistance. In this case, the total resistance for the flux from bulk albumin to bulk water consists of the individual transport resistances in albumin and in water. The term describing the transport resistance in water comprises the albumin-water partition coefficient as well as the diffusion coefficient and diffusion path length in water. The diffusion coefficients in water are very similar for all test chemicals. The partition coefficients, instead, differ by up to two orders of magnitudes for the chemicals tested here. Hence, one can expect that a correlation between the albumin-water partition coefficients and the desorption rate constants should be found, if the overall transfer process was dominated by the transport resistance in water. Fig. 8 shows that such a correlation does not exist.

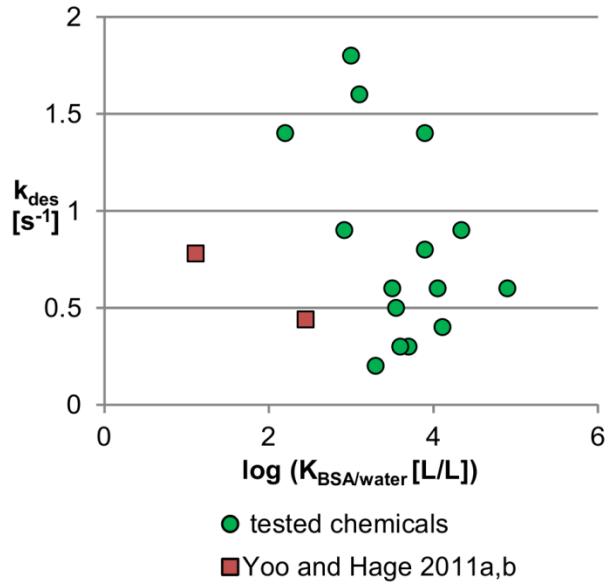


Fig. 8 Desorption rate constants k_{des} determined in this study (represented by green dots) and found in the literature (represented by red squares) versus the log of the corresponding albumin-water partition coefficients $K_{BSA/water}$

Note that the literature k_{des} values for ionic chemicals could not be included in this graph because no corresponding partition coefficients were available. According to the pKa of the chemicals [34] used in the literature, only two of these chemicals are present in their neutral forms at pH 7.40 (chloramphenicol and diazepam with the corresponding desorption rate constants $k_{des} = 0.78 \text{ s}^{-1}$ and $k_{des} = 0.44 \text{ s}^{-1}$ [9, 10]), those were included in Fig. 8. Thus we conclude that the transport resistance in water is not the limiting process for desorption kinetics.

Instead, the transport resistance in albumin, i.e. the diffusion coefficient, should be the dominating process. According to Fang [35], diffusion coefficients in polymers scale with $M^{-\alpha}$, where M is the molar mass of the compound and α is larger than one with an upper limit of ten. Consequently, one can expect that k_{des} should scale with the molar mass in the same way, if it was dominated by diffusion in albumin. And indeed, the desorption rate constants determined here scale exponentially with the molar mass (Fig. 9).

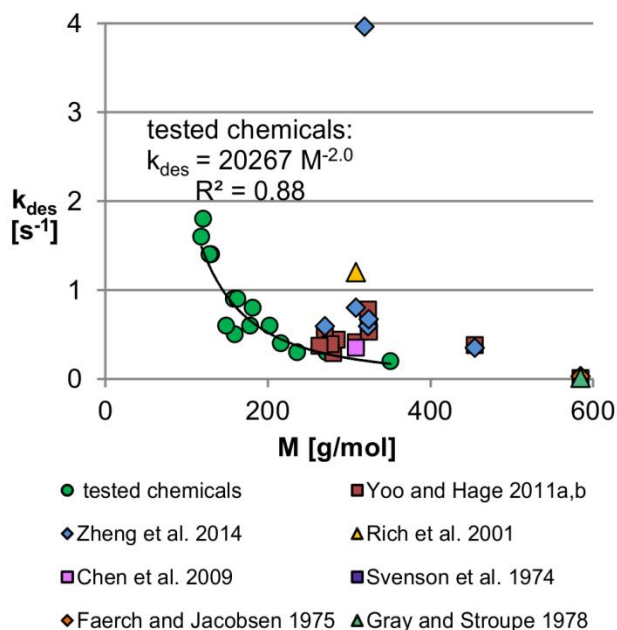


Fig. 9 Desorption rate constants k_{des} determined in this study (represented by green dots) and found in the literature (represented by colored symbols) versus the corresponding molar masses M . The solid line represents the fitted relationship between the desorption rate constants of our test chemicals and the molecular weights of the chemicals

The fitted relationship has the expected form with an exponent of -2:

$$k_{des} = 20267 * M^{-2.0} \quad (14)$$

Here, k_{des} refers to the desorption rate constant (s^{-1}) and M refers to the chemical's molar mass (g/mol).

Hence, the empirically found correlation between molecular weight and desorption rate constant is mechanistically very plausible. We conclude that this mechanistically based and empirically calibrated relationship enables prediction of desorption rate constants from albumin for various organic chemicals.

Fig. 9 also shows the literature values for k_{des} . Not all of these values fit to the observed correlation, but interestingly the extremely slow desorption rate constants for bilirubin, independently determined by Svenson, Faerch and Gray (determined $k_{des} = 0.009 \text{ s}^{-1}$, 0.03 s^{-1} and 0.01 s^{-1}), are roughly consistent with the correlation (calculated $k_{des} = 0.059 \text{ s}^{-1}$). We thus conclude that these extremely slow desorption rate constants are reliable and desorption rate constants ranging over a few orders of magnitude are plausible.

A possible explanation for the missing correlation for some of the other chemicals from the literature might be the different temperatures in the experiments. While the here presented experiments were performed at room temperature, some of the desorption rate constants in the literature were derived at $37 \text{ }^{\circ}\text{C}$. According to the paper from Svenson et al., a temperature increase from room temperature to $37 \text{ }^{\circ}\text{C}$ can lead to a two- to threefold faster desorption rate constant [8].

Another possible explanation for the missing correlation for some of the other chemicals from the literature might be an insufficient accuracy of the literature values due to some pitfalls in the used data evaluation: Common for all the studies is the assumption that the mass transfer kinetics removing the desorbed analyte from the freely dissolved state (i.e. extraction) is much faster than desorption of the analyte from albumin and, hence, equilibrium between the water phase and the extraction medium was assumed for evaluation of the experiments. This simplified scenario allows determination of the desorption rate constant from the slope of the semi logarithmic plot of the analyte concentration over sampling time. We suggest that this procedure is inaccurate: Although the extraction of the analyte from water is faster than desorption, the extraction kinetics still affects the resulting concentration profile. In fact, the desorbed analyte is not immediately removed from water and, therefore, affects the concentration gradient between the water phase and albumin. This results in a decelerated concentration decrease in the sample. Consequently, neglecting the extraction kinetics can lead to underestimation of desorption rate constants. To illustrate this statement, Fig. 10 shows how the derived k_{des} for one of our own test chemicals would differ, if extraction kinetics was neglected.

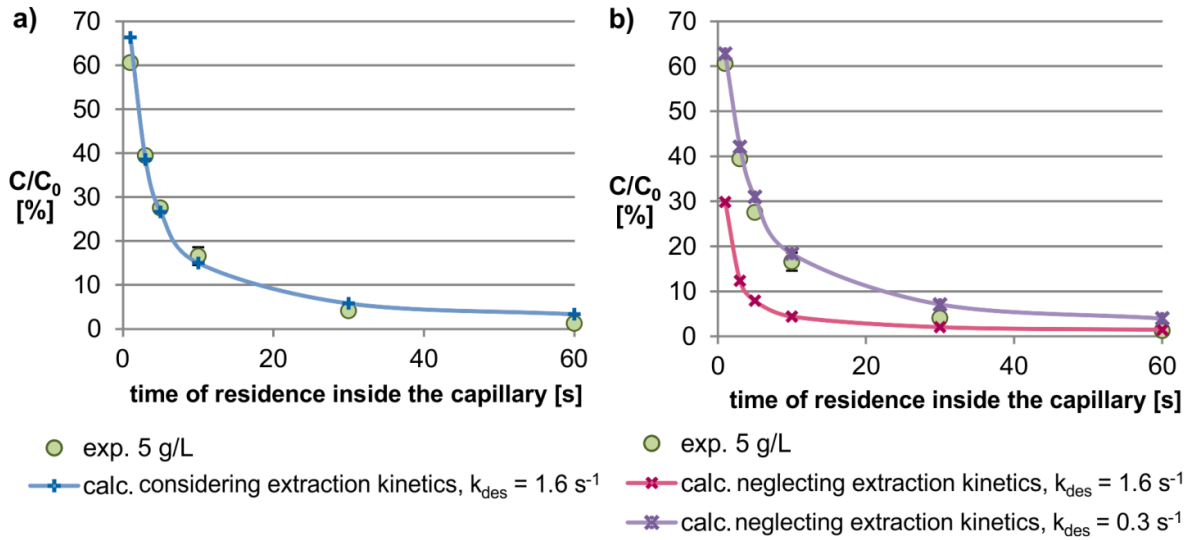


Fig. 10 Illustration how neglect of extraction kinetics affects the determined k_{des} using the example of allylbenzene extracted from BSA ($C = 5 \text{ g/L}$). Part a) shows the fit with $k_{des} = 1.6 \text{ s}^{-1}$ resulting from our data analysis procedure, which considers extraction kinetics of the freely dissolved allylbenzene into PDMS. Part b) shows calculation results when extraction kinetics are neglected. Neglecting extraction kinetics leads to an erroneously underestimated $k_{des} = 0.3 \text{ s}^{-1}$

Fig. 10a shows the results of our analysis procedure, which considers the extraction kinetics by using the extraction rate constant presented above ($k_{extr} = 2.7 \text{ s}^{-1}$). This procedure reveals the true desorption rate constant $k_{des} = 1.6 \text{ s}^{-1}$. Fig. 10b shows the results of an analysis procedure which neglects the extraction kinetics by assuming an extremely fast extraction rate constant ($k_{extr} = 1000 \text{ s}^{-1}$). This leads to an underestimated desorption rate constant $k_{des} = 0.3 \text{ s}^{-1}$. Using this second procedure, a slower desorption rate constant is erroneously needed to fit the same experimental data, because the decelerated concentration decrease due to the extraction kinetics is not taken into account. However, one has to note that this aspect is less important for slower desorption rate constants than for faster ones: If desorption occurs very slowly (compared to extraction), the extraction kinetics become less relevant for the overall transport kinetics, i.e. neglecting extraction kinetics distorts slower desorption rate constants less than faster ones.

Another pitfall of the simplified data analysis using linear regression of logarithmic concentration-time curves is that partition properties are neglected. If equilibrium between the extraction material and the sample is reached, the measured concentration profile will result in a plateau depending on the partition properties. Erroneously including parts of this plateau in the logarithmic plot from which the slope is to be determined leads to a lower slope again corresponding to an underestimation of the desorption rate constant. These

pitfalls might have decreased the accuracy of the published desorption rate constants. The more explicit data analysis presented here considers both the extraction kinetics from the water phase as well as the partition properties and thus avoids these pitfalls.

3.3.4. A first glance on physiological relevance of desorption kinetics from albumin

The determined k_{des} can now be used to estimate the impact of desorption kinetics on uptake and metabolism of chemicals in the human liver. For doing so, application of a suitable model representing the features of the physiological situation (residence time, diffusion distances, albumin concentration) is necessary. A rough idea on the importance of this process can, however, already be gained from a direct comparison of our experimental curves with the *in vivo* situation in a human: A residence time of 4 s, which corresponds to the typical residence time of blood in the sinusoids of the liver [2], was not sufficient for complete desorption of the test chemicals from albumin in our test system.

For a more accurate comparison, suitable calculations considering the following aspects are necessary:

- 1) dimensions of the liver sinusoids are different than dimensions in our capillary (average sinusoid diameter is only 7 – 9 μm [36]),
- 2) the albumin concentration present in blood is higher than in our experiments (physiological albumin concentration in plasma is around 40 g/L [37]),
- 3) the flow pattern might be different and
- 4) additional limitations due to blood flow or permeation into the hepatocytes are possible.

Smaller dimensions of the sinusoids lead to shorter diffusion path lengths, which results in a faster extraction into the surrounding hepatocytes. A higher albumin concentration leads to a higher albumin-bound fraction. Both a faster extraction and a higher albumin-bound fraction increase the importance of desorption kinetics for physiological scenarios compared to our experiments. The next chapter shows how these physiological features can be implemented into a suitable liver model to quantify the impact of desorption kinetics on hepatic metabolism.

4. Modelling the impact of desorption kinetics from albumin on hepatic metabolism

4.1. Calculations using a well-stirred liver model approach

4.1.1. Implementation of desorption kinetics into a well-stirred liver model

For mathematical quantification of hepatic metabolism, the liver is most commonly considered as a single well-stirred compartment. The well-stirred liver model is mathematically simpler than the parallel tube liver model and easier to apply. In the classical well-stirred liver model, all components of the liver, e.g. blood within the liver, blood transport proteins and hepatocytes, are assumed to be in instantaneous equilibrium with respect to the chemical [13]. Such a one-compartment model can represent blood flow limitation but it cannot represent limitations caused by slow desorption kinetics from transport proteins or slow permeation into the hepatocytes. It is thus desirable to modify the classical well-stirred liver model in a way that permeation and desorption can be considered while the simplicity of a well-stirred compartment model is kept. In order to incorporate desorption kinetics into the model one has to treat blood transport proteins as an additional compartment. If furthermore permeation kinetics are to be considered, a three-compartment model is needed where blood transport proteins, the rest of blood without transport proteins and hepatocytes represent three different well-stirred compartments.

For a quantitative understanding of the metabolic efficiency of the liver we then need to know the chemical concentrations in blood entering and leaving the liver for given boundary conditions. Under constant boundary conditions, i.e. constant blood flow and constant concentration in the inflowing blood as well as constant metabolic capacity and constant volumes of all system components, the liver will reach a steady-state situation. This means that the outflowing blood concentration does not change with time anymore. To derive an explicit solution for the steady-state extraction efficiency that covers the combined influence of blood flow rate, intrinsic metabolic capacity, permeation and desorption kinetics on the outflowing blood concentration, two mass balance approaches are combined: one for the freely dissolved concentration in blood and one for the bound concentration in blood entering and leaving the liver in a steady-state situation (Fig. 11).

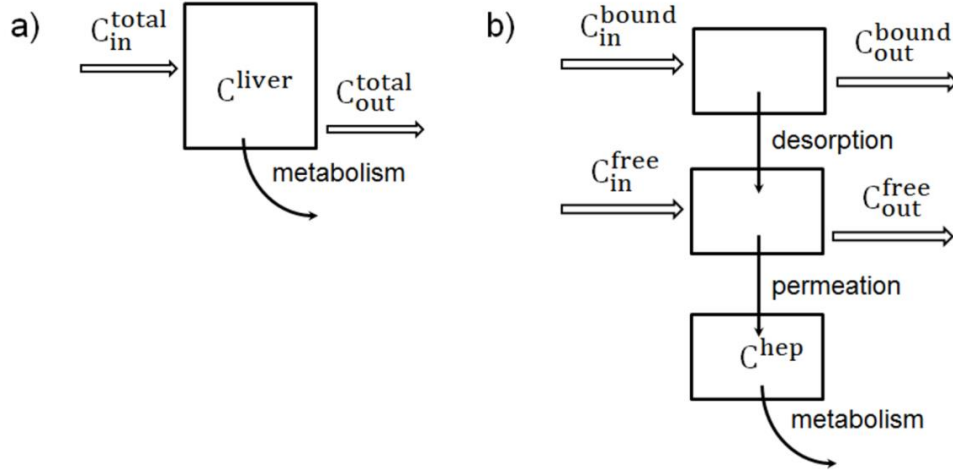


Fig. 11 Scheme of the classical well-stirred liver model (part a) and the here presented liver model, which considers the liver as an aggregation of three separate well-stirred sub-compartments (part b). Both models quantify the metabolic efficiency based on the chemical concentrations in blood entering and leaving the liver. The classical well-stirred liver model considers only blood flow limitation. The sub-compartmental model additionally considers desorption and permeation kinetics by differentiating freely dissolved and albumin-bound chemical concentration (C^{free} and C^{bound})

The difference between freely dissolved compound in the blood flowing in and out of liver equals the loss/gain due to permeation into/from the hepatocytes and the loss/gain due to sorptive exchange with the transport protein albumin, both expressed as first order (diffusion controlled) kinetic processes:

$$\begin{aligned}
 Q * C_{water} (C_{in}^{free} - C_{out}^{free}) \\
 &= P_{hep} * A * (C_{out}^{free} - C_{hep}^{free}) - k_{des} * V_{alb} \\
 &\quad * (C_{out}^{bound} - C_{out}^{free} * K_{AW})
 \end{aligned} \tag{15}$$

where Q is the volumetric blood flow rate (in mL_{blood}/s), C_{water} is the volume concentration of water in blood (in mL_{water}/mL_{blood}) and C_{in}^{free} and C_{out}^{free} are the freely dissolved concentrations of the compound in in- and outflowing blood (in mol/mL_{water}). P_{hep} is the total permeability between blood and hepatocytes (in cm/s), A is the exchange surface area between blood and hepatocytes (in cm²), C_{hep}^{free} is the freely dissolved concentration of the compound in the hepatocytes (in mol/mL_{water}), k_{des} is the desorption rate constant (in s⁻¹), V_{alb} is the albumin volume (in mL_{alb}), C_{out}^{bound} is the albumin bound concentration of the compound in blood (in mol/mL_{albumin}) and K_{AW} is the albumin-water partition coefficient (mL_{alb}/mL_{water}) of the studied compound. The albumin-water partition coefficient is a measure for the partition properties of a compound and is used here as an alternative to the

association constant K_a (in L/mol). Both constants can be converted into each other via the molar mass and the density of albumin, for detailed explanation we refer to appendix of [21]. Using the albumin-water partition coefficient is more convenient for the here presented mass balance approach.

Information on the intrinsic metabolic capacity of the hepatocytes is implicitly contained in this mass balance approach, because the freely dissolved concentration of the compound in the hepatocytes of course depends on metabolism. The detailed mathematic formulation of the metabolism term is derived from the fact that, in case of steady state, the mass of compound metabolized per unit time in the hepatocytes equals the mass that permeates into the hepatocytes per unit time:

$$P_{hep} * A * (C_{out}^{free} - C_{hep}^{free}) = k_{int} * V_{hep}^{total} * C_{hep}^{total} \quad (16)$$

In this approach, we express the metabolic capacity by the intrinsic metabolism rate constant k_{int} with the unit s^{-1} that multiplies with the total compound concentration in the hepatocytes C_{hep}^{total} (in mol/mL_{hepatocytes}) and the total hepatocyte volume V_{hep}^{total} (in mL_{hepatocytes}) to yield the metabolism rate. An alternative parameter for the intrinsic metabolic capacity is the intrinsic clearance, which corresponds to the volume that is cleared from the chemical by metabolism per time unit. Both parameters can be used for quantification of metabolism as long as both are used in a consistent way throughout the entire formalism.

The second mass balance approach considers the sorbed concentrations. The difference between compound flowing in and out of the liver blood pool in the sorbed state equals the loss due to the kinetic desorption process within the liver blood pool. The desorption process is driven by the difference between the actual sorbed concentration C^{bound} (which equals C_{out}^{bound} in a well-stirred hepatic blood pool) and the hypothetical sorbed concentration that is expected under equilibrium conditions, $C^{free} * K_{AW}$ (which equals $C_{out}^{free} * K_{AW}$ in a well-stirred hepatic blood pool):

$$Q * C_{alb} (C_{in}^{bound} - C_{out}^{bound}) = k_{des} * V_{alb} * (C_{out}^{bound} - C_{out}^{free} * K_{AW}) \quad (17)$$

Here, Q again is the volumetric blood flow rate (in mL_{blood}/s), C_{alb} is the volume concentration of albumin in blood (in mL_{alb}/mL_{blood}) and C_{in}^{bound} and C_{out}^{bound} are the albumin bound concentrations of the compound in in- and outflowing blood (in mol/mL_{alb}).

Rearrangement of the two equations allows calculation of the extraction efficiencies E^f and E^b for the freely dissolved and the sorbed concentrations, respectively (see appendix A for details):

$$E^f = \frac{P_{hep}A \left(1 - \frac{P_{hep}A}{k_{int}V_{hep}^{total}K_{hep/water} + P_{hep}A} \right) - \frac{k_{des}V_{alb}(QC_{alb}K_{AW} + k_{des}V_{alb}K_{AW})}{k_{des}V_{alb} + Q C_{alb}} + k_{des}V_{alb}K_{AW}}{QC_{water} + P_{hep}A \left(1 - \frac{P_{hep}A}{k_{int}V_{hep}^{total}K_{hep/water} + P_{hep}A} \right) + k_{des}V_{alb} \left(\frac{-k_{des}V_{alb}K_{AW}}{k_{des}V_{alb} + Q C_{alb}} + K_{AW} \right)} \quad (18)$$

and

$$E^b = \frac{k_{des}V_{alb} - k_{des}V_{alb}(1 - E^f)}{Q C_{alb} + k_{des}V_{alb}} \quad (19)$$

By this, eq. (18) and eq. (19) are the explicit solutions for the here presented modified well-stirred liver model that allows consideration of desorption kinetics. These two extraction efficiencies E^f and E^b can be combined so that the total extraction efficiency E can be calculated according to:

$$E = f_u E^f + f_b E^b \quad (20)$$

Here, f_u refers to the freely dissolved fraction of the compound in blood and f_b refers to the albumin-bound fraction in blood. The freely dissolved fraction f_u of a chemical can be derived from the albumin-water partition coefficient according to:

$$f_u = \frac{1}{\left(1 + K_{AW} * \frac{V_{alb}}{V_{water}} \right)} \quad (21)$$

The albumin-bound fraction in blood can then be derived from $f_b = 1 - f_u$.

The hepatic clearance Cl_h can be calculated from the total extraction efficiency according to:

$$Cl_h = Q * E \quad (22)$$

For a fixed blood flow rate Q , the hepatic clearance changes proportional to the total extraction efficiency. For the following discussion all calculations were made based on the same input value for a typical physiological liver blood flow rate and the discussion will focus on resulting changes of the extraction efficiency when different desorption rate constants are used.

4.1.2. Physiological input data

For our goal to investigate the effect of desorption kinetics on the extraction efficiency, we need to select realistic parameter values. These include physiological blood flow rates in the sinusoids of the human liver, permeability from the sinusoids into the hepatocytes, exchange

area between the sinusoids and hepatocytes, desorption rate constants from albumin, metabolism rate constants, equilibrium partition coefficients to albumin and the hepatocytes, the albumin concentration in the blood and the volumes of hepatocytes and blood that is in direct exchange with the hepatocytes.

In the literature, different values for physiological liver blood flow rates in human exist, ranging from 900 to 1700 mL/min [38]. The permeability is not the focus of this work, we thus used permeabilities sufficiently high to avoid a potential limitation due to slow permeation. Desorption rate constants were varied in the range of published experimental values (k_{des} ranging from 2 to 0.02 s⁻¹) [5, 6, 8, 39]. Metabolism rate constants were varied such that the resulting extraction efficiencies range from low values up to 0.9, which appears to be the relevant range. For the equilibrium partitioning towards albumin, we covered a broad range of albumin-water partition coefficients (K_{AW} ranging from 1 to 100000 mL_{alb}/mL_{water}). This range was chosen to include weakly sorbing compounds which are preferably present freely dissolved in blood, i.e. the freely dissolved fraction f_u of these compounds approaches the value 1, as well as strongly sorbing compounds which are preferably bound to albumin, i.e. the freely dissolved fraction f_u approaches the value 0. The freely dissolved fractions were calculated from the used albumin-water partition coefficients according to equation (21). Another required input information is the equilibrium partitioning towards the hepatocytes, i.e. the hepatocyte-water partition coefficient of the compounds. For neutral organic compounds, it is intuitive that the partition behaviour towards the hepatocytes should roughly correlate with the partition behaviour towards albumin. Indeed, the hepatocyte-water partition coefficient can be deduced from combining the contributions from protein, lipid and water of the hepatocytes to the overall sorption to hepatocytes [40] (see appendix B for example calculations). We, therefore, decided that it made sense to not vary both partition coefficients independently from each other but to derive the hepatocyte-water partition coefficient from the albumin-water partition coefficient via a plausible empirical relationship (see appendix B).

Hepatic elimination of course depends on the quantity of metabolic active cells. It is known from the literature that roughly 30% of the liver volume are blood [41]. It thus follows that 70% of the liver volume are liver cells and among these 65% [42] are assumed to be hepatocytes. Assuming a liver volume of 1.4 L (experimental values ranging from 1.1 – 1.7 L [38, 43, 44]), the volume of hepatocytes thus corresponds to about 660 mL. To correctly consider permeation and desorption, we also need to quantify the blood volume that exchanges compounds with the hepatocytes, i.e. the sinusoidal blood volume. This information is difficult to estimate and according to our knowledge only two values are

available in the literature. These correspond to 250 mL and 170 mL for our assumed liver volume. At the same time, existing experimental values for blood flow velocities in sinusoids range from 0.02 cm/s to 0.28 cm/s with a mean of 0.1 cm/s [45] and the sinusoidal length is known to be about 400–500 μm [46]. These values should actually be consistent with the published liver blood flow rates and sinusoidal volumes and thus offer a possibility to check if the used values are sensible. Blood flow rate Q combined with sinusoidal volume V as well as flow velocity v combined with the sinusoid length l can both be used to calculate the residence time of blood in the sinusoids. Accordingly, the following relationship for these four parameters can be formulated:

$$\frac{V}{Q} = \frac{l}{v} \quad (23)$$

Rearrangement of equation (23) gives the following expression for the blood flow rate Q :

$$Q = \frac{V}{l} * v \quad (24)$$

Combining an assumed sinusoidal volume of 200 mL with a sinusoid length of 500 μm and a flow velocity of 0.1 cm/s gives a blood flow rate of 24000 mL/min. This calculated blood flow rate greatly exceeds the experimental values found in the literature and is not realistic in a physiological sense. If we assume that the reported blood flow rate is accurate, than one or several of the other physiological parameters (sinusoidal volume, sinusoid length or flow velocity) need to be adjusted so that a consistent data set is achieved. We assume that, among these, the sinusoid length is the best characterized parameter. In our opinion, only small deviations due to the three-dimensional arrangement of the sinusoids are conceivable so that we correct the sinusoid length by no more than 100 μm from 500 μm to 600 μm . For the flow velocities inside the sinusoids, we suggest that the measured range should not be exceeded because the optical methods [45] used for the measurement should actually be quite reliable. Thus we suggest to use a value of 0.03 cm/s, which is at the lower end of the range Puhl et al. measured [45]. This value is also given in anatomical textbooks as a common value for blood flow velocities in capillaries [47]. Consequently, the last parameter, which remains to be adjusted is the sinusoidal volume. Indeed, it follows that the sinusoidal volume needs to be set to 50 mL – much lower than reported – when combination of the sinusoid length of 600 μm and flow velocity of 0.03 cm/s shall yield sensible results for the blood flow rate. With these numbers the calculated blood flow rate is 1500 mL/min, which is within the range of published experimental blood flow rates.

Accordingly we consider these values for sinusoid length, flow velocity and sinusoid volume as internally consistent and physiologically realistic.

The last required input information is the albumin concentration in blood. The concentration of serum albumin in human plasma is about 40 g/L [37]. Considering that approximately 60% of the total blood volume is plasma [48], it follows that the albumin concentration in blood is 24 g/L. For our calculations we assume that albumin is the only sorbing component in blood.

4.2. Calculations using a parallel tube liver model approach

4.2.1. Implementation of desorption kinetics into a parallel tube liver model

Another frequently used model for hepatic metabolism is the parallel tube liver model. In the parallel tube liver model, the liver is considered as an aggregation of identical cylindrical tubes surrounded by hepatocytes with a concentration gradient along the tubes. The parallel tube model is thus a more realistic representation of the physiological situation than the well-stirred model but at the same time it is mathematically more complex. The most simplistic version of the parallel tube liver model assumes instantaneous equilibrium between blood and hepatocytes at any point of the tube. However, with this simplistic version consideration of desorption kinetics and permeation kinetics is not possible. To include the effects of desorption and permeation, the model has to include a first order desorption kinetics and a first order permeation kinetics at any point of the tube.

The desired model thus has to discriminate albumin, aqueous blood and hepatocytes as separate compartments and needs to be discretized spatially along flow direction to represent the developing concentration gradient. In principle, these properties are already implemented in the transport model that was developed for data analysis of the desorption kinetics experiments. Accordingly, the developed transport model served as an optimal basis for the development of the parallel tube liver model. The existing transport model considers convective and dispersive transport of bound and unbound compound through the capillary, compound flux from the bound to the unbound state by a first order desorption kinetics and extraction of unbound compound into the extraction material of the capillary by a first order extraction kinetics. These three transport processes are also required in a parallel tube liver model to represent transport via blood flow, desorption from albumin and permeation into the hepatocytes. The only required modification to refine the existing transport model into a parallel tube liver model is the implementation of a metabolism term.

In the final parallel tube liver model, one tube (representing one liver sinusoid) is discretized into 100 sections along flow direction. Each section consists of separate compartments for the unbound compound concentration, bound compound concentration, compound concentration in the hepatocytes and albumin concentration in blood. Each of these compartments in one section was assumed as well-mixed. To calculate the compound concentration change in blood during passage through the tube, the contributions of each kinetic process to the overall concentration change are calculated for each spatial section and each time increment. The discretization in time is 0.0001 s. The transport of bound and unbound compound as well as of albumin itself via blood flow is represented by a convection-dispersion equation:

$$J = -A_{flow} D \frac{\partial C}{\partial x} + v A C \quad (25)$$

The flux J (mol/s) is given by the cross-sectional area A_{flow} (cm²), the dispersion coefficient D (cm²/s), the path length x (cm) and the convective velocity v (cm/s). C refers to the concentration of either bound compound, unbound compound or albumin.

The compound flux J (mol/s) from the albumin-bound state into the freely dissolved state is described by a first order desorption kinetics:

$$J = -k_{des} * V_{alb} * (C^{bound} - C^{free} * K_{AW}) \quad (26)$$

where k_{des} refers to the desorption rate constant (s⁻¹) and V_{alb} to the albumin volume (mL_{albumin}), C^{bound} and C^{free} are the unbound and bound concentrations of the chemical (mol/mL_{albumin} and mol/mL_{water}) in blood and K_{AW} is the albumin-water partition coefficient (mL_{alb}/mL_{water}).

Analogously, the compound flux (mol/s) from the freely dissolved state into the hepatocytes is represented by a first order permeation kinetics:

$$J = -P_{hep} * A * (C^{free} - C_{hep}^{free}) \quad (27)$$

Here, P_{hep} is the permeability between blood and hepatocytes (in cm/s), A is the exchange surface area between blood and hepatocytes (in cm²), C^{free} again is the unbound concentration of the chemical (mol/mL_{water}) in blood and C_{hep}^{free} is the unbound concentration of the compound in the hepatocytes (in mol/mL_{water}).

As the last required kinetic process, the compound elimination via metabolism is considered by a first order metabolism kinetics:

$$J = k_{int} * V_{hep}^{total} * C_{hep}^{total} \quad (28)$$

Here the compound flux or, more precisely, the metabolism rate (mol/s) is given by the intrinsic metabolism rate constant k_{int} (s^{-1}), the total compound concentration in the hepatocytes C_{hep}^{total} (mol/mL_{hepatocytes}) and the total hepatocyte volume V_{hep}^{total} (in mL_{hepatocytes}).

Derivation of an explicit solution is not possible for the parallel tube model. Instead the equations were solved numerically via implementation into a visual basic script, which conducted the computations in MS excel. For determination of total extraction efficiency, the change of bound and unbound compound concentration in outflowing blood was modelled until steady-state condition was reached, i.e. until the compound concentration in outflowing blood remained constant. The total extraction efficiency was then calculated as follows:

$$E = \frac{C_{in}^{total} - C_{out}^{total}}{C_{in}^{total}} \quad (29)$$

In this equation, C^{total} (mol/mL_{blood}) refers to the total concentration of the compound in inflowing or outflowing blood and can be calculated from $\frac{C^{free}V_{free} + C^{bound}V_{alb}}{V_{sinusoid}^{total}}$, C^{bound} and C^{free} are the unbound and bound concentrations of the chemical (mol/mL_{albumin} and mol/mL_{water}) in inflowing or in outflowing blood, V_{free} is the water volume in sinusoid blood (mL_{water}), V_{alb} is the albumin volume in sinusoid blood (mL_{albumin}) and $V_{sinusoid}^{total}$ is the total sinusoid blood volume (mL_{blood}).

4.2.2. Physiological input data

In chapter 4.1.2, a collection of physiologically sensible values for liver blood flow rates, dimensions of sinusoids, albumin concentration in blood, permeability and metabolism was presented for application of the modified well-stirred liver model. The same values are now used for the here presented parallel tube liver model to enable direct comparison of the results of both models.

Accordingly, we again use two different metabolism rate constants ($0.01 s^{-1}$ and $0.001 s^{-1}$) and vary the desorption rate constants from $0.02 s^{-1}$ to $20 s^{-1}$. In this range, $0.02 s^{-1}$ is the lower limit of known desorption rate constants and $20 s^{-1}$ represents a scenario where no desorption limitation occurs. The permeability again is set to high values that cause no limitations, because this work shall focus exclusively on limitations caused by slow desorption. The required information on the equilibrium partitioning towards the hepatocytes is derived from albumin-water partition coefficients as described above (chapter 4.1.2.) and

the used albumin-water partition coefficients K_{AW} again range from 1 to 100000 mL_{alb}/mL_{water}. The albumin concentration in blood of 24 g/L is derived from the known concentration of serum albumin in human plasma of 40 g/L [37] and the fact that 60% of the total blood volume is plasma [48]. Consistent to the calculations with the modified well-stirred liver model, a blood flow velocity in the sinusoids of 0.03 cm/s and a sinusoid length of 600 μ m is used.

Apart from these parameters, that were required in exactly the same form in our modified well-stirred liver model, there are a few additional parameters that are exclusively needed in the here presented parallel tube model. These differences in parametrization arise from the fact that the modified well-stirred liver model described the whole liver whereas the parallel tube model describes one single sinusoid. Nevertheless the extraction efficiency calculated with the parallel tube liver model also represents that of the entire liver. The reason for this is that extraction efficiency is a relative value derived from the steady-state blood concentrations that have to be the same in the entire liver when all sinusoids are assumed to be identical. The additional parameters needed in the parallel tube model are the flow cross section of one sinusoid, the volume of one sinusoid and the volume of hepatocytes surrounding one sinusoid. The flow cross section of one sinusoid can be calculated from the sinusoid diameter. According to Wake et al., the sinusoid diameter is 9 μ m [36] and accordingly a flow cross section of $8.7 \cdot 10^{-6}$ cm² results. Combining the sinusoid diameter with the sinusoid length, a sinusoid volume of $3.8 \cdot 10^{-8}$ mL can be calculated. To ensure consistency between the modified well-stirred liver model and the model used here, the ratio between volume of one sinusoid and the volume of hepatocytes surrounding one sinusoid is kept equal to the ratio between total sinusoidal blood volume and total hepatocyte volume. In the modified well-stirred model, we had a total sinusoidal blood volume of 50 mL for a total hepatocyte volume of about 660 mL. Accordingly, for one single sinusoid with a volume of $3.8 \cdot 10^{-8}$ mL a corresponding hepatocyte volume of $4.9 \cdot 10^{-7}$ mL results.

4.3. Comparison of the results of both liver models

4.3.1. Partition properties of the compound affect E

Before starting to quantify the influence of desorption kinetics on the total extraction efficiency of a compound, a few characteristics resulting from the partition properties of the compound need to be considered, because the impact of desorption kinetics will always be related to the impact of partition properties. To evaluate the sole impact of the partition

properties on extraction efficiency and clearance of a compound, a simplified scenario in which desorption and permeation kinetics are set to sufficiently high values so that no limitations result ($k_{des} = 20 \text{ s}^{-1}$, $P_{hep} = 1000 \text{ cm/s}$) was modelled first.

For the calculation of this simplified scenario, different albumin-water partition coefficients, which dictate the freely dissolved fractions f_u in blood and which are a measure of a compound's partition properties, are combined with three different k_{int} and the resulting total extraction efficiencies are compared. Fig. 12 shows the resulting total extraction efficiencies, calculated either with the well-stirred or with the parallel tube modelling approach. For all calculations physiological blood flow rates were used.

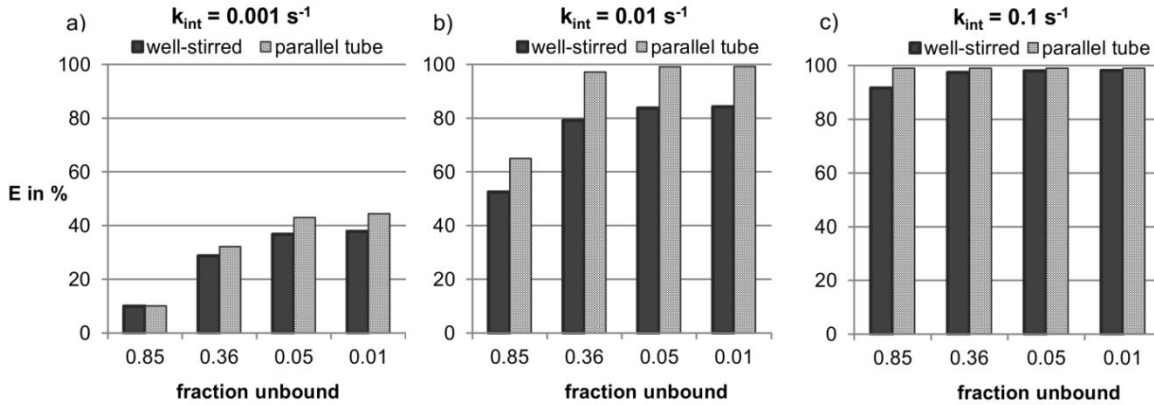


Fig. 12 Extraction efficiencies calculated either with the well-stirred modelling approach or with the parallel tube modelling approach as a function of the freely dissolved fraction f_u in blood and the metabolism rate constant k_{int} when desorption kinetics are very fast ($k_{des} = 20 \text{ s}^{-1}$). Permeation kinetics are set such that no limitation ($P_{hep} = 1000 \text{ cm/s}$) occurs.

A first comparison of the panels a, b and c shows that higher k_{int} of course lead to higher extraction efficiencies, because metabolism becomes faster. Combination of one k_{int} with different albumin-water partition coefficients and thus different freely dissolved fractions in blood leads to different total extraction efficiencies. In fact, the extraction efficiencies increase with decreasing freely dissolved fractions of the compounds. This observation might seem counter-intuitive at first. For its explanation, however, one can go back to the simplest approach for calculation of hepatic extraction efficiency based on the work of Rowland:

$$E = \frac{k_{liver} V_{liver} K_{liver/blood}}{Q + k_{liver} V_{liver} K_{liver/blood}} \quad (30)$$

This approach considers neither desorption kinetics nor permeation kinetics and is thus equivalent to the simplified scenario calculated above. Rowland's equation combines the

metabolism rate constant of the liver k_{liver} (in s^{-1}) with the volume of the liver V_{liver} (in mL_{liver}), the liver-blood partition coefficient $K_{liver/blood}$ (in mL_{blood}/mL_{liver}) and the liver blood flow rate Q (in mL_{blood}/h) to yield the hepatic extraction efficiency E .

The observation of increasing extraction efficiency with decreasing freely dissolved fraction can be explained as follows: A decreasing freely dissolved compound fraction in blood corresponds to a stronger partitioning towards albumin in blood. Compounds that show stronger partitioning towards albumin will also show stronger partitioning towards the liver, because liver and blood both consist of a non-sorbing aqueous portion and a sorbing non-aqueous portion and the sorbing portion of the liver is bigger than that of blood due to a higher protein and lipid content. The value of the liver-blood partition coefficient depends on the relative contributions of these different portions to overall sorption. The liver-blood partition coefficient thus increases with increasing sorbing character of the compound, and in eq. (30) it can be seen that an increased liver-blood partition coefficient leads to a higher extraction efficiency. However, the increase of the liver-blood partition coefficient is not unlimited but approaches a certain maximum. When sorption to the non-aqueous portion dominates the overall sorption, the value of the liver-blood partition coefficient is determined by the ratio of the non-aqueous portions of liver and blood and the upper limit of the liver-blood partition coefficient is reached. This issue is illustrated by panel a: While a decrease in the freely dissolved fraction from 0.85 to 0.05 leads to an increase of the calculated extraction efficiency by roughly 30%, a further decrease of the freely dissolved fraction to 0.01 leads only to minimal changes in extraction efficiency.

Furthermore, the extent to which the partition properties affect extraction efficiency is also dependent on the intrinsic metabolism rate constants themselves. High k_{int} reduce the relative impact of the partition properties on E , because metabolism is so fast that nearly everything that is delivered via blood flow is metabolized and the total extraction efficiency approaches the value of 100% (see panel c). In contrast, in case of very low k_{int} , the compounds would be removed out of the liver by blood flow faster than they can be metabolized and the total extraction efficiency would approach 0% regardless of the different partition properties.

Fig. 12 also shows that the results of the well-stirred modelling approach and the parallel tube modelling approach are similar, the differences in the calculated extraction efficiencies do not exceed 20%. The highest discrepancies between both models occur for the medium k_{int} , for the lowest and the highest k_{int} the differences between the calculated extraction efficiencies are smaller than 10%. The reason for this becomes obvious when one

simultaneously considers the values of the corresponding extraction efficiencies: The lowest k_{int} leads to rather low extraction efficiencies (panel a, $E < 50\%$). These low extraction efficiencies correspond to small concentration differences between inflowing and outflowing blood. In this case, the results of the parallel tube model, that explicitly considers the gradient along a sinusoid resulting from that concentration difference, approach the results of the well-stirred model that neglects the concentration gradient. In contrast, for the highest k_{int} the extraction efficiencies calculated with both models approach the maximum value of 100% and thus the results of both models converge.

4.3.2. Slow desorption can reduce E significantly

After realizing how the partition properties influence E , the influence of desorption kinetics on E is evaluated. For doing so, an intrinsic metabolism rate constant of $k_{int} = 0.01 \text{ s}^{-1}$ is used at first, because this k_{int} leads to total extraction efficiencies in the desired range (Fig. 12). For evaluation of the impact of desorption kinetics, the desorption rate constants were reduced stepwise from a value that has no impact on the total extraction efficiency in our scenarios ($k_{des} = 20 \text{ s}^{-1}$) to the lowest value that has been published in the literature ($k_{des} = 0.02 \text{ s}^{-1}$) and results were compared. Permeability again is set to a high value causing no limitation ($P_{hep} = 1000 \text{ cm/s}$). Fig. 13 summarizes the results of these calculations.

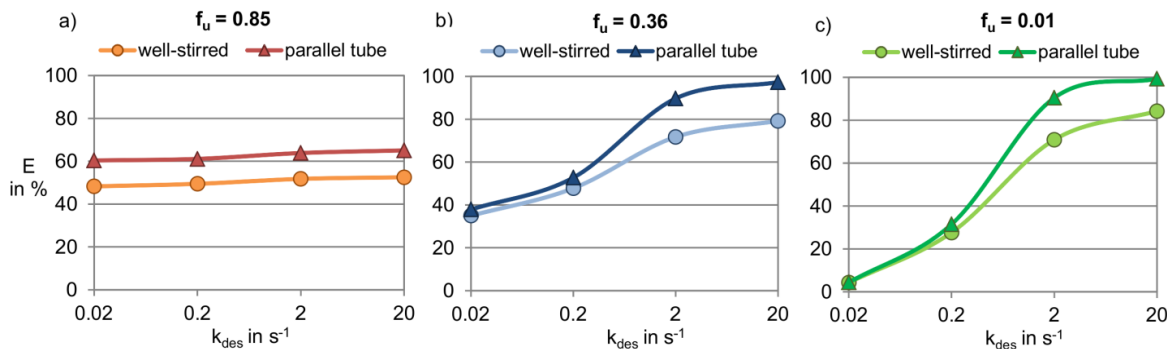


Fig. 13 Calculated extraction efficiencies for different desorption rate constants k_{des} and different freely dissolved fractions f_u . In this example, a metabolism rate constant $k_{int} = 0.01 \text{ s}^{-1}$, a high permeability $P_{hep} = 1000 \text{ cm/s}$ and physiological blood flow rates were used

It is intuitive that desorption kinetics have no impact on the total extraction efficiencies of weakly sorbing compounds, because the biggest fraction of these compounds is present freely dissolved in blood instead of bound to albumin. Weakly sorbing compounds are represented by panel a ($f_u = 0.85$) in Fig. 13 and show almost identical extraction efficiencies over the entire range of used k_{des} values.

With increasing sorbing character of the compound, the impact of desorption kinetics on the total extraction efficiencies grows, because the fraction bound to albumin in blood increases and only this fraction is sensitive to a potential desorption limitation. For moderately sorbing compounds ($f_u = 0.36$), represented by panel b, this leads to a reduction of total extraction efficiencies by factor 2 from more than 80% for non-limiting k_{des} to roughly 40% for the lowest k_{des} .

Strongly sorbing compounds ($f_u = 0.01$) are represented by panel c in Fig. 13. The total extraction efficiencies of these compounds are reduced by factor 20 from more than 80% for non-limiting k_{des} to 4% for the lowest k_{des} .

When comparing the differences between the both modelling approaches, one notices that the discrepancies again do not exceed 20%. For weakly sorbing compounds, the differences between the both models are even smaller than 10%. These differences stay similar over the whole range of tested k_{des} . For the moderately to strongly sorbing compounds, in contrast, the differences between both models are biggest for the non-limiting k_{des} , but the modelling results of both models converge with increasing desorption limitation. For these compounds, the compound concentration in the aqueous compartment of blood is smaller than for the weakly sorbing compounds. Accordingly, less chemical permeates into the hepatocytes and less chemical is metabolized. By this, the concentration gradient developing during sinusoid passage is also smaller and the results of the parallel tube model

approach those of the well-stirred model. However, when desorption is fast and the aqueous compartment of blood is restocked quickly with the compound due to quick desorption, more chemical can be metabolized and accordingly a bigger concentration gradient develops. This is the explanation why the discrepancies between both models change for moderately to strongly sorbing compounds depending on k_{des} .

4.3.3. Fast metabolism is a prerequisite for relevance of desorption kinetics

Apart from the partition properties of the compound, the metabolism itself is a second important determinant for the impact of desorption kinetics on E . It is intuitive that desorption kinetics become less important in case metabolism is very slow. Fig. 14 illustrates this statement. In this example, the used k_{des} comprise the same range as in Fig. 13. The intrinsic metabolism rate constant, however, is reduced to $k_{int} = 0.001 \text{ s}^{-1}$. We again exclude permeation limitation by setting permeability to a high value ($P_{hep} = 1000 \text{ cm/s}$) and use the physiological blood flow rate.

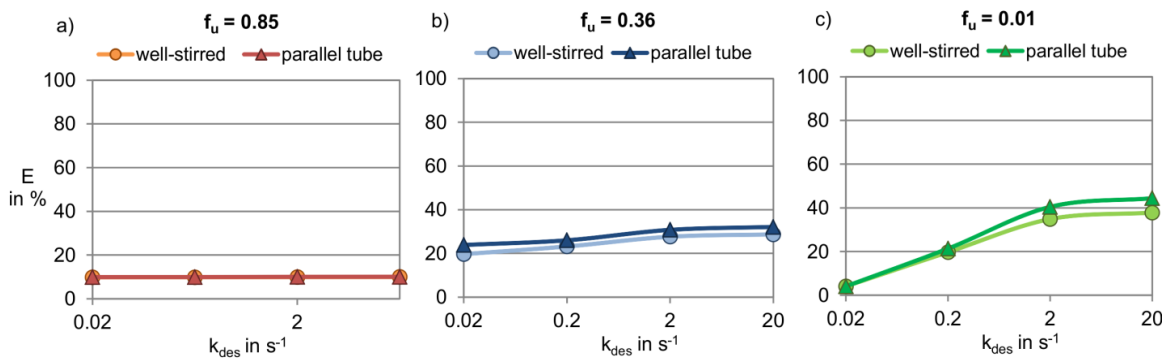


Fig. 14 Calculated extraction efficiencies for different desorption rate constants k_{des} and different freely dissolved fractions f_u . For these calculations, a lower metabolism rate constant of $k_{int} = 0.001 \text{ s}^{-1}$ is used, while permeability ($P_{hep} = 1000 \text{ cm/s}$) and blood flow rate are identical

The total extraction efficiencies are now generally lower than before, because the used metabolism rate constant $k_{int} = 0.001 \text{ s}^{-1}$ is smaller. Introducing desorption limitation by reducing k_{des} from 20 s^{-1} to 0.02 s^{-1} again has nearly no influence on the extraction efficiencies of weakly sorbing compounds, i.e. the data points are on the same level for the entire range of k_{des} . For moderately to strongly sorbing compounds, the total extraction efficiency again reduces as desorption limitation is introduced. This effect, however, is now lower than before: Instead of a reduction by a factor 20 that was observed with the faster metabolism rate constant for strongly sorbing compounds, the extraction efficiencies are now reduced by a factor 10 from roughly 40% to 4%.

4.4. Discussion

The calculations show that slow desorption from albumin is only relevant for hepatic metabolism of strongly sorbing compounds that are metabolized sufficiently fast in hepatocytes. For these compounds, the hepatic extraction efficiency and accordingly the hepatic clearance decrease with decreasing desorption rate constant k_{des} . The extent of this decrease depends not only on the value of k_{des} but also on the intrinsic metabolism rate constant and the partition properties of the compound.

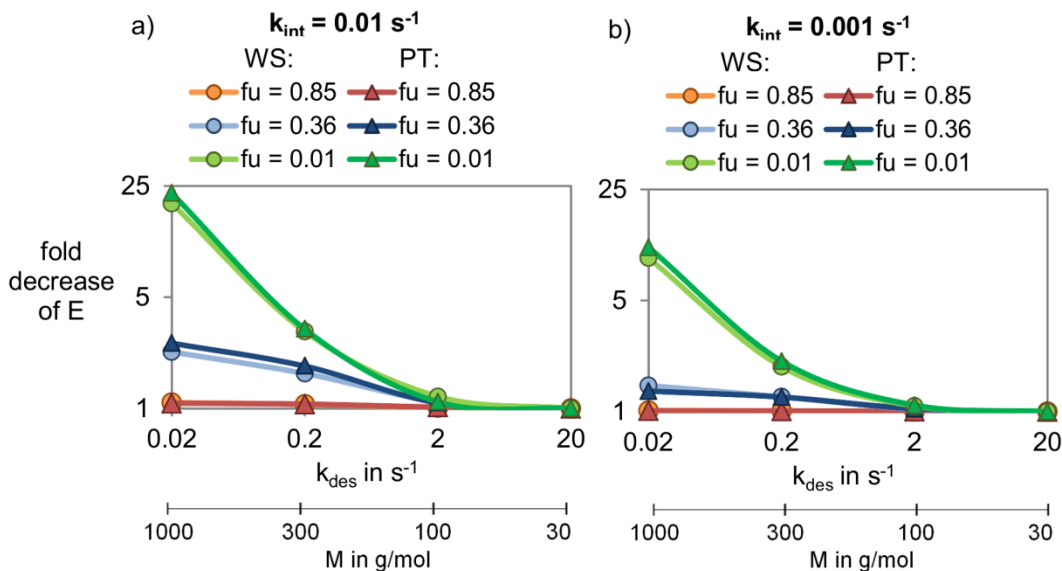


Fig. 15 Summary as to how the total extraction efficiencies E decrease depending on the value of the desorption rate constant k_{des} and the freely dissolved fraction f_u . Part a) shows the results for the fast metabolism rate constant $k_{int} = 0.01 \text{ s}^{-1}$, part b) shows the results in case of the slower metabolism with $k_{int} = 0.001 \text{ s}^{-1}$. Again a high permeability $P_{hep} = 1000 \text{ cm/s}$ and physiological blood flow rates were used. The exponential relationship between the molar mass M of a chemical and its desorption rate constant is indicated by the second x-axis

Fig. 15 sums up these findings by comparing the fold decrease of E when the same desorption rate constants are combined with different intrinsic metabolism rate constants and different freely dissolved fractions: Panel a) represents the calculations with $k_{int} = 0.01 \text{ s}^{-1}$ and panel b) represents the calculations with $k_{int} = 0.001 \text{ s}^{-1}$. Furthermore, the exponential relationship between desorption rate constants and molar mass of a chemical presented in chapter 3.3.3 is indicated by the second x-axis.

Additionally, the results of the well-stirred (WS, indicated as dots) as well as the results of the parallel tube modelling approach (PT, indicated as triangles) are shown in Fig. 15 to enable comparison between the models. The differences between both models are only

small. More precisely, the discrepancy in the calculated extraction efficiency does not exceed 20% in any of the modelled scenarios. We thus consider the well-stirred modelling approach as the method of choice for further calculations, because it does not require a complex numerical simulation but can be solved explicitly instead and thus is easier to apply.

The used freely dissolved fractions range from weakly sorbing compounds with $f_u = 0.85$ over moderately sorbing compounds with $f_u = 0.36$ to strongly sorbing compounds with $f_u = 0.01$. This theoretical classification can be related to example compounds from the fields of pharmaceuticals and contaminants: Examples for weakly sorbing compounds are simple polar compounds like paracetamol or metropolol with amino or hydroxyl groups, examples for moderately sorbing compounds are compound classes like phthalates, parabens and benzodiazepines (e.g. diazepam) and examples for strongly sorbing compounds are industrial chemicals like PCBs (polychlorinated biphenyls) or PAHs (polycyclic aromatic hydrocarbons).

When combining the slowest known desorption rate constant $k_{des} = 0.02 \text{ s}^{-1}$ with a strongly sorbing compound ($f_u = 0.01$) and a fast metabolism rate constant ($k_{int} = 0.01 \text{ s}^{-1}$), the calculated E is twentyfold lower than it was when instantaneous sorption equilibrium between albumin and water was assumed (Fig. 15a). According to the empirical relationship indicated by the second x-axis, k_{des} -values around 0.02 s^{-1} are only realistic for high molecular weight compounds. In the case of the above given examples for strongly sorbing compounds, this might be only possible for PCBs as the molar masses of PAHs mostly do not exceed 300 g/mol . A twentyfold lower extraction efficiency due to slow desorption can thus be regarded as an extreme scenario. For more common cases the impact of desorption kinetics on hepatic extraction efficiency will be lower. Chemicals with molar masses in the range of 200 g/mol to 300 g/mol have desorption rate constants in the order of 0.2 s^{-1} . Accordingly, for PAHs a reduction of E due to desorption kinetics by not more than factor 2 to 3 in case of fast metabolism appears to be realistic. Similar effects can be expected for moderately sorbing compounds like phthalates, parabens and benzodiazepines.

Slower metabolism ($k_{int} = 0.001 \text{ s}^{-1}$, Fig. 15b) diminishes the effect of desorption kinetics so that a reduction by no more than factor 10 results for strongly sorbing compounds with high molar masses. In case of weaker sorption or lower molar mass this effect diminishes further so that a reduction by no more than factor 2 results.

One has to note that we assume that albumin is the only sorbing component in blood. Blood lipids and blood cells were neglected, because neither their sorption capacities nor desorption kinetics from these blood components are known. If considerable sorption to these components occurred, the extraction efficiencies would not only depend on the

desorption kinetics from albumin but would also be influenced by the desorption kinetics from these other blood components. The presented models could also be applied to quantify the impact of desorption from other blood components on hepatic metabolism. For doing so, the parameters describing desorption kinetics from albumin and partition behaviour, i.e. binding affinity, to albumin need to be replaced by parameters describing the component of interest.

5. Conclusion

In this work, the desorption kinetics of organic chemicals from albumin were investigated and the impact of desorption kinetics on hepatic elimination of compounds was quantified.

The experimental investigation of desorption kinetics comprised determination of desorption rate constants for 15 different test chemicals belonging to different compound classes. Within the measured data set a relationship between the desorption rate constant of a compound and the compound's molar mass was observed. Mechanistic interpretation of the actual desorption step provided a plausible explanation for this observed relationship. Precisely, the desorption process was considered as a coupled diffusive transport across a phase boundary with the transport resistance within albumin being the dominating step in this transport process. The diffusive transport of a compound in albumin correlates with the molar mass of the compound and thus the same correlation has to result for desorption rate constant and molar mass. Accordingly, the empirically calibrated and mechanistically plausible relationship between desorption rate constant and molar mass can serve as a predictive tool for desorption rate constants of other chemicals. Considering the fact that our results were taken at room temperature, we suppose that the predicted k_{des} will reliably mark the lower limit of what can be expected for the physiological temperature of 37 °C.

To evaluate how big the impact of desorption kinetics on hepatic elimination is, suitable models of hepatic metabolism were developed. For this purpose, two different modelling approaches were used. The first modelling approach considered the liver as an aggregation of well-stirred compartments, whereas the second modelling approach represented the liver as an aggregation of parallel tubes. The first one is easier to apply and can be solved by an analytical solution, while the latter one is more realistic but requires a complex numerical approach. Comparison of the modelling results showed that differences between the results of both modelling approaches are small. Thus the well-stirred modelling approach was identified as the method of choice, because it provides results similar to the parallel tube model but requires less computational effort.

Application of the models showed that slow desorption can decrease hepatic elimination efficiency of compounds. The extent of this decrease, however, is always dependent on the combination of desorption kinetics, metabolism kinetics and the partition behaviour of the compound. Accordingly, a desorption rate constant can cause a decrease in extraction efficiency by a factor of ten for one chemical, while exactly the same desorption rate constant has nearly no effect on extraction efficiency of another chemical. For the most

cases, in fact, the impact of desorption kinetics on hepatic metabolism of a chemical will be rather small and a decrease of extraction efficiency by no more than a factor three will be realistic. Stronger decrease of extraction efficiency is unlikely, because it requires combination of extreme conditions in terms of desorption kinetics, metabolism kinetics and the partition properties of the compound.

In conclusion, this work provides the instruments to evaluate the relevance of desorption kinetics in a compound-specific manner. For prediction of desorption rate constants, the presented relationship between desorption rate constant and molar mass of a compound can be applied. This predictive tool requires no further information than the molar mass of the compound. The impact of desorption kinetics on hepatic metabolism can then be quantified via two explicit equations representing the analytical solution for hepatic elimination under steady-state condition. Both the predictive tool for desorption rate constants and the model for hepatic metabolism are mathematically easy to apply and require no time-consuming computations. By this, these instruments could be used routinely in pharmacokinetic and toxicokinetic predictions to assess the relevance of desorption kinetics for hepatic metabolism of a compound with little effort.

6. Abbreviations

3D	three dimensional
BSA	bovine serum albumin
E	hepatic extraction efficiency
GC	gas chromatography
GC-MS	gas chromatography-mass spectrometry
HSA	human serum albumin
k_{des}	desorption rate constant
k_{extr}	extraction rate constant
k_{int}	intrinsic metabolism rate constant of hepatocytes
LSER	linear solvation energy relationship
M	molar mass
MRM	multiple reaction monitoring
PAH	polycyclic aromatic hydrocarbons
PDMS	poly(dimethylsiloxane)
PT	parallel tube modelling approach
SIM	single ion monitoring
WS	well-stirred modelling approach

7. References

1. Mendel, C.M., The free hormone hypothesis: a physiologically based mathematical model*. *Endocrine Reviews*, 1989. 10(3): p. 232-274.
2. Schwen, L.O., et al., Representative sinusoids for hepatic four-scale pharmacokinetics simulations. *PloS one*, 2015. 10(7): p. e0133653.
3. Weisiger, R.A., Dissociation from albumin: a potentially rate-limiting step in the clearance of substances by the liver. *Proceedings of the National Academy of Sciences*, 1985. 82(5): p. 1563-7.
4. Chen, J., J.E. Schiel, and D.S. Hage, Noncompetitive peak decay analysis of drug–protein dissociation by high-performance affinity chromatography. *Journal of Separation Science*, 2009. 32(10): p. 1632-1641.
5. Faerch, T. and J. Jacobsen, Determination of association and dissociation rate constants for bilirubin-bovine serum albumin. *Archives of Biochemistry and Biophysics*, 1975. 168(2): p. 351-357.
6. Gray, R.D. and S.D. Stroupe, Kinetics and mechanism of bilirubin binding to human serum albumin. *Journal of Biological Chemistry*, 1978. 253(12): p. 4370-4377.
7. Rich, R.L., et al., High-resolution and high-throughput protocols for measuring drug/human serum albumin interactions using BIACORE. *Analytical Biochemistry*, 2001. 296(2): p. 197-207.
8. Svenson, A., E. Holmer, and L.-O. Andersson, A new method for the measurement of dissociation rates for complexes between small ligands and proteins as applied to the palmitate and bilirubin complexes with serum albumin. *Biochimica et Biophysica Acta*, 1974. 342(1): p. 54-59.
9. Yoo, M.J. and D.S. Hage, Use of peak decay analysis and affinity microcolumns containing silica monoliths for rapid determination of drug–protein dissociation rates. *Journal of Chromatography A*, 2011. 1218(15): p. 2072-2078.
10. Yoo, M.J. and D.S. Hage, High-throughput analysis of drug dissociation from serum proteins using affinity silica monoliths. *Journal of Separation Science*, 2011. 34(16-17): p. 2255-2263.
11. Zheng, X., et al., Determination of rate constants and equilibrium constants for solution-phase drug–protein interactions by ultrafast affinity extraction. *Analytical Chemistry*, 2014. 86(13): p. 6454-6460.
12. Kopinke, F.D., et al., Kinetics of desorption of organic compounds from dissolved organic matter. *Environmental Science & Technology*, 2011. 45(23): p. 10013-9.

13. Rowland, M., L.Z. Benet, and G.G. Graham, Clearance concepts in pharmacokinetics. *Journal of Pharmacokinetics and Biopharmaceutics*, 1973. 1(2): p. 123-136.
14. Winkler, K., S. Keiding, and N. Tygstrup, Clearance as a quantitative measure of liver function, in *The liver: Quantitative aspects of structure and function*. 1973, Karger Publishers. p. 144-155.
15. Pang, K.S. and M. Rowland, Hepatic clearance of drugs. I. Theoretical considerations of a "well-stirred" model and a "parallel tube" model. Influence of hepatic blood flow, plasma and blood cell binding, and the hepatocellular enzymatic activity on hepatic drug clearance. *Journal of Pharmacokinetics and Biopharmaceutics*, 1977. 5(6): p. 625-653.
16. Kirichuk, V.F. and A.N. Lutsevich, Modeling of drug elimination by the liver. 1. Main concepts and physiologically justified clearance models (a review). *Pharmaceutical Chemistry Journal*, 1996. 30(5): p. 285-292.
17. Lewis, A.E., The concept of hepatic clearance. *American journal of clinical pathology*, 1948. 18(10): p. 789-795.
18. Wilkinson, G.R. and D.G. Shand, Physiological approach to hepatic drug clearance. *Clinical Pharmacology & Therapeutics*, 1975. 18(4): p. 377-390.
19. Eisert, R. and J. Pawliszyn, Automated in-tube solid-phase microextraction coupled to high-performance liquid chromatography. *Analytical Chemistry*, 1997. 69(16): p. 3140-3147.
20. Ulrich, N., Endo S., Brown T. N., Watanabe N., Bronner G., Abraham M. H., Goss K. U. UFZ-LSER database v 3.2 2017; Available from: <http://www.ufz.de/lserd>.
21. Endo, S. and K.-U. Goss, Serum albumin binding of structurally diverse neutral organic compounds: data and models. *Chemical Research in Toxicology*, 2011. 24(12): p. 2293-2301.
22. Bradford, M.M., A rapid and sensitive method for the quantitation of microgram quantities of protein utilizing the principle of protein-dye binding. *Analytical Biochemistry*, 1976. 72(1): p. 248-254.
23. Hills, E.E., et al., Diffusion coefficients in ethanol and in water at 298 K: Linear free energy relationships. *Fluid Phase Equilibria*, 2011. 303(1): p. 45-55.
24. Rusina, T.P., F. Smedes, and J. Klanova, Diffusion coefficients of polychlorinated biphenyls and polycyclic aromatic hydrocarbons in polydimethylsiloxane and low-density polyethylene polymers. *Journal of Applied Polymer Science*, 2010. 116(3): p. 1803-1810.
25. Balmer, T.E., et al., Diffusion of alkanethiols in PDMS and its implications on microcontact printing (μ CP). *Langmuir*, 2005. 21(2): p. 622-632.

26. Wakeham, W.A., N.H. Salpadoru, and C.G. Caro, Diffusion coefficients for protein molecules in blood serum. *Atherosclerosis*, 1976. 25(2): p. 225-235.
27. Kramer, N.I., J.C.H. van Eijkeren, and J.L.M. Hermens, Influence of albumin on sorption kinetics in solid-phase microextraction: consequences for chemical analyses and uptake processes. *Analytical Chemistry*, 2007. 79(18): p. 6941-6948.
28. Endo, S., A. Pfennigsdorff, and K.-U. Goss, Salting-out effect in aqueous NaCl solutions: trends with size and polarity of solute molecules. *Environmental Science & Technology*, 2012. 46(3): p. 1496-1503.
29. El Kadi, N., et al., Unfolding and refolding of bovine serum albumin at acid pH: ultrasound and structural studies. *Biophysical Journal*, 2006. 91(9): p. 3397-3404.
30. Peters Jr, T., The Albumin Molecule: its Structure and Chemical Properties, in All About Albumin. 1995, Academic Press: San Diego. p. 9-77.
31. Ghuman, J., et al., Structural basis of the drug-binding specificity of human serum albumin. *Journal of Molecular Biology*, 2005. 353(1): p. 38-52.
32. Linden, L., K.-U. Goss, and S. Endo, 3D-QSAR predictions for bovine serum albumin–water partition coefficients of organic anions using quantum mechanically based descriptors. *Environmental Science: Processes & Impacts*, 2017. 19(3): p. 261-269.
33. Schwarzenbach, R.P., P.M. Gschwend, and D.M. Imboden, Environmental Organic Chemistry. 2016, Wiley. p. 583 - 585.
34. ChemAxon. Instant JChem Version 16.1.4.0. 2016; Available from: <http://www.chemaxon.com>.
35. Fang, X. and O. Vitrac, Predicting diffusion coefficients of chemicals in and through packaging materials. *Critical Reviews in Food Science and Nutrition*, 2017. 57(2): p. 275-312.
36. Wake, K. and T. Sato, "The Sinusoid" in the liver: lessons learned from the original definition by Charles Sedgwick Minot (1900). *The Anatomical Record*, 2015. 298(12): p. 2071-2080.
37. Peters Jr, T., Metabolism: Albumin in the Body, in All About Albumin. 1995, Academic Press: San Diego. p. 188-250.
38. Wynne, H.A., et al., The effect of age upon liver volume and apparent liver blood flow in healthy man. *Hepatology*, 1989. 9(2): p. 297-301.
39. Krause, S., N. Ulrich, and K.-U. Goss, Desorption kinetics of organic chemicals from albumin. *Archives of Toxicology*, 2018. 92(3): p. 1065-1074.
40. Endo, S., T.N. Brown, and K.-U. Goss, General model for estimating partition coefficients to organisms and their tissues using the biological compositions and

- polyparameter linear free energy relationships. *Environmental Science & Technology*, 2013. 47(12): p. 6630-6639.
41. Eipel, C., K. Abshagen, and B. Vollmar, Regulation of hepatic blood flow: The hepatic arterial buffer response revisited. *World Journal of Gastroenterology*, 2010. 16(48): p. 6046-57.
 42. Kuntz, E. and H.-D. Kuntz, *Hepatology Textbook and Atlas*. 2008: Springer.
 43. Davies, B. and T. Morris, Physiological parameters in laboratory animals and humans. *Pharmaceutical Research*, 1993. 10(7): p. 1093-1095.
 44. Johnson, T.N., et al., Changes in liver volume from birth to adulthood: A meta-analysis. *Liver Transplantation*, 2005. 11(12): p. 1481-1493.
 45. Puhl, G., et al., Noninvasive *in vivo* analysis of the human hepatic microcirculation using orthogonal polarized spectral imaging. *Transplantation*, 2003. 75(6): p. 756-761.
 46. Kuehnel, W., Digestive System, in *Color Atlas of Cytology, Histology, and Microscopic Anatomy*. 2003, Thieme. p. 272-339.
 47. Bullock, J., J. Boyle, and M.B. Wang, The Vascular System, in *Physiology*. 2001, Lippincott Williams & Wilkins. p. 128-134.
 48. Snyder, W., et al., ICRP Publication 23: report of the task group on reference man. 1975, International Commission on Radiological Protection.

Appendix

A. Rearranging the mass balance equations of the well-stirred modelling approach

To quantify the impact of desorption kinetics together with transcellular permeability and flow limitation in a modified well-stirred liver model, a first mass balance approach is used for the freely dissolved and a second mass balance approach is used for the sorbed concentrations entering and leaving the blood pool of the liver in a steady-state situation.

The first mass balance approach describes the difference between freely dissolved compound flowing in and out of the blood pool of the liver:

$$\begin{aligned}
 Q * C_{water} (C_{in}^{free} - C_{out}^{free}) \\
 = P_{hep} * A * (C_{out}^{free} - C_{hep}^{free}) - k_{des} * V_{alb} \\
 * (C_{out}^{bound} - C_{out}^{free} * K_{AW})
 \end{aligned} \tag{31}$$

where Q is the volumetric blood flow rate (in mL_{blood}/s), C_{water} is the volume concentration of water in blood (in mL_{water}/mL_{blood}) and C_{in}^{free} and C_{out}^{free} are the freely dissolved concentrations of the compound in in- and outflowing blood (in mol/mL_{water}). P_{hep} is the total permeability between blood and hepatocytes (in cm/s), A is the exchange surface area between blood and hepatocytes (in cm²), C_{hep}^{free} is the freely dissolved concentration of the compound in the hepatocytes (in mol/mL_{water}), k_{des} is the desorption rate constant (in s⁻¹), V_{alb} is the albumin volume (in mL_{alb}), C_{out}^{bound} is the albumin bound concentration of the compound in blood (in mol/mL_{albumin}) and K_{AW} is the albumin-water partition coefficient (mL_{alb}/mL_{water}) of the studied compound.

The second mass balance approach describes the difference between compound flowing in and out of the blood pool of the liver in the sorbed state:

$$Q * C_{alb} (C_{in}^{bound} - C_{out}^{bound}) = k_{des} * V_{alb} * (C_{out}^{bound} - C_{out}^{free} * K_{AW}) \tag{32}$$

Here, Q again is the volumetric blood flow rate (in mL_{blood}/s), C_{alb} is the volume concentration of albumin in blood (in mL_{alb}/mL_{blood}) and C_{in}^{bound} and C_{out}^{bound} are the albumin bound concentrations of the compound in in- and outflowing blood (in mol/mL_{alb}).

First we rearrange equation (31): C_{hep}^{free} is an unknown variable and needs to be replaced by an expression that contains only known variables. C_{hep}^{free} can be described with

a mass balance approach for the hepatocytes in a steady-state situation, that equates the netto permeation rate into the hepatocytes with the metabolism rate in the hepatocytes:

$$P_{hep} * A * (C_{out}^{free} - C_{hep}^{free}) = k_{int} * V_{hep}^{total} * C_{hep}^{total} \quad (33)$$

where k_{int} is the intrinsic metabolic rate constant in the hepatocytes (in s^{-1}), V_{hep}^{total} is the total volume of hepatocytes (in $mL_{hepatocytes}$) and C_{hep}^{total} is the total compound concentration in the hepatocytes (in $mol/mL_{hepatocytes}$). First, we need to replace C_{hep}^{total} by an expression based on C_{hep}^{free} :

$$C_{hep}^{free} = C_{hep}^{total} * f_{u\ in\ hep} * \frac{V_{hep}^{total}}{V_{hep}^{water}} \quad (34)$$

$$C_{hep}^{free} = C_{hep}^{total} * \frac{C_{hep}^{water} V_{hep}^{water}}{C_{hep}^{total} V_{hep}^{total}} * \frac{V_{hep}^{total}}{V_{hep}^{water}} \quad (35)$$

$$C_{hep}^{free} = C_{hep}^{total} * K_{water/hep} \quad (36)$$

Rearrangement for C_{hep}^{total} gives:

$$C_{hep}^{total} = C_{hep}^{free} * K_{hep/water} \quad (37)$$

Substitution into equation (33) gives:

$$P_{hep} * A * (C_{out}^{free} - C_{hep}^{free}) = k_{int} * V_{hep}^{total} * K_{hep/water} * C_{hep}^{free} \quad (38)$$

Now, we rearrange equation (38) for C_{hep}^{free} :

$$C_{hep}^{free} = \frac{P_{hep} A C_{out}^{free}}{k_{int} * V_{hep}^{total} * K_{hep/water} + P_{hep} * A} \quad (39)$$

Equation (39) can now be used to substitute C_{hep}^{free} in equation (31):

$$\begin{aligned} & Q * C_{water} (C_{in}^{free} - C_{out}^{free}) \\ &= P_{hep} * A * \left(C_{out}^{free} - \frac{P_{hep} A C_{out}^{free}}{k_{int} * V_{hep}^{total} * K_{\frac{hep}{water}} + P_{hep} * A} \right) - k_{des} \quad (40) \\ & * V_{alb} * (C_{out}^{bound} - C_{out}^{free} * K_{AW}) \end{aligned}$$

A second unknown variable in this equation is C_{out}^{bound} . To substitute C_{out}^{bound} , we rearrange the mass balance approach for the albumin-bound mass (eq. (32)):

$$C_{out}^{bound} = \frac{Q C_{alb} C_{in}^{bound} + k_{des} C_{out}^{free} * K_{AW}}{k_{des} + Q C_{alb}} \quad (41)$$

As the inflowing albumin-bound concentration is in equilibrium with the inflowing freely dissolved concentration, C_{in}^{bound} can be replaced by $C_{in}^{free} * K_{AW}$.

$$C_{out}^{bound} = \frac{Q C_{alb} C_{in}^{free} K_{AW} + k_{des} V_{alb} C_{out}^{free} * K_{AW}}{k_{des} V_{alb} + Q C_{alb}} \quad (42)$$

Substituting this into equation (40) gives:

$$\begin{aligned} & Q * C_{water} (C_{in}^{free} - C_{out}^{free}) \\ &= P_{hep} * A * \left(C_{out}^{free} - \frac{P_{hep} A C_{out}^{free}}{k_{int} * V_{hep}^{total} * K_{hep/water} + P_{hep} * A} \right) - k_{des} \\ & * V_{alb} * \left(\frac{Q C_{alb} C_{in}^{free} K_{AW} + k_{des} V_{alb} C_{out}^{free} * K_{AW}}{k_{des} V_{alb} + Q C_{alb}} - C_{out}^{free} * K_{AW} \right) \end{aligned} \quad (43)$$

Dividing by C_{in}^{free} allows rearrangement, because the extraction efficiency E^f of the freely dissolved fraction refers to

$$E^f = \frac{C_{in}^{free} - C_{out}^{free}}{C_{in}^{free}}$$

and accordingly $\frac{C_{out}^{free}}{C_{in}^{free}}$ equals $(1 - E^f)$:

$$\begin{aligned} Q C_{water} E^f &= P_{hep} * A * (1 - E^f) \left(1 - \frac{P_{hep} * A}{k_{int} * V_{hep}^{total} * K_{hep/water} + P_{hep} * A} \right) \\ & - \frac{k_{des} V_{alb} Q C_{alb} K_{AW}}{k_{des} V_{alb} + Q C_{alb}} - (1 - E^f) \left(\frac{k_{des} V_{alb} k_{des} V_{alb} K_{AW}}{k_{des} V_{alb} + Q C_{alb}} \right) \\ & + (1 - E^f) k_{des} V_{alb} K_{AW} \end{aligned} \quad (44)$$

Further rearrangement leads to the following equation for E^f :

$$E^f =$$

$$\begin{aligned} & \frac{P_{hep} A \left(1 - \frac{P_{hep} A}{k_{int} V_{hep}^{total} K_{hep/water} + P_{hep} A} \right) - \frac{k_{des} V_{alb} (Q C_{alb} K_{AW} + k_{des} V_{alb} K_{AW})}{k_{des} V_{alb} + Q C_{alb}} + k_{des} V_{alb} K_{AW}}{Q C_{water} + k_{perm} A \left(1 - \frac{P_{hep} A}{k_{int} V_{hep}^{total} K_{hep/water} + P_{hep} A} \right) + k_{des} V_{alb} \left(\frac{-k_{des} V_{alb} K_{AW}}{k_{des} V_{alb} + Q C_{alb}} + K_{AW} \right)} \end{aligned} \quad (45)$$

To calculate the extraction efficiency E^b for the albumin-bound fraction, the mass balance approach for the albumin-bound fraction (32) can be rearranged as follows:

$$Q * C_{alb} \left(\frac{C_{in}^{bound} - C_{out}^{bound}}{C_{in}^{bound}} \right) = k_{des} * V_{alb} * \frac{C_{out}^{bound}}{C_{in}^{bound}} - k_{des} * V_{alb} * \frac{C_{out}^{free}}{C_{in}^{bound}} * K_{AW} \quad (46)$$

Here, $\frac{C_{in}^{bound} - C_{out}^{bound}}{C_{in}^{bound}}$ refers to E^b and accordingly $\frac{C_{out}^{bound}}{C_{in}^{bound}}$ can be replaced by $(1 - E^b)$:

$$Q C_{alb} E^b = k_{des} * V_{alb} * (1 - E^b) - k_{des} * V_{alb} * \frac{C_{out}^{free}}{C_{in}^{bound}} * K_{AW} \quad (47)$$

$$E^b = \frac{k_{des} * V_{alb} - k_{des} * V_{alb} * \frac{C_{out}^{free}}{C_{in}^{bound}} * K_{AW}}{Q C_{alb} + k_{des} * V_{alb}} \quad (48)$$

Again, the inflowing albumin-bound concentration is in equilibrium with the inflowing freely dissolved concentration and C_{in}^{bound} is replaced by $C_{in}^{free} * K_{AW}$. Replacing $\frac{C_{out}^{free}}{C_{in}^{free}}$ with the extraction efficiency of the freely dissolved fraction E^f by $\frac{C_{out}^{free}}{C_{in}^{free}} = (1 - E^f)$ yields:

$$E^b = \frac{k_{des} V_{alb} - k_{des} V_{alb} (1 - E^f)}{Q C_{alb} + k_{des} V_{alb}} \quad (49)$$

To calculate the total extraction efficiency the following equations are used:

$$E^{total} = \frac{M_{in}^{total} - M_{out}^{total}}{M_{in}^{total}} = \frac{(M_{in}^{free} + M_{in}^{bound}) - (M_{out}^{free} + M_{out}^{bound})}{M_{in}^{free} + M_{in}^{bound}} \quad (50)$$

Replacing M_{out}^{free} by $M_{in}^{free} - E^f M_{in}^{free}$ and M_{out}^{bound} by $M_{in}^{bound} - E^b M_{in}^{bound}$ gives:

$$E^{total} = \frac{(M_{in}^{free} + M_{in}^{bound})}{M_{in}^{free} + M_{in}^{bound}} - \frac{(M_{in}^{free} - E^f M_{in}^{free} + M_{in}^{bound} - E^b M_{in}^{bound})}{M_{in}^{free} + M_{in}^{bound}} \quad (51)$$

M_{in}^{free} corresponds to $f_u M_{in}^{total}$ and M_{in}^{bound} corresponds to $f_b M_{in}^{total}$, where f_u and f_b refer to the unbound and bound fractions of the compound.

$$E^{total} = 1 - \frac{(f_u M_{in}^{total} - E^f f_u M_{in}^{total} + f_b M_{in}^{total} - f_b E^b M_{in}^{total})}{M_{in}^{total}} \quad (52)$$

$$E^{total} = 1 - (f_u - E^f f_u + f_b - f_b E^b) \quad (53)$$

$$E^{total} = f_u E^f + f_b E^b \quad (54)$$

B. Calculation of hepatocyte-water partition coefficients

To calculate the hepatic extraction efficiency of a certain compound, information on the partition properties of the compound is required. In detail, two different partition coefficients are required, these are the albumin-water partition coefficient and the hepatocyte-water partition coefficient. Of course the partition behaviour towards the hepatocytes should correlate with the partition behaviour towards albumin for neutral organic compounds because both are mostly driven by hydrophobicity. As it is important to use a consistent pair of partition coefficients for every calculation, we looked for a plausible empirical relationship between the hepatocyte-water partition coefficient and the albumin-water partition coefficient.

From the literature we now that the hepatocyte-water partition coefficient of a compound can be derived from the composition of a hepatocyte and the compound's partition coefficients between water and the single components of the hepatocyte [1]. According to our knowledge, only information on the composition of the whole liver is available [2] and we refer to these values for estimation of the composition of hepatocytes. Accordingly, we assume that 74% of the volume of a hepatocyte is water and the remaining 26% refer to other components such as proteins and lipids. The hepatocyte-water partition coefficient $K_{hep/water}$ (in $L_{water}/L_{hepatocyte}$) can thus be calculated from:

$$K_{hep/water} = \phi_{W,hep}K_{water/water} + \phi_{non-aq. components,hep}K_{non-aq. components/water} \quad (55)$$

Here, $K_{water/water}$ refers to the water-water partition coefficient of the compound (in L_{water}/L_{water}), which always equals 1 and $K_{non-aq. components/water}$ to the partition coefficient of the compound between water and the other components of the hepatocyte (in $L_{water}/L_{non-aq. components}$). $\phi_{W,hep}$ and $\phi_{non-aq. components,hep}$ are the fractional contents of water and the other components of the hepatocyte (0.74 and 0.26).

The partition coefficient of the compound between water and the other components of the hepatocyte again can be derived from the composition and the partition coefficients between water and the single components:

$$\begin{aligned}
 &K_{non-aq. components/water} \\
 &= \phi_{SL,hep}K_{storage\ lipid/water} + \phi_{ML,hep}K_{membrane\ lipid/water} \quad (56) \\
 &+ \phi_{P,hep}K_{protein/water}
 \end{aligned}$$

Here, $K_{storage\ lipid/water}$ is the storage lipid-water partition coefficient (in $L_{water}/L_{storage\ lipid}$), $K_{membrane\ lipid/water}$ the membrane lipid-water partition coefficient (in $L_{water}/L_{membrane\ lipid}$) and $K_{protein/water}$ is the protein-water partition coefficient of the compound (in $L_{water}/L_{protein}$). These compound-specific partition coefficients were taken from the LSER (linear solvation energy relationship)-online database [3]. $\phi_{SL,hep}$, $\phi_{ML,hep}$ and $\phi_{P,hep}$ are the fractional water, storage lipid, membrane lipid and protein content of the non-aqueous hepatocyte components:

Table 3: Composition of the non-aqueous hepatocyte components.

parameter	symbol	value	reference
fractional protein content	$\phi_{P,hep}$	0.73	[1]
fractional storage lipid content	$\phi_{SL,hep}$	0.08	[1]
fractional membrane lipid content	$\phi_{ML,hep}$	0.19	[1]

As an example, we calculated the hepatocyte-water partition coefficients for a few of the compounds, which were recently used to investigate desorption rate constants. The used partition coefficients are listed in the following table:

Table 4: Partition coefficients for different biological phases.

compound	$\log K_{protein/water}$ [$L_{water}/L_{protein}$]=	$\log K_{membrane\ lipid/water}$ [$L_{water}/L_{membrane\ lipid}$]=	$\log K_{storage\ lipid/water}$ [$L_{water}/L_{Storage\ lipid}$]=	$\log K_{albumin/water}$ [$L_{water}/L_{albumin}$]=
naphthalene	2.24	3.48	3.51	2.93
1,2,4-trichlorobenzene	2.7	4.01	4.19	3.47
1,4-dibromobenzene	2.59	3.9	4.02	3.34
phenanthrene	3.35	4.74	4.88	3.94
n-propylbenzene	2.38	3.59	3.87	3.08
pyrene	3.85	5.35	5.4	4.4
1-chlorooctane	3.06	4.3	4.84	3.77
dipentylether	2.63	3.68	4.28	3.2
1,2,3,4-tetrachlorobenzene	3.11	4.48	4.72	3.86

n-hexylbenzene	3.65	4.98	5.6	4.27
allylbenzene	2.05	3.21	3.38	2.75
di-n-butylether	1.78	2.75	3.12	2.4
1,8-dibromooctane	3.29	4.6	4.93	3.94
chlorpyrifos	3.76	4.93	5.11	4.29

By applying equation (56) the corresponding partition coefficients between water and the non-aqueous hepatocyte components were calculated and compared with the albumin-water partition coefficients. It shows that the non-aqueous components-water partition coefficients roughly correspond to the albumin-water partition coefficient multiplied by 1.6.

Table 5: Comparison of partition coefficients.

compound	$K_{\text{albumin/water}}$ [L _{water} /L _{albumin}]=	$K_{\text{non-aq. components/water}}$ [L _{water} /L _{non-aq. comp.}]=	$K_{\text{non-aq. comp./water}}$ / $K_{\text{albumin/water}}$
naphthalene	851.1	956.7	1.1
1,2,4-trichlorobenzene	2951.2	3525.5	1.2
1,4-dibromobenzene	2187.8	2617.3	1.2
phenanthrene	8709.6	18039.3	2.1
n-propylbenzene	1202.3	1493.7	1.2
pyrene	25118.9	67548.0	2.7
1-chlorooctane	5888.4	9997.9	1.7
dipentylether	1584.9	2697.9	1.7
1,2,3,4-tetrachlorobenzene	7244.4	10786.0	1.5
n-hexylbenzene	18620.9	52253.1	2.8
allylbenzene	562.3	578.4	1.0
di-n-butylether	251.2	253.6	1.0
1,8-dibromooctane	8709.6	15628.0	1.8
chlorpyrifos	19498.4	30482.8	1.6

For simplicity, we thus used $1.6 * K_{\text{albumin/water}}$ to derive the value for non-aqueous components-water partition coefficients from the albumin-water partition coefficient. According to equation (55), the hepatocyte-water partition coefficient is then calculated from:

$$K_{\text{hep/water}} = 0.74 * 1 + 0.26 * 1.6 * K_{\text{albumin/water}} \quad (57)$$

This empirical relationship is used for calculation of the needed hepatocyte-water partition coefficients.

C. References

1. Endo, S., T.N. Brown, and K.-U. Goss, General model for estimating partition coefficients to organisms and their tissues using the biological compositions and polyparameter linear free energy relationships. *Environmental Science & Technology*, 2013. 47(12): p. 6630-6639.
2. Schmitt, W., General approach for the calculation of tissue to plasma partition coefficients. *Toxicology In Vitro*, 2008. 22(2): p. 457-467.
3. Ulrich, N., Endo S., Brown T. N., Watanabe N., Bronner G., Abraham M. H., Goss K. U. UFZ-LSER database v 3.2 2017; Available from: <http://www.ufz.de/lserd>.

D. Published Papers

D.1. Desorption kinetics of organic chemicals from albumin



Desorption kinetics of organic chemicals from albumin

Sophia Krause¹ · Nadin Ulrich¹ · Kai-Uwe Goss^{1,2}

Received: 26 June 2017 / Accepted: 8 November 2017
© Springer-Verlag GmbH Germany, part of Springer Nature 2017

Abstract

When present in blood, most chemicals tend to bind to the plasma protein albumin. For distribution into surrounding tissues, desorption from albumin is necessary, because only the unbound form of a chemical is assumed to be able to cross cell membranes. For metabolism of chemicals, the liver is a particularly important organ. One potentially limiting step for hepatic uptake of the chemicals is desorption from albumin, because blood passes the human liver within seconds. Desorption kinetics from albumin can thus be an important parameter for our pharmacokinetic and toxicokinetic understanding of chemicals. This work presents a dataset of measured desorption rate constants and reveals a possibility for their prediction. Additionally, the obtained extraction profiles directly indicate physiological relevance of desorption kinetics, because desorption of the test chemicals is still incomplete after time frames comparable to the residence time of blood in the liver.

Keywords Albumin · Desorption kinetics · Protein-binding

Introduction

Blood is the most important transport vector for chemical substances inside organisms. For many chemicals, only a small portion of the chemicals is present freely dissolved in the plasma. The bigger portion is bound to different blood components. Among these, albumin is known to be one of the crucial components for binding. Albumin functions as a transport protein for many endogenous ligands (e.g., steroid hormones or metabolites) and also binds a lot of exogenous ligands (e.g., pharmaceuticals) (Fasano et al. 2005; Vandenberg et al. 1972).

Before these bound ligands can be distributed or metabolized in surrounding tissues, desorption from the protein is necessary (Mendel 1989; Mielke et al. 2017). An especially important organ for metabolism of chemicals is the liver.

Considering the fact that the residence time of blood in the human liver is only a few seconds (Schwen et al. 2015), it follows that the desorption kinetics might become the limiting step for the overall metabolism of a chemical in the liver. Although this issue has already been discussed in the literature (Berezhkovskiy 2012; Weisiger 1985), current toxicokinetic and pharmacokinetic models neglect the desorption kinetics by assuming instantaneous sorption equilibrium in blood (e.g. Poulin and Haddad 2013; Riley et al. 2005). Furthermore, there are only very few studies available in the literature investigating desorption kinetics from albumin experimentally. The results of these studies indicate a broad range of desorption rate constants for different chemicals, varying from 0.009 to 3.96 s⁻¹ (Chen et al. 2009; Faerch and Jacobsen 1975; Gray and Stroupe 1978; Rich et al. 2001; Svenson et al. 1974; Yoo and Hage 2011a, b; Zheng et al. 2014).

The aim of this study is the systematic investigation of the desorption kinetics from albumin. For this purpose, we use a new modification of a time-resolved extraction method to determine desorption rate constants of 15 different neutral organic chemicals.

Electronic supplementary material The online version of this article (<https://doi.org/10.1007/s00204-017-2117-4>) contains supplementary material, which is available to authorized users.

✉ Sophia Krause
sophia.krause@ufz.de

¹ Department of Analytical Environmental Chemistry, Helmholtz Centre for Environmental Research UFZ, Permoserstr. 15, 04318 Leipzig, Germany

² Institute of Chemistry, University of Halle-Wittenberg, Kurt-Mothes-Str. 2, 06120 Halle, Germany

Materials and methods

Materials

Stock solutions of the chemicals were prepared either in methanol or in isopropanol. Lyophilized human and bovine serum albumin was obtained from Sigma Life Science (> 98%, essentially fatty acid free) and dissolved in a phosphate buffer (150 mM NaCl, 10 mM phosphate, pH 7.40). Albumin suspensions were spiked with stock solutions of each chemical to prepare the sample solutions. The methanol or isopropanol content did not exceed 0.5 v/v %. The 007-1 gas chromatography (GC) capillary (inner diameter 0.25 mm, layer 100% polydimethylsiloxane (PDMS), layer thickness 8 μm) used for the time-resolved extraction was purchased from Quadrex Corporation. PDMS-coated glass fibers (diameter of the glass core 0.123 mm, PDMS layer thickness 30 μm) were produced by Polymicro Technologies Inc. Fibers and GC capillary were cut in pieces of 20 cm length and cleaned before usage by purging with methanol.

Experimental setup and principle

The principle for the performed measurement of desorption kinetics from albumin was a time-resolved extraction of the test chemical from an albumin suspension, which passes through a 20 cm piece of a GC capillary. The used method was a modification of the method introduced by Eisert and Pawliszyn (1997) and extended by Kopinke et al. (2011). The differences to the system of Kopinke et al. were: (1) the coating of the GC capillary was thicker (8 μm instead of 1 μm) and (2) a PDMS-coated glass fiber (30 μm coating thickness) instead of a metal wire was inserted in the GC capillary. Both changes resulted in a gain of sorption capacity due to a bigger PDMS volume. Introducing the glass fiber into the GC capillary (Fig. 1) reduced the maximum diffusion path length from the albumin suspension to the PDMS phase perpendicular to flow direction from 177 μm (empty capillary) to ≈ 25.5 μm (filled capillary, assuming non-centered glass fiber position). The slit volume was 3.34 μL .

During experiments, the sample solution ($V = 200$ μL) was pumped through the GC capillary with defined flow rates (VIT-FIT syringe pump, Lambda Laboratory Instruments). The flow rates (24–0.2 mL h^{-1}) determined the residence time of the sample inside the capillary. As soon as the test chemical desorbed from the protein inside the capillary, it was removed from the sample solution due to sorption into the PDMS layers. Only that fraction of the test chemical, which did not desorb fast enough from the albumin, passed through the capillary and was collected for analysis. This remaining concentration of the test chemical in the capillary effluent was compared to the concentration

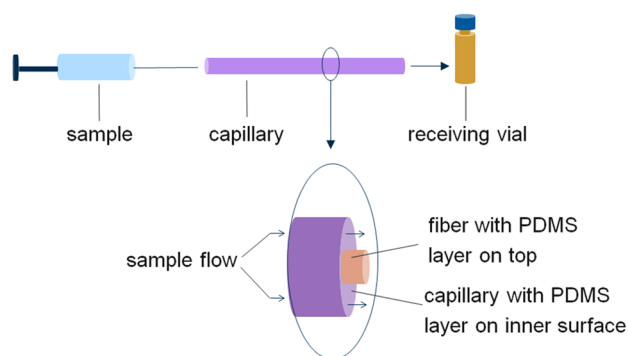


Fig. 1 Scheme of the used experimental setup. The sample solution (test chemical dissolved either in water or in albumin suspension) is pumped through a capillary in which a fiber is introduced and collected after passage through the capillary for concentration determination. Capillary as well as fiber are coated with PDMS, the freely dissolved test chemical sorbs into the PDMS layers and is extracted from the sample solution

in the input suspension. To avoid losses by volatilization, samples were collected directly in septum-closed vials after passage through the capillary. The vials were prefilled with cyclohexane as extraction solvent, cyclohexane contained hexachlorobenzene as internal standard. For extraction, samples were gently shaken for 3 min. Efficiency of extraction was calculated for each chemical using partition coefficients estimated based on the compound's physicochemical properties (Ulrich et al. 2017) and did not undershoot 99%. The input suspension was extracted in the same manner. Concentration of the test chemicals in the extracts was analyzed by via gas chromatography–mass spectrometry (GC–MS) (7890A/5975C and 7890B/7010, Agilent Technologies). For analysis, the cyclohexane extracts were injected in cold splitless mode, separated with an HP-5 column (HP-5MS UI, 30 m, inner diameter 0.25 mm, film thickness 0.25 μm , Agilent Technologies) and analyzed in SIM or MRM mode.

Time-resolved extraction experiments

As a reference, pure aqueous solutions (clean water without albumin) of the chemicals were pumped through the capillary with flow rates corresponding to residence times inside the capillary ranging from 0.5 up to 5 s. These experiments allowed derivation of the extraction rate constants k_{extr} of the freely dissolved chemical from the water phase into the PDMS.

In a next step, experiments were conducted with albumin suspensions. In these latter experiments the overall transport kinetics that we measured had contributions from two kinetic steps: (a) desorption from albumin itself into the freely dissolved state and (b) extraction from the freely dissolved state into PDMS. Obviously, a sensitive determination of the sole desorption kinetics from albumin is only possible if

the extraction kinetics from the water phase are corrected for in the experiments with albumin. This was why the reference experiments with water were needed. Human serum albumin (HSA) as well as bovine serum albumin (BSA) were used to reveal possible differences in desorption kinetics. The used albumin concentrations ranged from 0.1 to 10 g L⁻¹, individually chosen for each chemical according to its partition properties. The ratio of bound-to-unbound albumin (assuming 1:1-binding of the chemical) was calculated to avoid saturation of binding sites. Under these conditions, desorption from albumin could be assumed as independent from the used albumin concentration, i.e., experiments with different albumin concentrations should result in the same desorption rate constants k_{des} for a given chemical. Based on this assumption, each chemical was extracted from two albumin suspensions, differing in their concentrations. This procedure allowed confirmation of the determined k_{des} . The used flow rates corresponded to residence times ranging from 0.5 up to 60 s. All experiments were conducted at room temperature.

Limitations of the method

For successful application of the method, the following conditions had to be met:

1. The albumin-bound fraction of the chemical in the input albumin suspension would preferably be above 70–80%,
2. Sufficient capacity of PDMS for nearly complete extraction of the chemical from the albumin suspension under equilibrium conditions,
3. Extraction from water into PDMS faster than desorption from albumin into water,
4. Negligible loss of albumin due to sorption to the PDMS coating inside the capillary.

To ensure a high albumin-bound fraction in the input suspension, the used albumin concentrations were adapted for each chemical according to its partition properties. Partitioning between albumin and water was calculated using BSA-water partition coefficients either from literature (Endo and Goss 2011) or (in case no literature data was available) from the LSER (linear solvation energy relationship)-database (Ulrich et al. 2017), which provides partition coefficients estimated based on a compound's physicochemical properties. Only in a few experiments the sorbed amount was smaller than 70%, which resulted in a loss of accuracy in the derived desorption rate constants due to a smaller measuring range.

To meet the second condition of sufficient PDMS capacity, the experimental setup was optimized by testing GC capillaries with different layer thicknesses. The optimal setup consisted of a capillary with a 8 μm PDMS coating into which a glass fiber

with a 30 μm PDMS coating was inserted. Fast extraction of the test chemicals from water into PDMS was confirmed via comparing results from reference experiments with aqueous solutions of the chemicals to results from albumin suspension extraction.

To check to which extent a loss of albumin due to sorption to the PDMS coating inside the capillary occurs, the albumin concentration of the capillary effluent was measured and compared with concentrations of the original input albumin suspensions. Concentration determination was performed via absorption measurements at 280 nm as well as at 595 nm (Bradford assay, Bradford 1976). The calculated mean recoveries did not undershoot 99.1% (see SI Sect. 1), the loss of albumin thus could be considered as negligible.

Data analysis

Based on the generated data, desorption rate constants were determined by fitting a transport model. It was examined beforehand in separate calculations, which processes needed to be considered in this transport model (see SI Sect. 2).

As a result a numerical model was developed based on dispersion and convection of both, the albumin and the freely dissolved chemical (see SI Sect. 3). Driving factor for extraction of the chemical was the establishment of partition equilibrium for the chemical between albumin, PDMS and water. Partition equilibrium between albumin, PDMS and water was calculated using albumin–water and PDMS–water partition coefficients either from literature (Endo and Goss 2011) or from estimations based on the physicochemical properties of the compound (Ulrich et al. 2017). The extraction kinetics into the PDMS as well as the desorption kinetics from albumin were both assumed to be first-order kinetics.

Additionally, the model included the facilitated transport of the test chemicals from the suspension to the PDMS. This facilitated transport resulted from diffusion of the albumin-bound fraction of the chemical together with the albumin perpendicular to the flow direction, which happened in addition to diffusion of the freely dissolved chemical. The facilitated transport was represented using accelerated extraction rate constants when modeling the albumin extraction experiments. These accelerated extraction rate constants were calculated individually for each chemical and albumin concentration based on the extraction rate constants found in the reference experiments with clean water. For this calculation, we used an approach analog to the one from Kramer et al. (2007) (see SI Sect. 3).

Results

Determination of extraction rate constants

The obtained extraction profiles showed that extraction kinetics from water were similar for all chemicals. This observation is in agreement with expectations because diffusion of the used chemicals in water is very similar (estimated diffusion coefficients range from 3.5×10^{-6} to $8.4 \times 10^{-6} \text{ cm}^2 \text{ s}^{-1}$ (Hills et al. 2011)) and diffusion of the chemicals in PDMS itself had been shown not to be rate limiting in our setup (see SI Sect. 2). Figure 2 shows the extraction profiles of three different chemicals as an example. Shown are mean values of duplicates, standard deviations are indicated as error bars. While the PDMS-water partition coefficients of these chemicals differed by about 1 log-unit, sorption equilibrium was reached for all chemicals within 3 s residence time in the capillary and all chemicals were extracted to about 99%.

Fitting the curves with the transport model revealed a rate constant $k_{\text{extr}} = 2.7 \text{ s}^{-1}$ for extraction of the most chemicals. The only exceptions were chlorpyrifos, 1-nitrooctane and 1-chlorooctane, for which slightly different extraction rate constants were determined ($k_{\text{extr}} = 2.3 \text{ s}^{-1}$ for chlorpyrifos and $k_{\text{extr}} = 2.9 \text{ s}^{-1}$ for 1-nitrooctane and 1-chlorooctane). The determined extraction rate constants were used to calculate the accelerated extraction rate constants, which were needed for transport modeling of the extractions from albumin suspensions (see SI Sect. 3).

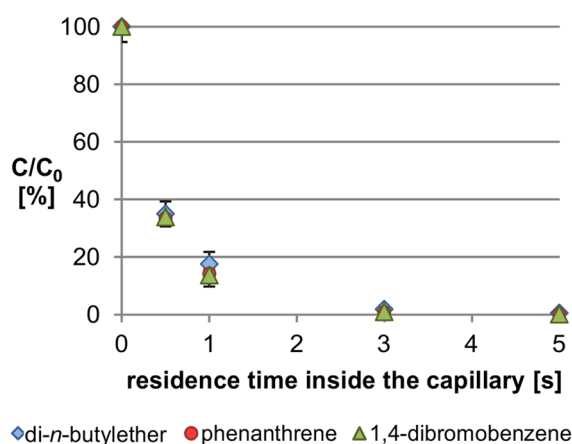


Fig. 2 Extraction of di-*n*-butylether ($C_0 = 1 \text{ mg L}^{-1}$), phenanthrene ($C_0 = 0.05 \text{ mg L}^{-1}$) and 1,4-dibromobenzene ($C_0 = 0.2 \text{ mg L}^{-1}$) from water, all test chemicals were extracted to about 99% within 3 s. Shown are mean values of duplicates, standard deviations are indicated as error bars. In cases where error bars are invisible, they are covered by the symbols

Comparison between HSA and BSA

The experiments with HSA instead of BSA yielded extraction profiles, which were overlaying to the extraction profiles measured in the BSA experiments. These experiments thus showed no evidence for dependence of desorption kinetics from the albumin type. Further comparison between HSA and BSA was omitted and the succeeding experiments were all conducted with BSA.

Determination of desorption rate constants

All experiments showed a substantially slower extraction from the albumin suspension compared to the extraction from water. Figure 3 shows the extraction of 1,2,3,4-tetrachlorobenzene from BSA compared to its extraction from water. Again, mean values of duplicates are shown and standard deviations are indicated as error bars.

After 60 s residence time in the capillary, the remaining concentration of 1,2,3,4-tetrachlorobenzene in the sample was almost zero. Obviously, 60 s were sufficient for desorption and establishment of partition equilibrium between water, albumin and PDMS. With shorter residence times the remaining concentration increased due to incomplete desorption. For the shortest residence time, the concentration in the capillary effluent was mainly governed by the partition equilibrium between water and albumin in the input suspension indicating no significant desorption going on during passage through the column.

Summarizing these observations, the edges of the extraction profiles can be considered as dominated by the partition

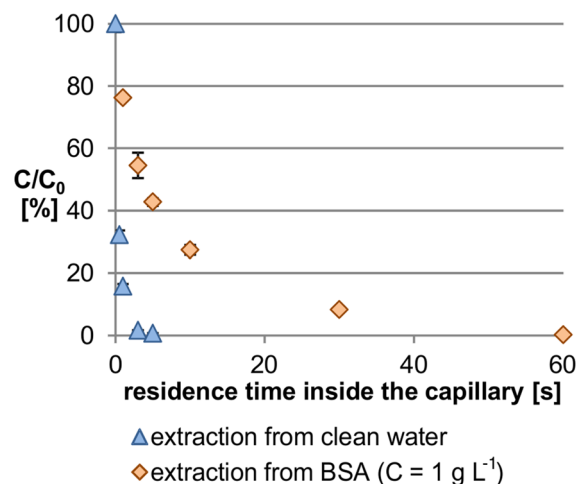


Fig. 3 Extraction of 1,2,3,4-tetrachlorobenzene ($C_0 = 0.1 \text{ mg L}^{-1}$) from water and from a BSA suspension ($C = 1 \text{ g L}^{-1}$). Shown are mean values of duplicates, standard deviations are indicated as error bars. In cases where error bars are invisible, they are covered by the symbols

properties of the chemicals, whereas the steepness of the intermediate part of the extraction profile mostly reflects the influence of the desorption rate constant.

The generated data were modeled with the developed transport model to obtain desorption rate constants for each chemical. For confirmation, each chemical was extracted from two albumin suspensions with different concentrations. Assuming that the desorption kinetics were independent from the albumin concentration, the desorption rate constant had to be the same for both experiments (Fig. 4). This allowed confirmation of the predetermined k_{extr} and the fitted k_{des} : while a single extraction curve could still be fitted equally well with different combinations of k_{extr} and k_{des} (because a wrong k_{extr} could be corrected by fitting an also wrong k_{des}), the simultaneous fitting of two extraction curves with different albumin concentrations could only succeed if both rate constants were correct.

Table 1 shows the determined desorption rate constants for 15 test chemicals. Additionally, the corresponding partition coefficients (from literature (Endo and Goss 2011) or estimated based on the physicochemical properties of the compound (Ulrich et al. 2017)) used for calculating equilibria and transport modeling are shown. All partition coefficients were corrected for the salting-out effect (Endo et al. 2012), because the salt content of the used buffer influences the partitioning of the chemicals. In some cases the published albumin–water partition coefficients were additionally

Table 1 List of test chemicals with determined desorption rate constants (k_{des}) and corresponding albumin–water and PDMS–water partition coefficients ($K_{\text{BSA/water}}$ and $K_{\text{PDMS/water}}$, from literature or estimated based on the physicochemical properties of the compound)

Test chemical	k_{des} (s^{-1})	$\log K_{\text{BSA/water}}$ (L L^{-1})	$\log K_{\text{PDMS/water}}$ (L L^{-1})
1-Nitrooctane	0.5	3.55	3.03
1-Chlorooctane	0.6	3.50	4.40
1,8-Dibromooctane	0.3	3.70	4.30
Di- <i>n</i> -butylether	1.4	2.20	3.24
Di- <i>n</i> -pentylether	0.9	2.92	3.85
<i>n</i> -Propylbenzene	1.8	3.00	3.49
<i>n</i> -Hexylbenzene	0.9	4.34	5.04
Allylbenzene	1.6	3.10	2.98
1,4-Dibromobenzene	0.3	3.60	3.49
1,2,4-Trichlorobenzene	0.8	3.90	3.70
1,2,3,4-Tetrachlorobenzene	0.4	4.11	4.11
Naphthalene	1.4	3.90	2.78
Phenanthrene	0.6	4.05	3.95
Pyrene	0.6	4.90	4.20
Chlorpyrifos	0.2	3.30	3.85

adjusted (by 0.3 log units maximum) to fit our data. This adjustment lies within the typical range of accuracy of the methods by which the albumin–water partition coefficients were determined. One exception was naphthalene, whose albumin–water partition coefficient needed to be adjusted by about 0.5 log units.

Discussion and conclusion

Desorption from BSA and HSA

Desorption kinetics of 15 neutral organic chemicals from albumin was investigated in this study. Initially, experiments were performed with both HSA and BSA to check for possible differences. These experiments showed no differences in desorption kinetics. Consequently, we assume that results from desorption experiments are transferable between the two species. Apart from our test with HSA and BSA, this assumption is also plausible in consideration of the similarities between the two proteins: both the amino acid sequence and the structure of the folded protein are very similar for HSA and BSA. The amino acid sequence homology between the two albumins is 76% (El Kadi et al. 2006), HSA consisting of 585 residues and BSA consisting of 583 residues (Peters Jr 1995a). Both amino acid chains are folded into three homologous domains, each domain consists of two subdomains (El Kadi et al. 2006; Ghuman et al. 2005). A recent study (Linden et al. 2017) suggested that albumin

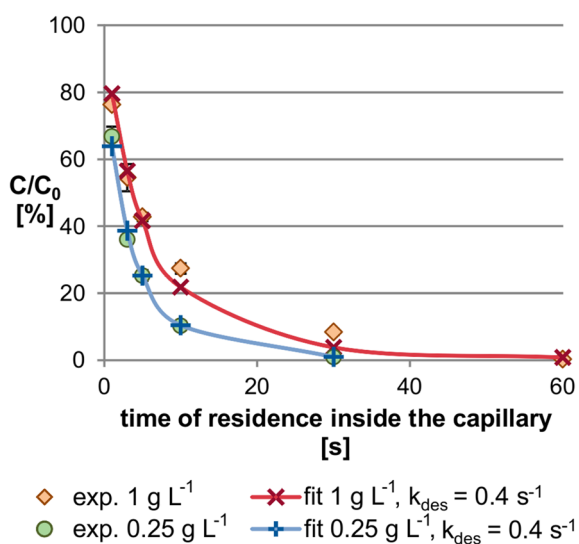


Fig. 4 Extraction of 1,2,3,4-tetrachlorobenzene ($C_0=0.1 \text{ mg L}^{-1}$) from bovine serum albumin suspensions. Different BSA concentrations are indicated as diamonds (1 g L^{-1}) and dots (0.25 g L^{-1}). Shown are mean values of duplicates, standard deviations are indicated as error bars. In cases where error bars are invisible, they are covered by the symbols. Corresponding fits with desorption rate constants $k_{\text{des}} = 0.4 \text{ s}^{-1}$ are indicated as crosses with interpolated lines between the calculated data points

binding effects for many chemicals arise from the 3-D structure of the molecule. In this study, binding for about 80 neutral and 40 ionic chemicals to albumin could be explained by considering three-dimensional features, but without discrimination between different binding sites. Consequently, the structural similarities between the two albumin types may result in similar binding of chemicals to HSA and BSA. Based on these structural similarities and our own results from initial tests, we thus assume that the found desorption rate constants from BSA also describe desorption from HSA.

Comparison to published k_{des}

The here determined desorption rate constants varied from 0.2 s^{-1} for the slowest to 1.8 s^{-1} for the fastest desorption rate constant. Thus, our results are in a similar range as the kinetic data published by Yoo, Chen and Rich (Chen et al. 2009; Rich et al. 2001; Yoo and Hage 2011a, b). Chen and Rich investigated the desorption kinetics of warfarin from HSA. Rich used surface plasmon resonance spectroscopy with BIACORE for real time detection of the desorption process and determined a desorption rate constant of 1.2 s^{-1} at $37 \text{ }^{\circ}\text{C}$, Chen found desorption rate constants of 0.56 and 0.66 s^{-1} at $37 \text{ }^{\circ}\text{C}$ using noncompetitive peak decay analysis in HSA-containing columns. Additionally applying a non-competitive peak decay method, Yoo determined desorption rate constants from human serum albumin for 12 drugs ranging from 0.29 to 0.78 s^{-1} at $37 \text{ }^{\circ}\text{C}$. The fastest desorption rate constant with 3.96 s^{-1} was measured by Zheng et al. (2014) for desorption of chlorpromazine from HSA at $37 \text{ }^{\circ}\text{C}$ using ultrafast affinity extraction in a HSA microcolumn.

In contrast, Svenson, Faerch and Gray investigated the desorption kinetics of bilirubin from albumin and found desorption rate constants smaller than our smallest value by around one order of magnitude (Faerch and Jacobsen 1975; Gray and Stroupe 1978; Svenson et al. 1974). Svenson used partitioning between soluble and immobilized albumin in combination with spectrophotometry and determined 0.009 s^{-1} as desorption rate constant from HSA at $25 \text{ }^{\circ}\text{C}$. Faerch determined a desorption rate constant of 0.03 s^{-1} from BSA at $37 \text{ }^{\circ}\text{C}$ by an enzymatic degradation method.

Again using a spectrophotometrical method, Gray determined a desorption rate constant of 0.01 s^{-1} from HSA at $4 \text{ }^{\circ}\text{C}$. Bilirubin was extracted from the HSA sample by adding BSA, the kinetics were monitored in a stopped flow spectrometer by means of the different absorption spectra of the two complexes.

These dramatic differences between the desorption rate constants of bilirubin, independently measured by three groups with different methods, and the desorption rate constants of all the other chemicals that we and other groups measured raise questions about the plausibility of the different results. Reinvestigation of the chemicals used in the

literature with the here presented time-resolved extraction method was not feasible, because PDMS is not a suitable extraction material for these chemicals. We thus checked if a mechanistic consideration of the desorption process can provide an explanation for these differences.

Mechanistic consideration of the desorption process

From a mechanistic point of view, the desorption process can be considered as a transfer process across a phase boundary. This transfer process requires diffusion within the albumin from the actual sorption sites to the water phase and diffusion across a stagnant water layer into the well-mixed water phase adjacent to the albumin. This coupled diffusive transport can be described by applying Fick's first law (see SI Sect. 4). After rearrangement of the equations it can be seen that desorption, i.e., k_{des} , mechanistically depends on two transport resistances in series: the resistance in albumin and in water (see SI Eq. (13)). The term describing the transport resistance in water comprises the albumin-water partition coefficient as well as the diffusion coefficient and diffusion path length in water. The diffusion coefficients in water are very similar for all test chemicals and the diffusion path length is the same as we assume that all chemicals sorb to the same sites. The partition coefficients, instead, differ by up to two orders of magnitudes for the chemicals tested here. Hence, one can expect that a correlation between the albumin-water partition coefficients and the desorption rate constants should be found, if the overall transfer process was dominated by the transport resistance in water. Figure 5 shows that such a correlation does not exist. Note that the literature k_{des} values for ionic chemicals could not be included in this graph because no corresponding partition coefficients were available. According to the pKa of the chemicals (ChemAxon 2016) used in the literature, only two of these chemicals are present in their neutral forms at pH 7.40 (chloramphenicol and diazepam with the corresponding desorption rate constants $k_{\text{des}} = 0.78 \text{ s}^{-1}$ and $k_{\text{des}} = 0.44 \text{ s}^{-1}$ (Yoo and Hage 2011a, b)), those are included in Fig. 5. Thus, we conclude that the transport resistance in water is not the limiting process for desorption kinetics.

Instead, the transport resistance in albumin, i.e., the diffusion coefficient, should be the dominating process. According to Fang and Vitrac (2017), diffusion coefficients in polymers scale with $\text{MW}^{-\alpha}$, where α is larger than one with an upper limit of ten. Hence, one can expect that k_{des} should scale with the molecular weight in the same way, if it was dominated by diffusion in albumin. And indeed, the desorption rate constants determined here scale exponentially with the molecular weight (Fig. 6).

The fitted relationship has the expected form with an exponent of -2 :

$$k_{\text{des}} = 20267 \times \text{MW}^{-2.0}, \quad (1)$$

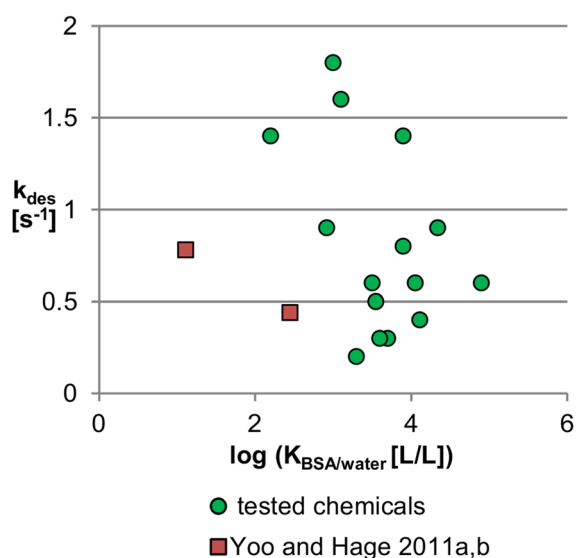


Fig. 5 Desorption rate constants k_{des} determined in this study (represented by green dots) and found in the literature (represented by red squares) versus the log of the corresponding albumin-water partition coefficients $K_{\text{BSA/water}}$ (Color figure online)

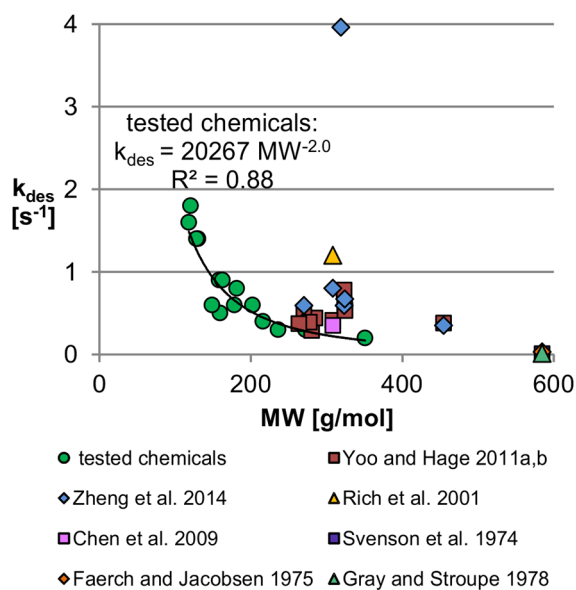


Fig. 6 Desorption rate constants k_{des} determined in this study (represented by green dots) and found in the literature (represented by colored symbols) versus the corresponding molecular weights MW. The solid line represents the fitted relationship between the desorption rate constants of our test chemicals and the molecular weights of the chemicals. (Color figure online)

Here, k_{des} refers to the desorption rate constant (s^{-1}) and MW refers to the chemicals molecular weight (g mol^{-1}).

Hence, the empirically found correlation between molecular weight and desorption rate constant is mechanistically very plausible. We conclude that this mechanistically based

and empirically calibrated relationship enables prediction of desorption rate constants from albumin for various organic chemicals.

Figure 6 also shows the literature values for k_{des} . Not all of these values fit to the observed correlation, but interestingly the extremely slow desorption rate constants for bilirubin, independently determined by Svenson, Faerch and Gray (determined $k_{\text{des}} = 0.009, 0.03$ and 0.01 s^{-1}), are consistent with the correlation (calculated $k_{\text{des}} = 0.059 \text{ s}^{-1}$). We thus conclude that these extremely slow desorption rate constants are reliable and desorption rate constants ranging over a few orders of magnitude are plausible.

A possible explanation for the missing correlation for some of the other chemicals from the literature might be an insufficient accuracy of the literature values due to some pitfalls in the used data evaluation: Common for all the studies is the assumption that the mass transfer kinetics removing the desorbed analyte from the freely dissolved state (i.e., extraction) is much faster than desorption of the analyte from albumin and, hence, equilibrium between the water phase and the extraction medium could be assumed for evaluation of the experiments. This simplified scenario allows determination of the desorption rate constant from the slope of the semi logarithmic plot of the analyte concentration over sampling time. We suggest that this procedure is inaccurate: Although the extraction of the analyte from water is faster than desorption, the extraction kinetics still affects the resulting concentration profile. In fact, the desorbed analyte is not immediately removed from water and, therefore, affects the concentration gradient between the water phase and albumin. This results in a decelerated concentration decrease in the sample. Consequently, neglecting the extraction kinetics can lead to underestimation of desorption rate constants. To illustrate this statement, Fig. 7 shows how the derived k_{des} for one of our own test chemicals would differ, if extraction kinetics was neglected.

Figure 7a shows the results of our analysis procedure, which considers the extraction kinetics using the extraction rate constant presented above ($k_{\text{extr}} = 2.7 \text{ s}^{-1}$). This procedure reveals the true desorption rate constant $k_{\text{des}} = 1.6 \text{ s}^{-1}$. Figure 7b shows the results of an analysis procedure which neglects the extraction kinetics by assuming an extremely fast extraction rate constant ($k_{\text{extr}} = 1000 \text{ s}^{-1}$). This leads to an underestimated desorption rate constant $k_{\text{des}} = 0.3 \text{ s}^{-1}$. Using this second procedure, a slower desorption rate constant is erroneously needed to fit the same experimental data, because the decelerated concentration decrease due to the extraction kinetics is not taken into account. However, one has to note that this aspect is less important for slower desorption rate constants than for faster desorption rate constants: If desorption occurs very slow (compared to extraction), the extraction kinetics become less relevant for the overall

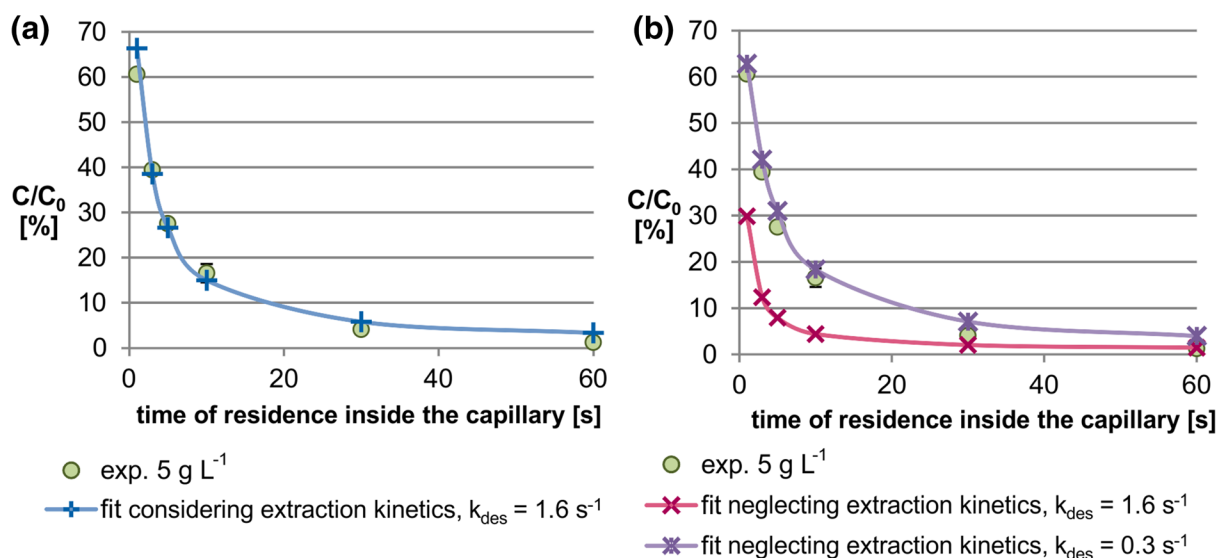


Fig. 7 Illustration how neglect of extraction kinetics affects the determined k_{des} using the example of allylbenzene extracted from BSA ($C=5 \text{ g L}^{-1}$). **a** The fit with $k_{des} = 1.6 \text{ s}^{-1}$ resulting from our data analysis procedure, which considers extraction kinetics of the freely

dissolved allylbenzene into PDMS. **b** Fits resulting from an alternative data analysis procedure, which neglects extraction kinetics. Neglecting extraction kinetics leads to an erroneously underestimated $k_{des} = 0.3 \text{ s}^{-1}$

transport kinetics, i.e., neglecting extraction kinetics distorts slower desorption rate constants less than faster ones.

Another pitfall of the simplified data analysis using linear regression of logarithmic concentration–time curves is that partition properties are neglected. If equilibrium between the extraction material and the sample is reached, the measured concentration profile will result in a plateau depending on the partition properties. Erroneously including parts of this plateau in the logarithmic plot from which the slope is to be determined leads to a lower slope again corresponding to an underestimation of the desorption rate constant. These two pitfalls might have decreased the accuracy of the published desorption rate constants. The more explicit data analysis presented in our study considers both the extraction kinetics from the water phase as well as the partition properties and thus avoids these pitfalls.

A further explanation for the missing correlation for some of the desorption rate constants from the literature might be the different temperatures in the experiments. While we performed our experiments at room temperature, some of the desorption rate constants in the literature were derived at $37 \text{ }^\circ\text{C}$. According to the paper from Svenson et al., a temperature increase from room temperature to $37 \text{ }^\circ\text{C}$ can lead to a two- to threefold faster desorption rate constant (Svenson et al. 1974).

Conclusion

In conclusion, the presented time-resolved extraction method combined with the transport model enables accurate investigation of desorption kinetics from albumin. The data obtained here suggest that k_{des} can be predicted from the molecular weight of a chemical according to Eq. (1). Considering the fact that our results were taken at room temperature, we suppose that the predicted k_{des} will reliably mark the lower limit of what can be expected for the physiological temperature of $37 \text{ }^\circ\text{C}$. The presented results can now be used to estimate the impact of desorption kinetics on uptake and metabolism of chemicals in the human liver. For doing so, application of a suitable model representing the features of the physiological situation (residence time, diffusion distances and albumin concentration) is necessary. A rough idea on the importance of this process can, however, already be gained from a direct comparison of our experimental curves with the in vivo situation in a human: A residence time of 4 s, which corresponds to the typical residence time of blood in the sinusoids of the liver (Schwen et al. 2015), was not sufficient for complete desorption of the test chemicals from albumin in our test system. For a more accurate comparison, suitable calculations considering the following aspects are necessary: (1) dimensions of the liver sinusoids are

different than dimensions in our capillary (average sinusoid diameter is only 7–9 μm (Wake and Sato 2015)), (2) the albumin concentration present in blood is higher than in our experiments (physiological albumin concentration in plasma is around 40 g L^{-1} (Peters Jr 1995b)), (3) the flow pattern might be different and (4) additional limitations due to blood flow or permeation into the hepatocytes are possible. Smaller dimensions of the sinusoids lead to shorter diffusion path lengths, which results in a faster extraction into the surrounding hepatocytes. A higher albumin concentration leads to a higher albumin-bound fraction. Both a faster extraction and a higher albumin-bound fraction increase the importance of desorption kinetics for physiological scenarios compared to our experiments. In a next step, we will implement these physiological features into the presented transport model to quantify the impact of desorption kinetics on hepatic metabolism *in vivo*.

Acknowledgements The authors thank Robert Köhler and Anett Georgi for technical support, Andrea Pfennigsdorff for lab assistance, Benjamin Schwarz for facilitating the measurement of a breakthrough curve and Satoshi Endo and Beate Escher for useful comments on our work. Additionally, we would like to thank the reviewers for their valuable comments which improved our manuscript strongly.

References

- Berezhkovskiy LM (2012) Determination of hepatic clearance with the account of drug–protein binding kinetics. *J Pharm Sci* 101(10):3936–3945. <https://doi.org/10.1002/jps.23235>
- Bradford MM (1976) A rapid and sensitive method for the quantitation of microgram quantities of protein utilizing the principle of protein–dye binding. *Anal Biochem* 72(1):248–254. [https://doi.org/10.1016/0003-2697\(76\)90527-3](https://doi.org/10.1016/0003-2697(76)90527-3)
- ChemAxon (2016) Instant JChem Version 16.1.4.0. Accessed April 2017. <http://www.chemaxon.com>
- Chen J, Schiel JE, Hage DS (2009) Noncompetitive peak decay analysis of drug–protein dissociation by high-performance affinity chromatography. *J Sep Sci* 32(10):1632–1641. <https://doi.org/10.1002/jssc.200900074>
- Eisert R, Pawliszyn J (1997) Automated in-tube solid-phase microextraction coupled to high-performance liquid chromatography. *Anal Chem* 69(16):3140–3147. <https://doi.org/10.1021/ac970319a>
- El Kadi N, Taulier N, Le Huérou JY et al (2006) Unfolding and refolding of bovine serum albumin at acid pH: ultrasound and structural studies. *Biophys J* 91(9):3397–3404. <https://doi.org/10.1529/biophysj.106.088963>
- Endo S, Goss K-U (2011) Serum albumin binding of structurally diverse neutral organic compounds: data and models. *Chem Res Toxicol* 24(12):2293–2301. <https://doi.org/10.1021/tx200431b>
- Endo S, Pfennigsdorff A, Goss K-U (2012) Salting-out effect in aqueous NaCl solutions: trends with size and polarity of solute molecules. *Environ Sci Technol* 46(3):1496–1503. <https://doi.org/10.1021/es203183z>
- Faerch T, Jacobsen J (1975) Determination of association and dissociation rate constants for bilirubin-bovine serum albumin. *Arch Biochem Biophys* 168(2):351–357. [https://doi.org/10.1016/0003-9861\(75\)90263-5](https://doi.org/10.1016/0003-9861(75)90263-5)
- Fang X, Vitrac O (2017) Predicting diffusion coefficients of chemicals in and through packaging materials. *Crit Rev Food Sci Nutr* 57(2):275–312. <https://doi.org/10.1080/10408398.2013.849654>
- Fasano M, Curry S, Terreno E et al (2005) The extraordinary ligand binding properties of human serum albumin. *IUBMB Life* 57(12):787–796. <https://doi.org/10.1080/15216540500404093>
- Ghuman J, Zunszain PA, Petitpas I, Bhattacharya AA, Otagiri M, Curry S (2005) Structural basis of the drug-binding specificity of human serum albumin. *J Mol Biol* 353(1):38–52. <https://doi.org/10.1016/j.jmb.2005.07.075>
- Gray RD, Stroupe SD (1978) Kinetics and mechanism of bilirubin binding to human serum albumin. *J Biol Chem* 253(12):4370–4377
- Hills EE, Abraham MH, Hersey A, Bevan CD (2011) Diffusion coefficients in ethanol and in water at 298 K: linear free energy relationships. *Fluid Phase Equilib* 303(1):45–55. <https://doi.org/10.1016/j.fluid.2011.01.002>
- Kopinke FD, Ramus K, Poerschmann J, Georgi A (2011) Kinetics of desorption of organic compounds from dissolved organic matter. *Environ Sci Technol* 45(23):10013–10019. <https://doi.org/10.1021/es2023835>
- Kramer NI, van Eijkeren JCH, Hermens JLM (2007) Influence of albumin on sorption kinetics in solid-phase microextraction: consequences for chemical analyses and uptake processes. *Anal Chem* 79(18):6941–6948. <https://doi.org/10.1021/ac070574n>
- Linden L, Goss K-U, Endo S (2017) 3D-QSAR predictions for bovine serum albumin–water partition coefficients of organic anions using quantum mechanically based descriptors. *Environ Sci Process Impacts* 19(3):261–269. <https://doi.org/10.1039/c6em00555a>
- Mendel CM (1989) The free hormone hypothesis: a physiologically based mathematical model. *Endocr Rev* 10(3):232–274. <https://doi.org/10.1210/edrv-10-3-232>
- Mielke H, Di Consiglio E, Kreutz R, Partosch F, Testai E, Gundert-Remy U (2017) The importance of protein binding for the *in vitro*–*in vivo* extrapolation (IVIVE)—example of ibuprofen, a highly protein-bound substance. *Arch Toxicol* 91(4):1663–1670. <https://doi.org/10.1007/s00204-016-1863-z>
- Peters T Jr (1995a) The albumin molecule: its structure and chemical properties. In: Peters T (ed) All about albumin. Academic Press, San Diego, pp 9–75
- Peters T Jr (1995b) Metabolism: albumin in the body. In: Peters T (ed) All about albumin. Academic Press, San Diego, pp 188–250
- Poulin P, Haddad S (2013) Toward a new paradigm for the efficient *in vitro*–*in vivo* extrapolation of metabolic clearance in humans from hepatocyte data. *J Pharm Sci* 102(9):3239–3251. <https://doi.org/10.1002/jps.23502>
- Rich RL, Day YSN, Morton TA, Myszka DG (2001) High-resolution and high-throughput protocols for measuring drug/human serum albumin interactions using BIACORE. *Anal Biochem* 296(2):197–207. <https://doi.org/10.1006/abio.2001.5314>
- Riley RJ, McGinness DF, Austin RP (2005) A unified model for predicting human hepatic, metabolic clearance from *in vitro* intrinsic clearance data in hepatocytes and microsomes. *Drug Metab Dispos* 33(9):1304–1311. <https://doi.org/10.1124/dmd.105.004259>
- Schwen LO, Schenk A, Kreutz C et al (2015) Representative sinusoids for hepatic four-scale pharmacokinetics simulations. *PLoS One* 10(7):e0133653. <https://doi.org/10.1371/journal.pone.0133653>
- Svenson A, Holmer E, Andersson L-O (1974) A new method for the measurement of dissociation rates for complexes between small ligands and proteins as applied to the palmitate and bilirubin complexes with serum albumin. *Biochim Biophys Acta Protein Struct* 342(1):54–59. [https://doi.org/10.1016/0005-2795\(74\)90105-6](https://doi.org/10.1016/0005-2795(74)90105-6)
- Ulrich N, Endo S, Brown TN, Watanabe N, Bronner G, Abraham MH, Goss KU (2017) UFZ-LSER database v 3.2. Accessed feb 2017. <http://www.ufz.de/lserd>

- Vandenbelt JM, Hansch C, Church C (1972) Binding of apolar molecules by serum albumin. *J Med Chem* 15(8):787–789. <https://doi.org/10.1021/jm00278a001>
- Wake K, Sato T (2015) “The Sinusoid” in the liver: lessons learned from the original definition by Charles Sedgwick Minot (1900). *Anat Rec* 298(12):2071–2080. <https://doi.org/10.1002/ar.23263>
- Weisiger RA (1985) Dissociation from albumin: a potentially rate-limiting step in the clearance of substances by the liver. *Proc Natl Acad Sci* 82(5):1563–1567
- Yoo MJ, Hage DS (2011a) High-throughput analysis of drug dissociation from serum proteins using affinity silica monoliths. *J Sep Sci* 34(16–17):2255–2263. <https://doi.org/10.1002/jssc.201100280>
- Yoo MJ, Hage DS (2011b) Use of peak decay analysis and affinity microcolumns containing silica monoliths for rapid determination of drug–protein dissociation rates. *J Chromatogr A* 1218(15):2072–2078. <https://doi.org/10.1016/j.chroma.2010.09.070>
- Zheng X, Li Z, Podariu MI, Hage DS (2014) Determination of rate constants and equilibrium constants for solution-phase drug–protein interactions by ultrafast affinity extraction. *Anal Chem* 86(13):6454–6460. <https://doi.org/10.1021/ac501031y>

D.2. The impact of desorption kinetics from albumin on hepatic extraction efficiency and hepatic clearance: a model study



The impact of desorption kinetics from albumin on hepatic extraction efficiency and hepatic clearance: a model study

Sophia Krause¹ · Kai-Uwe Goss^{1,2}

Received: 20 December 2017 / Accepted: 17 May 2018
© Springer-Verlag GmbH Germany, part of Springer Nature 2018

Abstract

Until now, the question whether slow desorption of compounds from transport proteins like the plasma protein albumin can affect hepatic uptake and thereby hepatic metabolism of these compounds has not yet been answered conclusively. This work now combines recently published experimental desorption rate constants with a liver model to address this question. For doing so, the used liver model differentiates the bound compound in blood, the unbound compound in blood and the compound within the hepatocytes as three well-stirred compartments. Our calculations show that slow desorption kinetics from albumin can indeed limit hepatic metabolism of a compound by decreasing hepatic extraction efficiency and hepatic clearance. The extent of this decrease, however, depends not only on the value of the desorption rate constant but also on how much of the compound is bound to albumin in blood and how fast intrinsic metabolism of the compound in the hepatocytes is. For strongly sorbing and sufficiently fast metabolized compounds, our calculations revealed a twentyfold lower hepatic extraction efficiency and hepatic clearance for the slowest known desorption rate constant compared to the case when instantaneous equilibrium between bound and unbound compound is assumed. The same desorption rate constant, however, has nearly no effect on hepatic extraction efficiency and hepatic clearance of weakly sorbing and slowly metabolized compounds. This work examines the relevance of desorption kinetics in various example scenarios and provides the general approach needed to quantify the effect of flow limitation, membrane permeability and desorption kinetics on hepatic metabolism at the same time.

Keywords Hepatic metabolism · Desorption kinetics · Albumin

Introduction

The rate of hepatic elimination of a compound present in blood depends not only on the intrinsic metabolic capacity of the liver but also on the delivery rate of the compound to the metabolically active sites. The metabolically active sites in the liver are metabolizing enzymes, which are located

within the hepatocytes. It follows that the delivery of a compound can thus be limited by blood flow into the liver and by permeation through cell membranes and adjacent water layers into the hepatocytes (Baker and Parton 2007; Gillette 1971; Wilkinson and Shand 1975). Apart from blood flow and permeation, desorption from blood components such as the plasma protein albumin is a further potential limitation for delivery (Weisiger 1985). The reason for this potential limitation is that many compounds are highly bound in blood but only the unbound fraction of the compounds can permeate into cells (Mendel 1989).

Most commonly, the mathematical treatment of the quantitative aspects of hepatic metabolism considers the liver as a well-stirred compartment. In this so-called well-stirred liver model, all components of the liver, e.g., blood within the liver and exiting the liver, blood proteins and hepatocytes, are assumed to be in instantaneous equilibrium with respect to the chemical (Rowland et al. 1973). The well-stirred liver model is mathematically simpler than other liver models (e.g., the parallel tube liver model) and easier

Electronic supplementary material The online version of this article (<https://doi.org/10.1007/s00204-018-2224-x>) contains supplementary material, which is available to authorized users.

✉ Sophia Krause
sophia.krause@ufz.de

✉ Kai-Uwe Goss
kai-uwe.goss@ufz.de

¹ Department of Analytical Environmental Chemistry, Helmholtz Centre for Environmental Research UFZ, Permoserstr. 15, 04318 Leipzig, Germany

² Institute of Chemistry, University of Halle-Wittenberg, Kurt-Mothes-Str. 2, 06120 Halle, Germany

to apply. The classical well-stirred one-compartment liver model can represent blood flow limitation but it cannot represent limitations caused by low membrane permeability or slow desorption kinetics from binding proteins. It is thus desirable to modify the classical well-stirred liver model in a way that permeation and desorption can be considered while the simplicity of a well-stirred compartment model is kept. To incorporate permeation kinetics into the model one has to treat the liver as a two-compartment model in which permeability limits the exchange between two separate well-stirred compartments, one representing the liver blood and the other representing the hepatocytes. If desorption kinetics are to be considered additionally, then a three-compartment model is needed where blood transport proteins represent a third well-stirred compartment.

Common parameters for characterization of the hepatic elimination capacity are hepatic clearance and hepatic extraction efficiency. The clearance is often imagined as the blood or plasma volume which is cleared from a compound per time unit and the extraction efficiency corresponds to the concentration difference between inflowing and outflowing blood relative to the concentration in inflowing blood. It is important to realize that both metrics are related but by no means equivalent; high extraction efficiency means that most of the chemical delivered to the liver by blood flow is metabolized. If the blood flow rate would now be increased (leaving blood concentration and metabolic capacity unaltered) then the extraction efficiency would decrease because the blood residence time in the liver decreases. In contrast, the amount of chemical metabolized per time (and thus the clearance) would increase at the same time, because the amount of chemical delivered to the hepatocytes would be higher.

In this publication, we want to quantify hepatic elimination by calculating the extraction efficiency and hepatic clearance under consideration of blood flow, membrane permeability and desorption kinetics from albumin in a model that depicts the liver as three well-stirred sub-compartments. Until now, consideration of desorption kinetics in addition to blood flow and permeability was rarely done in the literature, likely because little knowledge on desorption kinetics themselves existed. In a previous study (Krause et al. 2017), we measured desorption rate constants of organic chemicals from albumin with a time-resolved extraction method and found a mechanistically plausible correlation for their prediction. We now address the question how desorption kinetics impact hepatic elimination in humans using these recently published experimental values for desorption rate constants.

Methods

Implementation of desorption kinetics from albumin into a well-stirred model

For a quantitative understanding of the metabolic efficiency of the liver, we need to know the chemical concentrations in blood entering and leaving the liver for given boundary conditions. Under constant boundary conditions, i.e. constant blood flow and constant concentration in the inflowing blood as well as constant metabolic capacity and constant volumes of all system components, the liver will reach a steady-state situation. This means that the outflowing blood concentration does not change with time anymore. For the scenario that only considers blood flow limitation and metabolic capacity, an analytical solution for calculation of the extraction efficiency under steady-state condition exists in the literature already (Rowland et al. 1973).

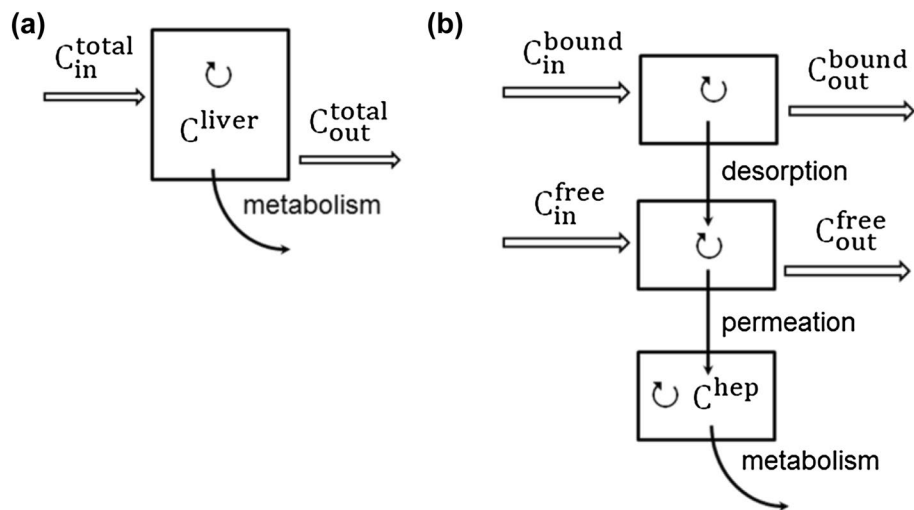
Here we now show how an analytical mathematical expression for the steady-state extraction efficiency that covers the combined influence of blood flow rate, intrinsic metabolic capacity, permeation and desorption kinetics on the outflowing blood concentration can be derived. For doing so, the liver is considered as an aggregation of three well-stirred compartments (Fig. 1) and two mass balance approaches are combined: one for the freely dissolved and one for the sorbed concentrations entering and leaving the blood pool of the liver in a steady-state situation.

The difference between freely dissolved compound flowing in and out of the blood pool of the liver equals the loss/gain due to permeation into/from the hepatocytes and the loss/gain due to sorptive exchange with albumin both expressed as first-order (diffusion controlled) kinetic processes:

$$Q \times C_{\text{water}} (C_{\text{in}}^{\text{free}} - C_{\text{out}}^{\text{free}}) = P_{\text{hep}} \times A \times (C_{\text{out}}^{\text{free}} - C_{\text{hep}}^{\text{free}}) - k_{\text{des}} \times V_{\text{alb}} \times (C_{\text{out}}^{\text{bound}} - C_{\text{out}}^{\text{free}} \times K_{\text{AW}}), \quad (1)$$

where Q is the volumetric blood flow rate (in mL_{blood}/s), C_{water} is the volume concentration of water in blood (in mL_{water}/mL_{blood}) and $C_{\text{in}}^{\text{free}}$ and $C_{\text{out}}^{\text{free}}$ are the freely dissolved concentrations of the compound in in- and outflowing blood (in mol/mL_{water}). P_{hep} is the total permeability between blood and hepatocytes (in cm/s), A is the exchange surface area between blood and hepatocytes (in cm²), $C_{\text{hep}}^{\text{free}}$ is the freely dissolved concentration of the compound in the hepatocytes (in mol/mL_{water}), k_{des} is the desorption rate constant (in 1/s), V_{alb} is the albumin volume (in mL_{alb}), $C_{\text{out}}^{\text{bound}}$ is the albumin bound concentration of the compound in blood (in mol/mL_{albumin}) and K_{AW} is the albumin–water partition coefficient (mL_{alb}/mL_{water}) of the studied compound. The

Fig. 1 Scheme of the classical well-stirred liver model (a) and the here-presented liver model, which considers the liver as an aggregation of three separate well-stirred sub-compartments (b). Both models quantify the metabolic efficiency based on the chemical concentrations in blood entering and leaving the liver. The classical well-stirred liver model considers only blood flow limitation. The sub-compartmental model additionally considers desorption and permeation kinetics by differentiating freely dissolved and albumin-bound chemical concentration (C^{free} and C^{bound})



albumin–water partition coefficient is a measure for the partition properties of a compound and is used here as an alternative to the association constant K_a (in L/mol). Both constants can be converted into each other via the molar mass and the density of albumin, for detailed explanation we refer to appendix of Endo and Goss (2011). Using the albumin–water partition coefficient is more convenient for the here-presented mass balance approach. Information on the intrinsic metabolic capacity of the hepatocytes is implicitly contained in this mass balance approach, because the freely dissolved concentration of the compound in the hepatocytes of course depends on metabolism. The detailed mathematic formulation of the metabolism term is derived from the fact that, in case of steady state, the mass of compound metabolized per unit time in the hepatocytes equals the mass that permeates into the hepatocytes per unit time:

$$P_{\text{hep}} \times A \times (C_{\text{out}}^{\text{free}} - C_{\text{hep}}^{\text{free}}) = k_{\text{int}} \times V_{\text{hep}}^{\text{total}} \times C_{\text{hep}}^{\text{total}}. \quad (2)$$

In this approach, we express the metabolic capacity by the intrinsic metabolism rate constant k_{int} with the unit 1/s that multiplies with the total compound concentration in the hepatocytes $C_{\text{hep}}^{\text{total}}$ (in mol/mL_{hepatocytes}) and the total hepatocyte volume $V_{\text{hep}}^{\text{total}}$ (in mL_{hepatocytes}) to yield the metabolism rate (in mol/s). An alternative parameter for the intrinsic

metabolic capacity is the intrinsic clearance, which corresponds to the volume that is cleared from the chemical by metabolism per time unit. Both parameters can be used for quantification of metabolism as long as both are used in a consistent way throughout the entire formalism.

The second mass balance approach considers the sorbed concentrations. The difference between compound flowing in and out of the blood pool of the liver in the sorbed state equals the loss due to the kinetic desorption process within the liver blood pool which is driven by the difference between the actual sorbed concentration C_{bound} (which equals $C_{\text{bound}}^{\text{bound}}$ in a well-stirred hepatic blood compartment) and the hypothetical sorbed concentration that is expected under equilibrium conditions, $C_{\text{out}}^{\text{free}} \times K_{\text{AW}}$ (which equals $C_{\text{out}}^{\text{free}} \times K_{\text{AW}}$ in a well-stirred hepatic blood compartment):

$$Q \times C_{\text{alb}} (C_{\text{in}}^{\text{bound}} - C_{\text{out}}^{\text{bound}}) = k_{\text{des}} \times V_{\text{alb}} \times (C_{\text{out}}^{\text{bound}} - C_{\text{out}}^{\text{free}} \times K_{\text{AW}}), \quad (3)$$

where Q again is the volumetric blood flow rate (in mL_{blood}/s), C_{alb} is the volume concentration of albumin in blood (in mL_{alb}/mL_{blood}) and $C_{\text{in}}^{\text{bound}}$ and $C_{\text{out}}^{\text{bound}}$ are the albumin bound concentrations of the compound in in- and out-flowing blood (in mol/mL_{alb}).

Rearrangement of the two equations allows calculation of the extraction efficiencies E^f and E^b for the freely dissolved and the sorbed concentrations, respectively (see SI Sect. 1 for details):

$$E^f = \frac{P_{\text{hep}}A \left(1 - \frac{P_{\text{hep}}A}{k_{\text{int}} \times V_{\text{hep}}^{\text{total}} \times K_{\text{hep/water}} + P_{\text{hep}}A} \right) - \frac{k_{\text{des}} V_{\text{alb}} (Q C_{\text{alb}} K_{\text{AW}} + k_{\text{des}} V_{\text{alb}} K_{\text{AW}})}{k_{\text{des}} V_{\text{alb}} + Q C_{\text{alb}}} + k_{\text{des}} V_{\text{alb}} K_{\text{AW}}}{QC_{\text{water}} + P_{\text{hep}}A \left(1 - \frac{P_{\text{hep}}A}{k_{\text{int}} \times V_{\text{hep}}^{\text{total}} \times K_{\text{hep/water}} + P_{\text{hep}}A} \right) + k_{\text{des}} V_{\text{alb}} \left(\frac{-k_{\text{des}} V_{\text{alb}} K_{\text{AW}}}{k_{\text{des}} V_{\text{alb}} + Q C_{\text{alb}}} + K_{\text{AW}} \right)} \quad (4)$$

and

$$E^b = \frac{k_{\text{des}} V_{\text{alb}} - k_{\text{des}} V_{\text{alb}} (1 - E^f)}{Q C_{\text{alb}} + k_{\text{des}} V_{\text{alb}}} \quad (5)$$

These two extraction efficiencies can be combined so that the total extraction efficiency E^{total} can be calculated according to:

$$E^{\text{total}} = f_u E^f + f_b E^b, \quad (6)$$

where f_u refers to the freely dissolved fraction of the compound in blood and f_b refers to the albumin-bound fraction in blood. The freely dissolved fraction f_u of a chemical can be derived from the albumin–water partition coefficient according to:

$$f_u = \frac{1}{\left(1 + K_{\text{AW}} \times \frac{V_{\text{alb}}}{V_{\text{water}}}\right)} \quad (7)$$

The albumin-bound fraction in blood can then be derived from $f_b = 1 - f_u$.

The hepatic clearance Cl_h can be calculated from the total extraction efficiency according to:

$$Cl_h = Q \times E^{\text{total}} \quad (8)$$

For a fixed blood flow rate Q , the hepatic clearance changes proportional to the total extraction efficiency. For the following discussion, all calculations were made based on the same input value for a typical physiological liver blood flow rate and the discussion will focus on resulting changes of the extraction efficiency when different desorption rate constants are used.

Input data

For our goal to investigate the effect of desorption kinetics on the extraction efficiency, we need to select realistic parameter values. These include physiological blood flow rates in the sinusoids of the human liver, permeability from the sinusoids into the hepatocytes, exchange area between the sinusoids and hepatocytes, desorption rate constants from albumin, metabolism rate constants, equilibrium partition coefficients to albumin and the hepatocytes, the albumin concentration in the blood and the volumes of hepatocytes and blood in direct exchange with the hepatocytes.

In the literature, different values for physiological blood flow rates in human exist, ranging from 900 to 1700 mL/min (Wynne et al. 1989). The permeability is not the focus of this work; we thus used permeabilities sufficiently high to avoid a potential limitation due to slow permeation. This topic will be investigated in a separate work. Desorption rate constants were varied in the range of published experimental values [k_{des} ranging from 2 to 0.02 1/s (Faerch and Jacobsen 1975;

Gray and Stroupe 1978; Krause et al. 2017; Svenson et al. 1974)]. Metabolism rate constants were varied such that the resulting extraction efficiencies range from low values up to 0.9, which appears to be the relevant range. For the equilibrium partitioning towards albumin, we covered a broad range of albumin–water partition coefficients (K_{AW} ranging from 1 to 100,000 mL_{alb}/mL_{water}). By this, we include a variety of different compounds in our calculations: weakly sorbing compounds which are preferably present freely dissolved in blood, i.e. the freely dissolved fraction f_u of these compounds approaches the value 1, are considered as well as strongly sorbing compounds which are preferably bound to albumin, i.e. the freely dissolved fraction f_u approaches the value 0. The freely dissolved fractions were calculated from the used albumin–water partition coefficients according to Eq. (7). Another required input information is the equilibrium partitioning towards the hepatocytes, i.e. the hepatocyte–water partition coefficient of the compound. For neutral organic compounds, it is intuitive that the partition behavior towards the hepatocytes should broadly correlate with the partition behavior towards albumin. Indeed, the hepatocyte–water partition coefficient can be deduced from combining the contributions from protein, lipid and water of the hepatocytes to the overall sorption to hepatocytes (Endo et al. 2013) (see SI Sect. 2 for example calculations). We, therefore, decided that it made sense to not vary both partition coefficients independently from each other but to derive the hepatocyte–water partition coefficient from the albumin–water partition coefficient via a plausible empirical relationship (see SI Sect. 2).

Hepatic elimination of course depends on the quantity of metabolic active cells. It is known from the literature that roughly 30% of the liver volume are blood (Eipel et al. 2010). It thus follows that 70% of the liver volume are liver cells and among these 65% (Kuntz 2008) are assumed to be hepatocytes. Assuming a liver volume of 1.4 L [experimental values ranging from 1.1 to 1.7 L (Davies and Morris 1993; Johnson et al. 2005; Wynne et al. 1989)], the volume of hepatocytes thus corresponds to about 660 mL. To correctly consider permeation and desorption, we also need to quantify the blood volume that exchanges compounds with the hepatocytes, i.e. the sinusoidal blood volume. This information is difficult to estimate and according to our knowledge only two values are available in the literature (Eipel et al. 2010; Villeneuve et al. 1996). These correspond to 250 and 170 mL for our assumed liver volume. At the same time, existing experimental values for blood flow velocities in sinusoids range from 0.02 to 0.28 cm/s with a mean of 0.1 cm/s (Puhl et al. 2003) and the sinusoidal length is known to be about 400–500 μm (Kuehnelt 2003). These values should actually be consistent with the published blood flow rates and sinusoidal volumes and thus offer a possibility to check if the used values are sensible. Blood flow rate Q

combined with sinusoidal volume V as well as flow velocity v combined with the sinusoid length l can both be used to calculate the residence time of blood in the sinusoids. Accordingly, the following relationship for these four parameters can be formulated:

$$\frac{V}{Q} = \frac{l}{v}. \quad (9)$$

Rearrangement of Eq. (9) gives the following expression for the blood flow rate Q :

$$Q = \frac{V}{l} \times v. \quad (10)$$

Combining an assumed sinusoidal volume of 200 mL with a sinusoid length of 500 μm and a flow velocity of 0.1 cm/s gives a blood flow rate of 24,000 mL/min. This calculated blood flow rate greatly exceeds the experimental values found in the literature and is not realistic in a physiological sense. If we assume that the reported blood flow rate is accurate, then one or several of the other physiological parameters (sinusoidal volume, sinusoid length or flow velocity) need to be adjusted so that a consistent data set is achieved. We assume that, among these, the sinusoid length is the best characterized parameter. In our opinion, only small deviations due to the three-dimensional arrangement of the sinusoids are conceivable so that we correct the sinusoid length by no more than 100 μm from 500 to 600 μm . For the flow velocities inside the sinusoids, we suggest that the measured range should not be exceeded because the optical methods used for the measurement should actually be quite reliable. Thus, we suggest to use a value of 0.03 cm/s, which is at the lower end of the range Puhl et al. measured (Puhl et al. 2003). This value is also given in anatomical textbooks as a common value for blood flow velocities in capillaries (Bullock et al. 2001). Consequently, the last parameter, which remains to be adjusted is the sinusoidal volume. Indeed, it follows that the sinusoidal volume needs to be set to 50 mL—much lower than reported—when combination of the sinusoid length of 600 μm and flow velocity of 0.03 cm/s shall yield sensible results for the blood flow rate. With these numbers the calculated blood flow rate is 1500 mL/min, which still is within the range of published experimental blood flow rates. Accordingly, we consider these values for sinusoid length, flow velocity and sinusoid volume as internally consistent and physiologically realistic.

The last required input information is the albumin concentration in blood. The concentration of serum albumin in human plasma is about 40 g/L (Peters Jr 1995). Considering that circa 60% of the total blood volume is plasma (Snyder et al. 1975), it follows that the albumin concentration in blood is 24 g/L. For our calculations we assume that albumin is the only sorbing component in blood.

Results and discussion

Partition properties of the compound affect E^{total}

Before starting to quantify the influence of desorption kinetics on the total extraction efficiency, a few characteristics resulting from the partition properties of the compound need to be considered, because the impact of desorption kinetics will always be related to the impact of partition properties. To evaluate the sole impact of the partition properties on extraction efficiency and clearance of a compound, we first start with a simplified scenario in which desorption and permeation kinetics are set to sufficiently high values so that no limitations result ($k_{\text{des}} = 20$ 1/s, $P_{\text{hep}} = 1000$ cm/s).

For the calculation of this simplified scenario, different albumin–water partition coefficients, which dictate the freely dissolved fractions f_u in blood and which are a measure of a compound's partition properties, are combined with different k_{int} and the resulting total extraction efficiencies are compared. Figure 2 shows the resulting total extraction efficiencies. For all calculations, a liver blood flow rate of 1500 mL/min was used.

Combination of one k_{int} with different albumin–water partition coefficients and thus different freely dissolved fractions in blood leads to different total extraction efficiencies. The reason for this is that compounds that show stronger partitioning towards albumin, i.e. have lower freely dissolved fractions, will also show stronger partitioning towards the hepatocytes and are thus metabolized more efficiently. The extent of this effect, however, is also dependent on the intrinsic metabolism rate constants themselves. Extremely high k_{int} reduces the relative impact of the partition properties on E^{total} , because metabolism is so fast that nearly everything that is delivered via blood flow is metabolized and the total extraction efficiency approaches the value of 100%. In contrast, in case of very low k_{int} , the compounds are removed out of the liver by blood flow faster than they

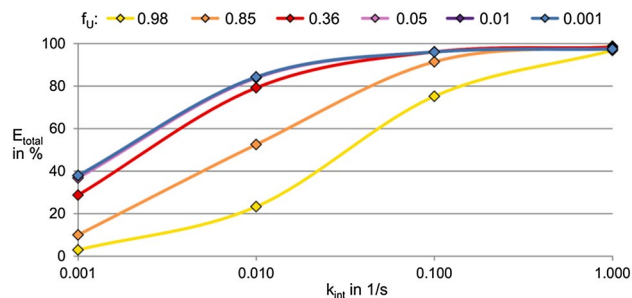


Fig. 2 Calculated extraction efficiencies as a function of the freely dissolved fraction f_u in blood and the metabolism rate constant k_{int} when desorption kinetics are very fast ($k_{\text{des}} = 20$ 1/s). Permeation kinetics are set such that no limitation ($P_{\text{hep}} = 1000$ cm/s) occurs. Liver blood flow rate is 1500 mL/h

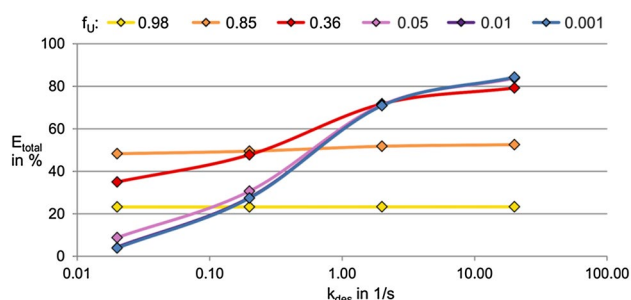


Fig. 3 Calculated extraction efficiencies for different desorption rate constants k_{des} and different freely dissolved fractions f_u . In this example, a metabolism rate constant $k_{int} = 0.01$ 1/s, a high permeability $P_{hep} = 1000$ cm/s and a blood flow rate $Q = 1500$ mL/min are used

can be metabolized and the total extraction efficiency approaches 0%.

Slow desorption can reduce E^{total} significantly

After realizing how the partition properties influence E^{total} , we now evaluate the influence of desorption kinetics on E^{total} . For doing so, we use an intrinsic metabolism rate constant of $k_{int} = 0.01$ 1/s, because this k_{int} leads to total extraction efficiencies in the desired range (Fig. 2). For evaluation of the impact of desorption kinetics, we reduce the desorption rate constants stepwise from a value that has no impact on the total extraction efficiency in our scenarios ($k_{des} = 20$ 1/s) to the lowest value that has been published in the literature ($k_{des} = 0.02$ 1/s) and compare the results. Permeability again is set to a high value causing no limitation ($P_{hep} = 1000$ cm/s) and a liver blood flow rate of 1500 mL/min is used. Figure 3 summarizes the results of these calculations.

It is intuitive that desorption kinetics have no impact on the total extraction efficiencies of weakly sorbing compounds because the biggest fraction of these compounds is present freely dissolved in blood instead of bound to albumin. Weakly sorbing compounds are represented by the yellow ($f_u = 0.98$) and orange data points ($f_u = 0.85$) in Fig. 3, which show almost identical extraction efficiencies no matter which k_{des} value is used in the calculation. Examples for such weakly sorbing compounds are simple polar compounds such as paracetamol or metoprolol with amino or hydroxyl groups.

With increasing sorbing character of the compound, the impact of desorption kinetics on the total extraction efficiencies grows, because the fraction bound to albumin in blood increases and this fraction is sensitive to a potential desorption limitation. For moderately sorbing compounds ($f_u = 0.36$), represented by the red data points, this leads to a reduction of total extraction efficiencies by factor 2 from 80% for non-limiting k_{des} to roughly 40% for the slowest k_{des} . A slightly stronger effect is observed for the strongly sorbing

compounds (magenta data points, $f_u = 0.05$). Here, a reduction of the total extraction efficiencies from 80% to roughly 10% results from slow desorption. Examples for the groups of moderately to strongly sorbing compounds are compound classes such as phthalates, parabens, benzodiazepines (e.g., diazepam) and propionic acid derivatives such as ibuprofen.

Very strongly sorbing compounds ($f_u < 0.01$) are represented by the blue and purple data points in Fig. 3. The latter, however, are overlain by the blue data points and, therefore, not visible. Examples for very strongly sorbing compounds could be industrial chemicals such as PCBs (polychlorinated biphenyls) or PAHs (polycyclic aromatic hydrocarbons). The total extraction efficiencies of these compounds are reduced by factor 20 from 84% for non-limiting k_{des} to 4% for the slowest k_{des} . The example of the blue and purple data points additionally shows that the impact of desorption kinetics has an upper limit. When a freely dissolved fraction of $f_u = 0.01$ is reached, further increase of the albumin–water partition coefficient does not impact the calculated E^{total} anymore. The reason for this is that the fraction bound to albumin approaches a value of 1 if a certain albumin–water partition coefficient is reached and further increase of the albumin–water partition coefficient only leads to minimal changes of the bound fraction.

Fast metabolism is a prerequisite for relevance of desorption kinetics

Apart from the partition properties of the compound, the metabolism itself is a second important determinant for the impact of desorption kinetics on E^{total} . It is intuitive that desorption kinetics become less important in case metabolism is very slow. Figure 4 illustrates this statement. In this example, the used k_{des} comprises the same range as in Fig. 3. The intrinsic metabolism rate constant, however, is reduced to $k_{int} = 0.001$ 1/s. We again exclude permeation limitation

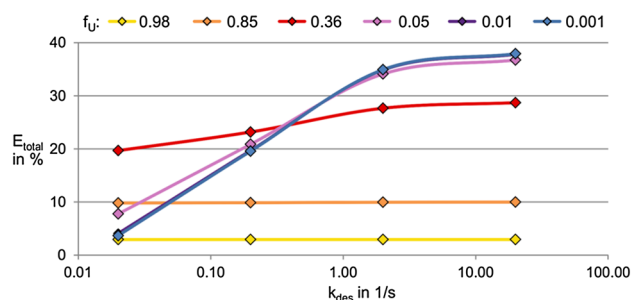


Fig. 4 Calculated total extraction efficiencies using again different desorption rate constants ($k_{des} = 0.02$ – 20 1/s), but this time in combination with a slower metabolism rate constant ($k_{int} = 0.001$ 1/s). We again use a high permeability $P_{hep} = 1000$ cm/s and the blood flow rate $Q = 1500$ mL/min

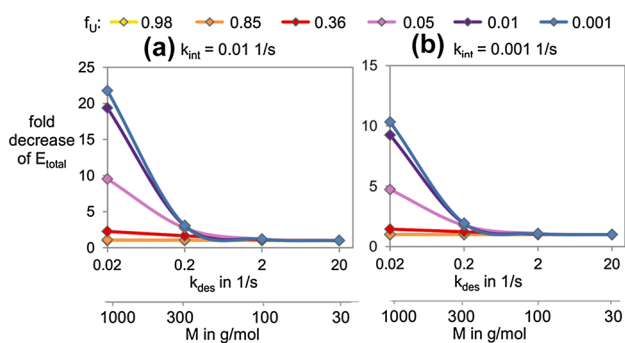


Fig. 5 Summary as to how the total extraction efficiencies decrease depending on the value of the desorption rate constant k_{des} and the freely dissolved fraction f_u . **a** The results for the fast metabolism rate constant $k_{\text{int}} = 0.01$ 1/s and **b** the results in case of the slower metabolism with $k_{\text{int}} = 0.001$ 1/s. Again a high permeability $P_{\text{hep}} = 1000$ cm/s and the physiological blood flow rate $Q = 1500$ mL/min were used. The previously found exponential relationship between the molar mass of a chemical and its desorption rate constant is indicated by the second x -axis (Krause et al. 2017)

by setting permeability to a high value ($P_{\text{hep}} = 1000$ cm/s) and use the physiological blood flow rate of 1500 mL/min.

The total extraction efficiencies are now generally lower than before, because the used metabolism rate constant $k_{\text{int}} = 0.001$ 1/s is smaller. Introducing desorption limitation by reducing k_{des} from 20 to 0.02 1/s again has nearly no influence on the extraction efficiencies of weakly sorbing compounds, i.e. the data points are on the same level for the entire range of k_{des} . For strongly sorbing compounds, the total extraction efficiency again reduces as desorption limitation is introduced. This effect, however, is now lower than before. Instead of a reduction by a factor 20, the extraction efficiencies for strongly sorbing compounds are now reduced by a factor 10 from 37 to 3.7%.

Figure 5 sums up these findings by comparing the fold decrease of E^{total} when the same desorption rate constants are combined with different intrinsic metabolism rate constants and different freely dissolved fractions: panel (a) represents the calculations with a $k_{\text{int}} = 0.01$ 1/s and panel (b) represents the calculations with a $k_{\text{int}} = 0.001$ 1/s.

When combining the slowest known desorption rate constant $k_{\text{des}} = 0.02$ 1/s with very strongly sorbing compounds ($f_u < 0.01$) and a fast metabolism rate constant ($k_{\text{int}} = 0.01$ 1/s), the calculated E^{total} is twentyfold lower than it was when instantaneous sorption equilibrium between albumin and water was assumed (Fig. 5a). In a previous publication (Krause et al. 2017), we reported a relationship between the desorption rate constants and molar mass of a chemical and we indicated this exponential relationship here by the second x -axis in Fig. 5. According to this empirical relationship k_{des} values around 0.02 1/s are only realistic for high molecular weight compounds. In the case of the above-given examples for very strongly sorbing compounds, this might be only

realistic for PCBs as the molar masses of PAHs mostly do not exceed 300 g/mol. A twentyfold lower extraction efficiency due to slow desorption can thus be regarded as an extreme scenario. For more common cases, the impact of desorption kinetics on hepatic extraction efficiency will be lower. Chemicals with molar masses in the range of 200 to 300 g/mol have desorption rate constants in the order of 0.2 1/s. For moderately to very strongly sorbing compounds such as phthalates, parabens, benzodiazepines, propionic acid derivatives and PAHs, a reduction of E^{total} due to desorption kinetics by not more than factor 2 to 3 in case of fast metabolism appears to be realistic. Slower metabolism ($k_{\text{int}} = 0.001$ 1/s, Fig. 5b) diminishes this effect further so that a reduction by not more than factor 2 results.

Conclusions

Our calculations show that slow desorption from albumin is only relevant for hepatic metabolism of strongly sorbing compounds that are metabolized sufficiently fast in hepatocytes. For these compounds, the hepatic extraction efficiency and accordingly the hepatic clearance decrease with decreasing desorption rate constant k_{des} . The extent of this decrease, however, depends not only on the value of k_{des} but also on the intrinsic metabolism rate constant and the partition properties of the compound. Accordingly, for some compounds, the extraction efficiency is decreased by a factor of 10, while for other compounds, the extraction efficiency is only decreased by a factor 2–3 or even less when desorption kinetics are considered in hepatic metabolism. A decrease by more than a factor of 10 is unlikely, because it requires combination of extreme conditions in terms of the values of k_{des} , k_{int} and the partition properties of the compound. Furthermore, one has to note that we assume that albumin is the only sorbing component in blood. We neglect other binding proteins, blood lipids and blood cells, because neither their sorption capacities nor desorption kinetics from these blood components are known. If considerable sorption to these components occurred, the extraction efficiencies would not only depend on the desorption kinetics from albumin but would also be influenced by the desorption kinetics from these other blood components. The presented model could also be applied to quantify the impact of desorption from other binding blood components on hepatic metabolism. For doing so, the parameters describing desorption kinetics from albumin and partition behavior, i.e. binding affinity, to albumin need to be replaced by parameters describing the binding component of interest.

Another important point is that the presented calculations are based on the well-stirred liver model. From the literature it is known, however, that the well-stirred liver

model is not suitable when the intrinsic clearance is fast compared to blood flow and a concentration gradient along the liver sinusoids develops (Kirichuk and Lutsevich 1996; Pang and Rowland 1977). Accordingly, the application of the so-called parallel tube model, which considers the liver as an aggregation of cylindrical tubes with a decrease in compound concentration along the tubes, might be interesting for those cases where high metabolism rate constants apply. Implementation of desorption kinetics into the parallel tube model requires a more complex, numerical approach, which will be the subject of future work.

Acknowledgements The authors thank Satoshi Endo for very helpful comments on this manuscript.

References

- Baker M, Parton T (2007) Kinetic determinants of hepatic clearance: plasma protein binding and hepatic uptake. *Xenobiotica* 37(10–11):1110–1134. <https://doi.org/10.1080/00498250701658296>
- Bullock J, Boyle J, Wang MB (2001) *The Vascular System, Physiology*. Lippincott Williams & Wilkins, pp 128–134
- Davies B, Morris T (1993) Physiological parameters in laboratory animals and humans. *Pharm Res* 10(7):1093–1095. <https://doi.org/10.1023/a:1018943613122>
- Eipel C, Abshagen K, Vollmar B (2010) Regulation of hepatic blood flow: the hepatic arterial buffer response revisited. *World J Gastroenterol* 16(48):6046–6057. <https://doi.org/10.3748/wjg.v16.i48.6046>
- Endo S, Goss K-U (2011) Serum albumin binding of structurally diverse neutral organic compounds: data and models. *Chem Res Toxicol* 24(12):2293–2301. <https://doi.org/10.1021/tx200431b>
- Endo S, Brown TN, Goss K-U (2013) General model for estimating partition coefficients to organisms and their tissues using the biological compositions and polyparameter linear free energy relationships. *Environ Sci Technol* 47(12):6630–6639. <https://doi.org/10.1021/es401772m>
- Faerch T, Jacobsen J (1975) Determination of association and dissociation rate constants for bilirubin-bovine serum albumin. *Arch Biochem Biophys* 168(2):351–357. [https://doi.org/10.1016/0003-9861\(75\)90263-5](https://doi.org/10.1016/0003-9861(75)90263-5)
- Gillette JR (1971) Factors affecting drug metabolism. *Ann N Y Acad Sci* 179(1):43–66. <https://doi.org/10.1111/j.1749-6632.1971.tb46890.x>
- Gray RD, Stroupe SD (1978) Kinetics and mechanism of bilirubin binding to human serum albumin. *J Biol Chem* 253(12):4370–4377
- Johnson TN, Tucker GT, Tanner MS, Rostami-Hodjegan A (2005) Changes in liver volume from birth to adulthood: a meta-analysis. *Liver Transpl* 11(12):1481–1493. <https://doi.org/10.1002/lt.20519>
- Kirichuk VF, Lutsevich AN (1996) Modeling of drug elimination by the liver. I. Main concepts and physiologically justified clearance models (a review). *Pharm Chem J* 30(5):285–292. <https://doi.org/10.1007/bf02333961>
- Krause S, Ulrich N, Goss K-U (2017) Desorption kinetics of organic chemicals from albumin. *Arch Toxicol*. <https://doi.org/10.1007/s00204-017-2117-4>
- Kuehnel W (2003) *Digestive system, color atlas of cytology, histology, and microscopic anatomy*. Thieme, pp 272–339
- Kuntz E, Kuntz H-D (2008) *Hepatology textbook and atlas*. Springer
- Mendel CM (1989) The free hormone hypothesis: a physiologically based mathematical model. *Endocr Rev* 10(3):232–274. <https://doi.org/10.1210/edrv-10-3-232>
- Pang KS, Rowland M (1977) Hepatic clearance of drugs. I. Theoretical considerations of a “well-stirred” model and a “parallel tube” model. Influence of hepatic blood flow, plasma and blood cell binding, and the hepatocellular enzymatic activity on hepatic drug clearance. *J Pharmacokinet Biopharm* 5(6):625–653. <https://doi.org/10.1007/bf01059688>
- Peters T Jr (1995) *Metabolism: albumin in the body, all about albumin*. Academic Press, San Diego, pp 188–250
- Puhl G, Schaser KD, Vollmar B, Menger MD, Settmacher U (2003) Noninvasive in vivo analysis of the human hepatic microcirculation using orthogonal polarization spectral imaging. *Transplantation* 75(6):756–761. <https://doi.org/10.1097/01.TP.0000056634.18191.1A>
- Rowland M, Benet LZ, Graham GG (1973) Clearance concepts in pharmacokinetics. *J Pharmacokinet Biopharm* 1(2):123–136. <https://doi.org/10.1007/bf01059626>
- Snyder W, Cook M, Nasset E, Karhausen L, Howells G, Tipton I (1975) *ICRP Publication 23: report of the task group on reference man*. Elmford. International Commission on Radiological Protection, NY
- Svenson A, Holmer E, Andersson L-O (1974) A new method for the measurement of dissociation rates for complexes between small ligands and proteins as applied to the palmitate and bilirubin complexes with serum albumin. *Biochim Biophys Acta Protein Struct* 342(1):54–59. [https://doi.org/10.1016/0005-2795\(74\)90105-6](https://doi.org/10.1016/0005-2795(74)90105-6)
- Villeneuve JP, Dagenais M, Huet PM, Roy A, Lapointe R, Marleau D (1996) The hepatic microcirculation in the isolated perfused human liver. *Hepatology* 23(1):24–31. <https://doi.org/10.1002/hep.510230104>
- Weisiger RA (1985) Dissociation from albumin: a potentially rate-limiting step in the clearance of substances by the liver. *Proc Natl Acad Sci* 82(5):1563–1567
- Wilkinson GR, Shand DG (1975) Physiological approach to hepatic drug clearance. *Clin Pharmacol Ther* 18(4):377–390
- Wynne HA, Cope LH, Mutch E, Rawlins MD, Woodhouse KW, James OF (1989) The effect of age upon liver volume and apparent liver blood flow in healthy man. *Hepatology* 9(2):297–301. <https://doi.org/10.1002/hep.1840090222>

List of figures

Fig. 1 Schematic representation of the experimental set-up for time-resolved extraction experiments	5
Fig. 2 Detailed scheme of the used experimental set-up	8
Fig. 3 Scheme of the spatial discretization in the diffusion model	9
Fig. 4 Scheme of the spatial discretization in the dispersion-convection model	11
Fig. 5 Extraction from water	13
Fig. 6 Extraction of 1,2,3,4-tetrachlorobenzene from water and BSA	14
Fig. 7 Extraction of 1,2,3,4-tetrachlorobenzene from BSA	15
Fig. 8 Desorption rate constants versus albumin-water partition coefficients	19
Fig. 9 Desorption rate constants versus molar masses	20
Fig. 10 Illustration how neglect of extraction kinetics affects k_{des}	22
Fig. 11 Scheme of the classical well-stirred liver model (part a) and the here presented liver model (part b).....	25
Fig. 12 Calculated extraction efficiencies as a function of the freely dissolved fraction f_u and the metabolism rate constant k_{int}	34
Fig. 13 Calculated extraction efficiencies for different desorption rate constants k_{des} and different freely dissolved fractions f_u	37
Fig. 14 Calculated extraction efficiencies for different desorption rate constants k_{des} and different freely dissolved fractions f_u	38
Fig. 15 Summary as to how the total extraction efficiencies E decrease depending on the value of the desorption rate constant k_{des} and the freely dissolved fraction f_u	39

List of tables

Table 1: Albumin recoveries after pumping albumin suspensions through the capillary.	7
Table 2: List of test chemicals with determined desorption rate constants (k_{des}) and corresponding albumin-water and PDMS-water partition coefficients	16
Table 3: Composition of the non-aqueous hepatocyte components.....	54
Table 4: Partition coefficients for different biological phases.....	54
Table 5: Comparison of partition coefficients.	55

Danksagung

An dieser Stelle möchte ich mich zuerst bei Prof. Kai-Uwe Goss und Dr. Nadin Ulrich für die exzellente Betreuung bedanken. Prof. Goss danke ich für die unzähligen, sehr lehrreichen Diskussionen, seine ständige Bereitschaft zur Besprechung diverser Modellierungsprobleme, Ermutigungen in Momenten der Frustration und die allgemeine Unterstützung bei der Erstellung dieser Arbeit, in der ich so viel Neues lernen konnte. Neben Prof. Goss gilt mein besonderer Dank auch Dr. Ulrich. Ohne ihre unermüdliche Hilfe bei experimentellen Fragestellungen, ihr Engagement bei technischen oder organisatorischen Problemen und ihr strategisches, auf das Vorankommen im Projekt orientierte Denken und Planen wäre diese Arbeit nicht das geworden, was sie ist. Eine bessere Betreuung hätte ich mir von beiden nicht wünschen können.

Als nächstes möchte ich mich bei meinen Kollegen für die stets sehr angenehme Arbeitsatmosphäre im Department Analytische Umweltchemie bedanken. Im Besonderen danke ich Andrea Pfennigsdorff; mit ihrer Hilfsbereitschaft, ihrer herzlichen Art und ihren aufmunternden Worten zum richtigen Zeitpunkt machte sie das Labor zu einem Ort, an dem ich sehr gern gearbeitet habe. Dank ihr habe ich mich von Anfang an willkommen gefühlt. Auch meinen Mit-Doktoranden Wolfgang Larisch, Lukas Linden, Kai Bittermann, Luise Henneberger, Andrea Ebert, Estella Garessus und Flora Allendorf danke ich. Sie haben meinen Arbeitsalltag gesellig gemacht, durch Diskussionen meine Arbeit bereichert und auch mal für die nötige Zerstreuung gesorgt. Besonders möchte ich mich nochmal bei Flora, Estella und Andrea für ihre moralische Unterstützung in der finalen Phase meiner Arbeit und ihre Geduld in Formulierungs- und Formatierungsdiskussionen bedanken.

Natürlich danke ich auch meiner Familie, die mir die Erstellung dieser Arbeit erst durch ihre Unterstützung ermöglicht hat und mich bei Zweifeln stets in meinem Weg bestärkt hat. Außerdem möchte ich auch meinem Freund danken, der über die ganze Zeit hinweg stets ein offenes Ohr für mich hatte, die Höhen meines Arbeitsalltages in Freude mit mir geteilt hat und die Tiefen durch tröstende Worte geglättet hat.

Zuletzt möchte ich mich auch für die moralische Unterstützung meiner langjährigen Freundinnen Tini, Maria und Steffi bedanken, die sich zeitgleich in das Projekt Doktorarbeit gestürzt haben und bei denen ich mich daher trotz räumlicher Entfernung so gut verstanden gefühlt habe wie bei sonst kaum jemandem.

Angaben zur Person und zum Bildungsgang

Name: Sophia Krause
Geburtsdatum: 09.03.1990
Geburtsort: Zwickau

2015 – 2018 **Helmholtz-Zentrum für Umweltforschung Leipzig**
Department Analytische Umweltchemie
Promotion: “Desorption kinetics from albumin and the influence on hepatic metabolism”

2012 – 2014 **Friedrich-Schiller-Universität Jena**
Studium der Biochemie
Abschluss: Master of Science
Abschlussarbeit bei der Analytik Jena AG Bereich F&E:
▪ Entwicklung eines Real Time-PCR-Nachweises für *Phytophthora*-Pflanzenpathogene

2008 – 2011 **Friedrich-Schiller-Universität Jena**
Studium der Biochemie/Molekularbiologie
Abschluss: Bachelor of Science
Abschlussarbeit im Plazentalabor des Universitätsklinikums Jena:
▪ Proteindetektion in humanen Zelllinien nach Zytokin-Stimulation

2000 – 2008 **Peter-Breuer-Gymnasium Zwickau**
Allgemeine Hochschulreife

Publikationen und Konferenzbeiträge

- 2016 ISES 2016, Utrecht: How the desorption kinetics from albumin may impact QIVIVE (Vortrag)
- 2018 Krause, S., N. Ulrich, and K.-U. Goss, Desorption kinetics of organic chemicals from albumin. *Archives of Toxicology*, 2018. 92(3): p. 1065-1074.
- 2018 German Pharm-Tox Summit 2018, Göttingen: Desorption kinetics of organic chemicals from albumin (Poster)
- 2018 Krause, S. and K.-U. Goss, The impact of desorption kinetics from albumin on hepatic extraction efficiency and hepatic clearance: a model study. *Archives of Toxicology*, 2018. 92(7): p. 2175-2182.
- 2018 Krause, S. and K.-U. Goss, *In vitro* - *in vivo* extrapolation of hepatic metabolism for different scenarios – a toolbox, *Chemical Research in Toxicology* (submitted)

Eidesstattliche Erklärung

Hiermit erkläre ich an Eides statt, dass ich diese Arbeit selbstständig und ohne fremde Hilfe verfasst habe, keine anderen als die angegebenen Quellen und Hilfsmittel benutzt habe und die den benutzten Werken inhaltlich oder wörtlich entnommenen Stellen als solche kenntliche gemacht habe.

Außerdem erkläre ich, dass ich noch keine vergeblichen Promotionsversuche unternommen habe und die vorliegende Dissertationsschrift weder in der gegenwärtigen noch in einer anderen Fassung bei einer anderen Fakultät vorgelegen hat.

Leipzig, 19.06.2018

(Sophia Krause)